# CAPACITY OF MULCH BIOBARRIERS TO SUPPORT COMPLETE ANAEROBIC DECHLORINATION OF AEROBIC, TCE-CONTAMINATED GROUNDWATER

A Thesis

Presented to the Faculty of the Graduate School

of Cornell University

In Partial Fulfillment of the Requirements for the Degree of

Master of Science

by

Yitian Sun

August 2014

## ABSTRACT

The rise of Industrial Revolution in the 19th century has brought not only fast economic growth, but also the release of large amounts of anthropogenic compounds into the environment. Trichloroethene (TCE), a confirmed human carcinogen, is one of the most commonly found contaminants in groundwater, therefore the remediation of this compound has been extensively studied and practiced in the past several decades.

For compounds like TCE that are highly oxidized, destruction by reduction reactions (called reductive dechlorination) is more favorable than oxidative reactions. Although a wide range of bioremediation methods have been applied, biological permeable reactive barriers, referred to as biobarriers are attractive for shallow groundwater contamination plumes because of their ability to capture groundwater contaminant plumes before they migrate off-site, and their low cost of operation and maintenance. However, little research has explored the ability of biobarriers to reach complete dechlorination of TCE in oxygenated groundwater. Additionally, the dissolved oxygen in groundwater has not been taken into consideration when estimating the longevity of a biobarrier, and the impact of dissolved oxygen to the dechlorination process in a biobarrier is unknown.

For this Master's thesis, a column study was conducted to study the capacity of a mulch biobarrier to fully dechlorinate TCE to ethene. Six mulch (pine bark) filled columns (2 control, 4 experimental) were constructed to study the dechlorination process of TCE, with the inoculation of KB-1™ enrichment culture (at a 1:1000 dilution level). The 1 mg/L TCE-containing

inflow water was oxygenated, to examine the impact of dissolved oxygen on mulch column performance. The mulch columns (with a hydraulic residence time of 3.3 days) were able to reduce the dissolved oxygen concentration from 7.9 mg/L to a level anaerobic enough to allow reductive dechlorination to happen within three cm into the columns. Four days after inoculation, *cis*-1,2-dichloroethene appeared in the columns and 8 days after inoculation, vinyl chloride showed up in trace amounts. Until 130 days of operation, levels of vinyl chloride or ethene remained low, but the dechlorination process then accelerated. By Day 212, two of the four inoculated columns reached 73% and 99% complete dechlorination (i.e. ethene comprised over 73% of the chlorinated ethenes detected at the effluent ends of the columns), and by Day 297, the other two columns also reached 95% and 99% complete dechlorination.

The longevity of the column was predicted to be 7 years, considering only the impact of dissolved oxygen on the consumption of mulch-derived electron donors. Using column parameters and results from another researcher's studies, a dissolved oxygen penetration front speed of 0.7 cm of column height per month was predicted—corresponding to 5 cm within 212 days. With time, signs of TCE penetration was observed in the four inoculated columns, suggesting oxygen intrusion further into the columns.

From PCR tests on DNA extracted from column liquids, the existence of key KB1 dechlorination populations, *Geobacter* and *Dehalococcoides*, were confirmed using the biomarker genes *pceA* for *Geobacter* and vcrA/16S rRNA for *Dehalococcoides*. qPCR tests failed to quantify these populations, but results with 16S rRNA gene primers suggested 100 to 100,000 times more 16S rRNA gene copies (not specific to known inoculated dechlorinators)

were associated with the mulch-attached biofilms than with planktonic phases (in column liquid).

## BIOGRAPHICAL SKETCH

Yitian came to the US for education in 2008, and obtained a Bachelor of Science degree from Iowa State University before coming to Cornell University. He did not know that he will be studying, and probably going to put his career in environmental engineering when he first came to the US, because he received an offer from Iowa State University as a computer science major. The second day he arrived in Ames, Iowa, he went to switch his major from that to civil engineering, because he thought civil engineering could build skyscrapers and that was way cooler than doing programming in a cubical for the rest of his life.

He would not once again switch his major to environmental engineering, if not have met Professor Sung in 2009. Yitian did not want to work in cafeteria anymore after working there for a whole summer in 2009, and decided to try working as an undergraduate research assistant, and he met Dr. Sung, who was in environmental engineering. As a great advisor and friend, Dr. Sung has let Yitian found his passion about environmental engineering. Yitian learned a lot about wastewater treatment and has done multiple research projects on wastewater related topics at Iowa State University, but he decided to learn more about environmental engineering so he came to Cornell University for a MS/PhD degree.

At Cornell University, he became more interested in groundwater remediation, and made his way to finishing up this thesis research. The tight US job market in environmental engineering may not end up keeping him here, but he has decided to stay in environmental engineering field rather than getting a computer science degree and start rolling in money.

*To my lover and best friend, Qi Meng*

## ACKNOWLEDGEMENTS

Firstly, I would like to give my appreciation to Dr. Ruth Richardson and Dr. James Gossett, for their unstoppable wisdom and great patience in guiding me through the two-year research adventure and finally successfully finished my thesis. Their ways of thinking of how to solve a research problem is the most inspiring thing I have learned at Cornell University.

Secondly, I would like to express my love and appreciation to my family: my mom and dad (not including my girlfriend yet at this point). I admire their courage in giving up the money for buying a sport coupe version of 2014 Maserati, and put it on my six-year foreign education. They always say (and so does everybody) that the education I received is priceless, but I would really like to make the money someday and pay them back. Money may be paid back eventually, but the other kind of debt they have offered me, their love, can never be paid back, although I would try my best for the rest of my life.

Thirdly, I want to thank Professor Len W. Lion for offering my twice the teaching assistant opportunity, and also encouraged me to help with Professor Damian Helbling's lab course. The teaching experience I gained from assisting the two professors in their undergraduate environmental engineering core courses have helped me developed strong communication skill, and also reinforced my knowledge about the fundamentals in our field. Professor Damian Helbling's joining will surely open up new gates for our department.

Then, I want to thank my girlfriend, for her accompanying and love, and most importantly, her support and understanding when I face difficulties in my life. I will try my best to let her feel the same way.

Last but not least, I want to give my thanks to all the people that have helped me, laughed with me, and accepted me as a friend. This include the entire Richardson Lab Group, Runtian, The Scott Land & Yard Group, and my friends and advisors I met at Cornell University.

## TABLE OF CONTENTS

# LIST OF TABLES

## LIST OF FIGURES

## LIST OF ABBREVIATIONS

| | |
|---|---|
| **PCE** | **Tetrachloroethene** |
| **TCE** | **Trichloroethene** |
| ***cis*-DCE** | ***cis*-1,2-dichloroethene** |
| **VC** | **Vinyl chloride** |
| **DO** | **Dissolved oxygen** |
| **PRB** | **Permeable Reactive Barrier** |
| **MCL** | **Maximum Contaminant Level** |
| **DNAPL** | **Dense Non-Aqueous Phase Liquid** |
| **DMC** | ***Dehalococcoides mccartyi*** |
| **EPA** | **Environmental Protection Agency** |
| **PCR** | **Polymerase Chain Reaction** |
| **qPCR** | **Quantitative Polymerase Chain Reaction** |
| **LoDs** | **Limits of Detection** |

# CHAPTER 1 INTRODUCTION

## *1.1 Context*

With the rise of the Industrial Revolution in the 19$^{th}$ century, many toxic anthropogenic compounds were released to the environment before environmental awareness grew and regulations were developed. Among the released chemicals, trichloroethene (TCE) is very commonly found, and poses a threat to human health, including risks of cancer from TCE and its daughter product vinyl chloride (VC). Therefore, the remediation of TCE has been studied and practiced over the last several decades, and good progress has been made.

Despite natural attenuation for TCE occurring at some contaminant sites, engineered treatment methods are needed to ensure fast and thorough destruction of the compound. For compounds like TCE that are highly oxidized, destruction by reduction reactions is more favorable and when dealing with chlorinated organics, the reaction is called reductive dechlorination. A reducing environment (anaerobic) and suitable electron donor(s) are required for the reductive dechlorination of TCE, and among the remediation methods developed, biological permeable reactive barriers (also commonly referred to as biobarriers) have gained attention for their ability to capture groundwater contaminant plumes before they migrate off-site, their potential of long-term passive treatment, and their low cost of operation and maintenance.

In several previous TCE-treating biobarrier studies, complete TCE dechlorination to ethene was seldom achieved, with VC as the end product in some studies. Since VC also poses a great threat to human health, complete dechlorination to the harmless compound ethene is crucial for the success of biobarrier systems. Although the reductive dechlorination of TCE requires an anaerobic environment, groundwater, especially shallow groundwater (where biobarriers are mostly applied to due to the cost of excavation during construction), can contain dissolved oxygen in the mg/L range. This issue has not been addressed in previous biobarrier studies, and the effect of incoming dissolved oxygen on the dechlorination performance in a biobarrier, as well as the threat to the longevity of the biobarrier need to be studied. Additionally, knowledge about the distribution of the TCE-dechlorinating microorganisms in a biobarrier is useful for engineers to make better judgments when operating a biobarrier system. Therefore, this thesis research has used pine bark mulch filled columns, inoculated with KB-1$^{TM}$ culture, to treat oxygenated, TCE-contaminated water. The dechlorination process, methane levels, and dissolved oxygen concentrations were monitored along the length of the columns, and the distributions of microbial populations were tracked using molecular biomarkers.

### *1.2 Objectives*

The objectives of this thesis research were: 1) to determine if complete dechlorination of TCE can be achieved in mulch biobarrier columns receiving aerobic waters; 2) to estimate the longevity of the mulch biobarrier in terms of dechlorination performance; and 3) to monitor the distribution and quantities of the KB-1 dechlorinator populations.

# CHAPTER 2 BACKGROUND

## *2.1 The Threat of Chlorinated Ethenes*

Human impact on the environment has increased over the ages, especially with the rise of the Industrial Revolution. Many toxic anthropogenic (man-made) compounds were introduced to the environment, and it is difficult for the assimilative capacities of natural systems to adapt and keep pace (Leisinger, 1983). The Superfund Program was established in 1980 (USEPA, Superfund: Basic Information) to ensure funds for environmental cleanup. Out of 1430 of the most severe hazardous waste polluted sites on the National Priorities List (NPL), trichloroethene (TCE) has been found in 852 of them (ATSDR, 2003). It was also documented that tetrachloroethene (PCE) and TCE are the two biggest environmental risk drivers in the U.S. and other countries, due to their mass production and numerous incidences of uncontrolled release (Moran, et al., 2007).

TCE is a nonflammable, volatile, colorless liquid at room temperature with a sweet odor and sweet, burning taste (ATSDR, 1997). Even though TCE could show up in household products such as typewriter correction fluid, paint removers, adhesives and spot removers, it is mostly used as a solvent to remove grease from fabricated metal parts, and the evaporation of this chemical into air during such activity is by far the biggest source in the environment (ATSDR, 1997; EPA, 2001).

People living near hazardous waste sites may be exposed to TCE in the air or in well water they use for drinking, bathing, or cooking. The reported maximum contaminant level (MCL) for drinking water is 5 micrograms per liter, based on liver problems and increased risk of cancer in adults (USEPA, 2009). TCE enters the human body through air breathing, water drinking and direct skin contact. Exposure to high levels of TCE has adverse effects on the central nervous systems, immune system and endocrine system in adults (TEACH, 2007).

TCE can enter soil and groundwater near chemical waste sites. According to EPA regulations, land disposal of hazardous waste containing greater than or equal to 1,000 mg/kg halogenated organic compounds has been restricted (USEPA, 1987e). A residual amount of TCE that persists in dense, non-aqueous-phase liquids (usually referred to as DNAPLs) experiences a very slow dissolution process, making it harder to collect and treat using the popular pump-and-treat strategy for groundwater remediation.

To investigate the environmental impact of TCE, many researchers have looked into its mobility in the subsurface environment. The experimentally measured soil organic carbon sorption coefficients (Koc) for TCE range from 106 to 460 L/kg (Garbarini & Lion, 1986). This indicates a medium-to-high mobility of TCE in soil. TCE has also been found to be highly mobile in sandy soil (Wilson, et al., 1981). The high Henry's Law Constant of TCE also indicates a high volatility of the compound (Gossett, 1987).

### *2.2 Transformation and Removal of Trichloroethene*

#### *2.2.1 Physical Properties*

In the atmosphere, TCE transforms into hydroxyl radicals through photochemical reactions (Singh, et al., 1982). In many surface waters, neither biodegradation nor hydrolysis occurs at a rapid rate, so TCE is expected to volatilize into the atmosphere (ATSDR, 1997). When pure TCE seeps into soil, it moves through the unsaturated zone into saturated zone and displaces soil pore water, due to its dense non-aqueous phase liquid characteristics, and will continue to sink until it reaches an impermeable layer such as clay (ATSDR, 1997). As a result, treatment is needed for TCE in groundwater to prevent TCE from getting into drinking water wells and being breathed into human bodies due to vaporization into homes (vapor intrusion).

#### *2.2.2 Aerobic TCE Degradation*

For compounds like TCE that are highly oxidized, removal using abiotic or biotic reductive dechlorination is more favorable than oxidative processes. Aerobically, chlorinated ethenes can go through cometabolism by monooxygenases of methanotrophs or other monooxygenases that oxidize alkanes, alkenes and aromatic hydrocarbons, with carbon dioxide as the end product (Wilson & Wilson, 1985; McCarty, et al., 1998). With addition of organic compounds such as methane and toluene, this mechanism can be effective in removing TCE up to 1,000 to 1,200 µg/L, but with higher TCE concentrations, the solubility of oxygen appears to be limiting and the system becomes less efficient, such as when treating source zone TCE (McCarty, et al., 1998).

Oxidation of TCE using chemical reactions is also a common practice in the remediation field. Permanganate, hydrogen peroxide, ozone, peroxodisulfate, and activated persulfate are all effective choices according to the US EPA (Huling & Pivetz, 2006).

### *2.2.3 Anaerobic TCE Degradation*

Reductive dechlorination, as oppose to TCE oxidation, involves a sequential reactions where the chlorine atoms on the alkene molecule are replaced by hydrogen atoms one by one, forming the reaction chain: TCE to DCE (dichloroethene), DCE to vinyl chloride (VC), and finally VC to the non-toxic compound, ethene. This process can happen either via abiotic processes (Butler & Hayes, 1999; Henderson & Demond, 2007) or biotic processes (Bouwer & McCarty, 1983; Loffler & Edwards, 2006). Note that an incomplete dechlorination with VC as the end product may cause even more problems, as the MCL in drinking water for VC is 2 micrograms per liter, even lower than that of TCE (USEPA, 2009). VC is also identified by The U.S. Department of Health and Human Services as a known carcinogen (IARC, 1974). Thus, complete reductive dechlorination is essential to all remediation practices, whether abiotic or biotic.

#### *2.2.3.1 Abiotic Reductive Dechlorination of TCE*

The reductive dechlorination achieved by chemical reactions mainly involves the use of zero-valent iron (ZVI, $Fe^0$) or iron sulfide (FeS). More detailed reaction mechanisms and examples of applications are covered in the permeable reactive barrier section 2.3.2.3.

#### *2.2.3.2 Biological Reductive Dechlorination of TCE*

Biological reductive dechlorination of PCE/TCE is carried by different families and strains of bacteria. Among them, the most prominent is *Dehalococcoides*. *Dehalococcoides mccartyi* strains (DMC) are the only known microorganisms capable of dechlorinating *cis*-DCE and VC to ethene (Maymó-Gatell, et al., 1997; Löffler, et al., 2013). The specific strain, *Dehalococcoides mccartyi* strain 195 (formerly *Dehalococcoides ethenogenes* strain 195), is the only strain that completely dechlorinates PCE to ethene by itself. While it can rapidly respire PCE, TCE, and cis-DCE, it dechlorinates VC by a slower co-metabolic process (Maymó-Gatell, et al., 1999). Dechlorinators other than DMC, such as *Geobacter*, *Sulfurospirillum*, *Desulfitobacterium*, and *Dehalobacter* can partially dechlorinate PCE or TCE to *cis*-DCE (Löffler & Edwards, 2006).

The reductive dechlorination processes performed by microorganisms are catalyzed by enzymes called reductive dehalogenases (RDases), which are encoded by the RDase subunit A gene (rdhA) (Tang, et al., 2013). A few rdhA genes that act on chlorinated ethenes have been functionally characterized, such as *PceA* (Magnuson, et al., 2000), *TceA* (Magnuson, et al., 2000), *VcrA* (Müller, et al., 2004) and *BvcA* (Tang, et al., 2013). Table 2.1 below summarizes the information for important dechlorinators found to date, including the rdhA(s) they carry, electron donors and acceptors, and the end dechlorination product. Table 2.2 shows RDases

relevant to PCE/TCE dechlorination.

**Table 2.1: Summary of the dechlorinators of interest and the functions of their characterized rdhA(s).**

| Dechlorinators | GenBank assession no. | Characterized rdhA(s) with functions | Electron acceptors | Electron donors | End product(s) | References |
|---|---|---|---|---|---|---|
| ***Dehalococcoides strains*** | | | | | | |
| Strain 195 | AF004928 | *pceA* (PCE → TCE), *tceA* (TCE → VC) | PCE, TCE, *cis*-DCE, 1,1-DCE, VC (co-metabolic) | $H_2$ | ethene | Maymó-Gatell, et al., 1997, 1999; Seshadri et al., 2005; Löffler et al., 2012 |
| Strain BAV1 | AY165308 | *bvcA* (DCEs, VC → ethene) | PCE&TCE (cometabolic), DCEs, DCA, VC | $H_2$ | ethene | Tang et al., 2013 |
| Strain CBDB1 | AF230641 | *cbrA* (1,2,3,4-TeCB → 1,2,4-TCB)(1,2,3-TCB → 1,3-DCB) | PCE, TCE | $H_2$ | *trans*-DCE | Adrian et al., 2000 |
| Strain FL2 | AF357918.2 | *tceA* (TCE → VC) | PCE (co-metabolic), TCE, *cis*-DCE, *trans*-DCE, VC (co-metabolic) | $H_2$ | VC, ethene | He, et al., 2005 |
| Strain GT | | *vcrA* (DCEs, VC → ethene) | TCE, *cis*-DCE, 1,1-DCE, VC | $H_2$ | ethene | Sung et al., 2006 |
| Strain VS | AY322364 | *vcrA* (DCEs, VC → ethene) | TCE, DCEs, VC | $H_2$ | ethene | Cupples et al., 2003; Müller et al., 2004 |
| ***KB-1 related dechlorinators*** | | | | | | |
| *Dehalococcoides* Strains (multiple) | | KB1_VcrA (DCEs, VC → ethene), KB1_BvcA (DCEs, VC → ethene), KB1_TceA (TCE → VC) | TCE, *cis*-DCE, VC | $H_2$ | ethene | Duhamel and Edwards, 2006 |
| *Geobacter lovleyi* strain KB1 | AY914177 (strain SZ) | KB1_PceA (PCE, TCE → *cis*-DCE) | PCE, TCE | $H_2$, acetate | *cis*-DCE | Duhamel and Edwards, 2006 |

Several mixed cultures containing VC-respiring DMC Strains (i.e. DMC sp. strain BAV1, strain GT or strain VS) were studied and sustained by research groups (Duhamel, et al., 2002; Richardson, et al., 2002; Vainberg, et al., 2009). Among them, the KB-1$^{TM}$ culture from SiREM Labs of Guelph, Ontario, Canada is one of the commercially available cultures that been widely used in bioremediation projects worldwide.

**Table 2.2: Summary of the reductive dehalogenases (RDases) relevant to PCE/TCE dechlorination.**

| RDases for PCE/TCE dechlorination | Catalytic activity in dechlorination | Reference |
|---|---|---|
| pceA | PCE → TCE | Magnuson et al., 2000 |
| tceA | TCE → VC | Magnuson et al., 2000 |
| vcrA | DCEs, VC → ethene | Müller et al., 2004 |
| bvcA | DCEs, VC → ethene | Tang et al., 2013 |

The KB-1 culture was initially derived from an enrichment culture started by the Edwards lab at the University of Toronto (Duhamel, et al., 2002). This culture, named KB1-UT, is known for its ability to completely dechlorinate PCE to ethene via TCE, *cis*-DCE, and VC. To date, this culture contains (at least two) *Dehalococcoides* strains and one *Geobacter* strain that are all responsible for dechlorination. From tests done on TCE-induced KB-1 culture from Edwards' lab, the *Dehalococcoides* strains expressed four reductive dechlorination genes: KB1_VcrA, KB1_BvcA, KB1_TceA and KB1_RdhA5. From tests done on VC-induced KB-1 culture, one more gene transcript showed up as KB1_RhA1 (Tang, et al., 2013). The *Geobacter* strain in the KB-1$^{TM}$

culture is very similar to (95% amino-acid identity) *Geobacter lovleyi* strain SZ, and the strain is named Geobacter strain KB-1 (Tang, et al., 2013). It is capable of dechlorinating PCE and TCE to cis-DCE via an RDase encoded by a *pceA* gene. The electron donor for this *Geobacter* strain is presumed to be acetate instead of hydrogen, which is the common electron donor for *Dehalococcoides* (Wagner, et al., 2012).

The commercial KB-1 culture (referring to as KB-1$^{TM}$) from SiREM Labs is a commercial product that can enhance remediation of a range of chlorinated solvents and recalcitrant compounds such as: chlorinated ethenes, chlorinated ethanes, chlorinated methanes, chlorinated propanes, RDX (Royal Demolition Explosive), and chlorofluorocarbons (SiREM: *www.siremlab.com/products/kb-1*). To highlight KB-1$^{TM}$'s capability in terms of dechlorination, it contains two VC-respiring RdhA genes similar to *vcrA* and *bvcA*. *VcrA* was initially described in DMC Strain VS (Müller, et al., 2004) and *bvcA* in DMC Strain BAV1 (Krajmalnik-Brown, et al., 2004). The *bvcA* gene was initially known to be associated with VC dechlorination (Krajmalnik-Brown, et al., 2004), but later on found also be able to dechlorinate *cis*-DCE and 1,2-DCA (Tang, et al., 2013). It is believed that different strains of DMC in KB-1$^{TM}$ contain *vcrA* and *bvcA* homologs.

#### *2.2.3.3 Suitable Growth Conditions for Biological Reductive Dechlorination*

In the reductive dechlorination process, the electron acceptors are chlorinated compounds, such as TCE, *cis*-DCE and VC, and the direct electron donor is hydrogen if DMC is considered. In the past, methanol, formate, acetic acid, glucose and hydrogen were all found as

suitable electron donors for PCE-dechlorinating cultures containing *Dehalococcoides* (Freedman & Gossett, 1989), but later on, it is found that hydrogen is the only direct electron donor for the dechlorination process for all known *Dehalococcoides* mccartyi strains (DMC) (Maymó-Gatell, et al., 1995). However, organic acids are usually injected to the subsurface, because the fermentation process by various fermenters in the mixed culture will provide hydrogen in situ, and it is not practical to inject hydrogen gas. It is interesting that while vitamin $B_{12}$ and biotin are essential growth factors for DMC, the DMC cannot synthesize them. Instead, they have to rely on other organisms to produce them (Seshadri, et al., 2005). Normally, organic acids that generate hydrogen upon fermentation (such as lactate, butyrate and benzoate) are all considered suitable electron donors for the dechlorination process. Selected hydrogen releasing electron donors and hydrogen consuming reactions that occur in dechlorinating mixed cultures are shown below in Table 2.3.

**Table 2.3: Hydrogen releasing and consuming reactions related to reductive dechlorination.**

| **Selected Hydrogen Releasing Reactions** | |
|---|---|
| *Electron Donor* | *Reactions* |
| Acetate | $acetate^- + 4H_2O \rightarrow 2HCO_3^- + H^+ + 4H_2$ |
| Propionate | $propionate^- + 3H_2O \rightarrow acetate^- + HCO_3^- + H^+ + 3H_2$ |
| Butyrate | $butyrate^- + 2H_2O \rightarrow 2acetate^- + H^+ + 2H_2$ |
| Ethanol | $ethanol + H_2O \rightarrow acetate^- + H^+ + 2H_2$ |
| Methanol | $methanol + 2H_2O \rightarrow HCO_3^- + H^+ + 3H_2$ |
| Lactate | $lactate^- + 2H_2O \rightarrow acetate^- + HCO_3^- + H^+ + H_2$ |
| **Selected Hydrogen Consuming Reactions** | |
| *With Chlorinated Electron Acceptor* | *Reactions* |
| PCE | $PCE + H_2 \rightarrow TCE + H^+ + Cl^-$ |
| TCE | $TCE + H_2 \rightarrow$ *cis*-$DCE + H^+ + Cl^-$ |
| *cis*-DCE | *cis*-$DCE + H_2 \rightarrow VC + H^+ + Cl^-$ |
| VC | $VC + H_2 \rightarrow ethene + H^+ + Cl^-$ |
| *Sulfate reduction* | $4H_2 + SO_4^{2-} \rightarrow S^{2-} + 4H_2O$ |
| *Iron reduction* | $2Fe^{3+} + H_2 \rightarrow 2Fe^{2+} + 2H^+$ |
| *Other Hydrogen Consuming Microorganisms* | *Reactions* |
| Acetogens | $2HCO_3^- + 4H_2 + H^+ \rightarrow acetate^- + 4H_2O$ |
| Hydrogentrophic Methanogens | $HCO_3^- + 4H_2 + H^+ \rightarrow methane + 3H_2O$ |

Adapted from (Fennell & Gossett, 1998), (He, et al., 2002), (Shen & Wilson, 2007) and (Lovley, 1987).

Besides being electron donors, some organic compounds are utilized as carbon sources to support the growth of the dechlorinators. Acetate is the only direct carbon source for DMC, but it can be produced during fermentation of high molecular weight electron donors (Maymó-Gatell, et al., 1997), with reactions shown in Table 2.3.

A reducing environment is crucial for keeping the robustness of the dechlorinators in the subsurface (ITRC, 2008). The existence of dissolved oxygen (DO) in the subsurface

environment will directly inhibit the dechlorination process. Although the maximum oxygen tolerance levels of different dechlorinators have not been studied, it is known that a DO about 1.6 mg/L can inactivate the KB-1$^{TM}$ culture's dechlorination, but in one study, when DO was again dropped to less than 0.2 mg/L, the dechlorination ability returned (Heavner, 2013). It is generally easy to deplete DO, simply by adding electron and carbon donors for the dechlorinators. In that way, the DO will be quickly consumed by facultative microbes, and an anoxic condition as well as low redox potential condition will be created, and the subsurface will be suitable for reductive dechlorination.

Groundwater DO levels vary from air-saturated concentrations to nearly zero, depending on the depth of the point of interest below groundwater table, groundwater conditions (chemically and biologically available organic carbon levels) and geochemical conditions. In 1979, a simple conceptual groundwater DO model was made, for the distribution of DO in groundwater (Champ, et al., 1979): groundwater found in shallow subsurface contains DO at near air-saturated concentrations, and as it gets deeper below water table where gas exchange with the atmosphere becomes insignificant, and coupled with DO consumption by microbial uptake and oxidation of reduced minerals, the DO level can drop to near zero. Besides that, DO concentrations may increase along flowpaths due to contact with oxygen in the overlying vadose zone (Rose & Long, 1988), or decrease along flowpaths due to the oxidation of organic or inorganic compounds persisting in groundwater. In summary, when considering an in-situ bioremediation design, the groundwater DO at a site needs to be carefully monitored and controlled.

### *2.3 Groundwater Remediation Technologies*

#### *2.3.1 Ex-situ*

Existing remediation strategies for groundwater contamination can be divided into two groups, ex-situ remediation and in-situ remediation. In Ex-situ remediation, the representative strategy is to pump the groundwater above ground and treat it with chemical, physical or biological processes. The treatment can be on-site or off-site. The main advantage of this approach is that it does not require thorough understanding of the subsurface environment, and the remedial activity is easier to control and monitor compared to in-situ methods (Reddy, 2008). However, the costs can be quite high and it can often take many decades to remediate a site.

#### *2.3.2 In-situ*

In-situ remediation methods take place in the subsurface where either the contamination source zone or the groundwater contaminant plume is located. Popular *in-situ* remediation strategies include physical removal, with common methods like air stripping, carbon adsorption, soil venting and in-well aeration; chemical destruction, such as in-situ chemical oxidation (ISCO); and biological destruction, with the help of microorganisms existing in the subsurface or bioaugmented into the subsurface (ITRC, 2008; Reddy, 2008).

##### *2.3.2.1 In-Situ: Physical Removal Strategies*

In physical in-situ remediation strategies, air stripping and combined air stripping and carbon adsorption have received considerable attention since the early 1980s (Rusell, et al.,

1992). Air stripping takes advantage of some contaminants' high Henry's Law constants, moving contaminants from the dissolved phase into air, and then either releasing to the atmosphere or conducting gas-phase adsorption using activated carbon. The disadvantage is obvious: a great potential of polluting the air or high cost in replacing activated carbon sorbent. Soil venting and in-well aeration also take advantage of the high volatility of TCE and some other organic contaminants (Rusell, et al., 1992). In-situ remediation methods require good understanding of subsurface conditions, but they are more economical compared to ex-situ methods, as the in-situ methods require little site disruption and provide better safety for on-site workers and the general public near the remedial project (Reddy, 2008).

#### *2.3.2.2 In-Situ: In-situ Chemical Oxidation*

In-situ chemical oxidation (ISCO) can be used in either surface or subsurface conditions. When targeting TCE, iron (II)-assisted persulfate and permanganate are commonly used (Liang, et al., 2004) (Huling & Pivetz, 2006). The advantage of this technology is that chemical oxidation occurs quickly. As soon as the chemical gets in contact with the contaminant, the contaminant gets oxidized. The disadvantage of ISCO is that the reactions are usually short-lived, which means the chemical cannot be well-distributed through one-time injection. It usually requires multiple injections and close injection spacing, meaning high cost (Huling & Pivetz, 2006).

### *2.3.2.3 In-situ: Permeable Reactive Barriers*

Among in-situ methods, permeable reactive barriers (PRBs) are a relatively new technology (Henderson & Demond, 2007; Wilkin & Puls, 2004; Reddy, 2008). As seen in Figure 2.1, a PRB is a porous barrier or wall of material, with either soil with soil amendments added or an entirely non-soil solid material, such as mulch or compost (Reddy, 2008). It is often constructed perpendicular to the flow of contaminated groundwater, to maximize the contact with the plume, and biotic or abiotic remediation strategies can then be applied in the PRB to stop the migration of the contaminated plume (Henderson & Demond, 2007).

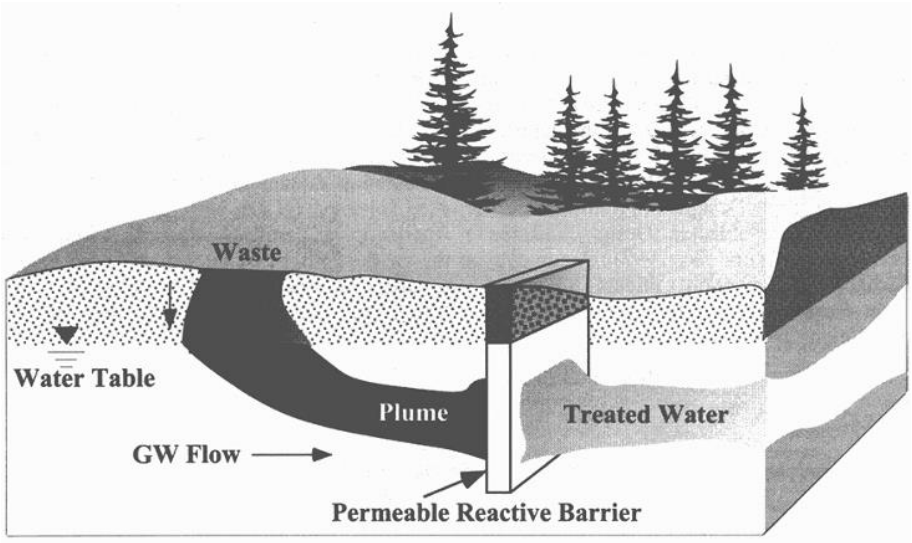


**Figure 2.1: A schematic of a PRB placed perpendicular to the groundwater contaminant plume (Reddy, 2008).**

The PRB system offers several positive features: (1) *in situ* plume capture and treatment, especially suitable for large volumes of water containing low concentrations of contaminants (Blowes, et al., 1999); (2) simultaneous treatment of multiple contaminants, such as organics (chlorinated ethenes for example), heavy metals, radionuclides, and nutrients (RTDF, 2001); (3)

low operation and maintenance costs (Powell & Powell, 2002); and (4) long-term passive treatment possible from selection of reactive media (Reddy, 2008). However, there are limitations to this technology as well, which include: (1) potential for decreasing reactivity overe time (ZVI PRB as an example); (2) only valid for shallow groundwater treatment due to construction costs; and (3) lengthy treatment time compared to some alternative remediation approaches such as ISCO (Reddy, 2008). Some PRBs were constructed in the 1990s, such as the pilot-scale PRB installed at the Borden, Ontario site in 1991 (Gillham & O'Hannesin, 1992) and the full-scale PRB installed at the Intersil Site in Sunnyvale, CA in 1995 (Warner, et al., 2005). A list of PRBs installed before 2001 was prepared by the Permeable Reactive Barrier Action Team under The Remediation Technologies Development Forum, which summarized PRB applications to different types of contaminants (chlorinated solvents, metals and inorganics, fuel hydrocarbons, nutrients, radionuclides, and other organic compounds) at full-scale or pilot-scale. (RTDF, 2001). For the purpose of this thesis research, only details on the treatment of chlorinated ethenes will be covered.

In abiotic PRBs, granular or nano-sized zero-valent iron (ZVI or nZVI) or iron sulfide are commonly applied for TCE dechlorination. Under the resulting reducing environment, Fe (II) sorbed to iron oxides, green rust, and iron sulfides can be formed, and they have all been observed to abiotically reduce chlorinated solvents (Amonette, et al., 2000; Lee & Batchelor, 2002; Butler & Hayes, 1999). Among them, iron sulfides (both amorphous FeS and poorly crystalline mackinawite) were frequently found in ZVI PRB systems (Phillips, et al., 2000;

Benner, et al., 1999), and the formation of acetylene (ethyne) is a signature of the successful PCE/TCE abiotic reduction (He, et al., 2008).

For zero-valent iron application in PRBs, a dozen site applications occurred in Europe and the U.S. It was found that porosity reduction in a few years could cause complete failure (Henderson & Demond, 2007), and complete dechlorination was either not achieved or not reported. Of the operating PRBs in the US, only 40 have provided sufficient public information on field conditions and performance issues (Henderson & Demond, 2007)). Given the increase in the price of zero-valent iron, high sensitivity to site conditions (groundwater containing sulfate, and soil containing iron minerals), and poor dechlorination results (plugging due to mineral formation, incomplete dechlorination process), biotic PRB remediation strategies may be favored over ZVI PRBs (Shen & Wilson, 2007).

Besides iron-based treatment, sorption-type treatments (including ion exchange, for ionized contaminants) are also common in the application of PRB. The materials that have been applied to PRBs for direct sorption control include: granular activated carbon (GAC), bone char, apatite, zeolites, coal, peat, synthetic resins, compost, wood chips, wheat straw, cheese whey, tire chips, paper sludge and waste green sands (ITRC, 2005).

### *2.4 Enhanced In-situ Reductive Dechlorination (ERD)*

#### *2.4.1 In-situ Bioremediation Other Than In Permeable Reactive Barriers*

The mechanism of biological reductive dechlorination of TCE is covered in Section 2.2.3.2, including the chemistry and biology of the process. This section only discusses the applications of bioremediation. Enhanced reductive dechlorination (ERD), as opposed to monitored natural attenuation, involves in-situ injection or placement of fermentable organic substrates (electron donor), and very commonly, bioaugmentation is also involved (Scheutz, et al., 2008). Different system configurations are usually used for different treatment purposes. For liquid substrates, injection wells are usually used. A grid configuration (a matrix of wells drilled directly on top of the area being treated) can be used for treating a contaminated source zone area, while a linear barrier configuration (also called a containment barrier, which is a line of injection wells placed perpendicular to the flow direction of the contaminant plume) is usually employed when trying to intercept a contaminant plume (Scheutz, et al., 2008). One application of linear barrier configuration in a TCE remediation project was discussed in this thesis, in section 4.6.4. The use of solid substrates in ERD is called a biobarrier, which is covered in the next section. The selection of fermentable organic substrates, cultures used for bioaugmentation, as well as the system configuration are carefully considered after acquiring knowledge of subsurface site conditions. Compared with conventional remedial technologies (e.g., ISCO or pump-and-treat), remediation via enhanced reductive dechlorination has longer effectiveness with a lower overall cost (Leeson, et al., 2004).

### *2.4.2 Bioremediation with Permeable Reactive Barriers — (Biobarriers)*

A PRB used for bioremediation is also called biobarrier or biowall (In this thesis, the term biobarrier is used.). To set up a biobarrier, one either can line up rows of substrate injection

wells for liquid substrate, or excavate a trench to be filled with solid substrate as with abiotic PRBs. The location of the biobarrier should be perpendicular to the groundwater flow to best intercept contaminants (Leeson, et al., 2004). There are three types of biobarriers: active, semi-passive and passive. Active biobarriers re-circulate the substrate inside of the reaction zone to achieve fast reaction rates and rapid removal of contaminants. Semi-passive biobarriers requires periodic injection of substrates to maintain the ongoing biological activity within the barrier. When the contaminants of concern are electron acceptors (as with TCE reductive dechlorination), the added substrates are usually organic electron donors. The substrates used in active and semi-passive biobarrier are usually readily degradable organic compounds to ensure quick contaminant removal, but the total cumulative amount of substrate consumed is higher than in passive biobarriers. Passive biobarriers, on the other hand, need only one time addition of solid substrates or one time injection of slowly degrading liquid substrates (Cowan, 2000). The substrates used will support the biological activity over a long period of time in the reaction zone, usually over 5 to 10 years if a solid substrate is used (Leeson, et al., 2004).

Biobarriers are able to treat various types of contaminants due to their easy modification, such as selecting reactive media, controlling contaminant residence time, and choices of biological enhancements to the remedial action (Reddy, 2008). There are several key design parameters pertaining to biobarriers: appropriate reactive medium or a mixture of several media; a hydraulic conductivity slightly higher than surrounding subsurface environment to avoid any bypass flow; biobarrier dimensions that are large enough to intercept

the entire contaminant plume; and enough residence time for the contaminants to be removed or degraded (Reddy, 2008).

When selecting media for a biobarrier, typical choices for a slow-release, long-lasting substrate include engineered liquid media such as HRC™ and EVO™ from REGENESIS and solid media such as tree mulch (Leeson, et al., 2004). Although HRC™ (REGENESIS, https://www.regenesis.com/contaminated-site-remediation-products/enhanced-anaerobic-bioremediation/hrc/) and EVO™ (Terra Systems, http://www.terrasystems.net/products.htm) have the ability to slowly release electron donors and carbon sources to the dechlorinators, they tend to not last very long — not because of their reaction rates, but rather because they will be flushed out slowly by groundwater flow. They also do not have the ability to control the contaminant plume size, unless a costly recirculating well system is used. However, solid substrates used in a biobarrier can effectively provide electron donor and carbon source for the dechlorination process, and will not be flushed away. The solid substrate also provides the natural or bioaugmented microorganisms a superior, highly sorptive solid surface on which to grow.

### *2.4.3 Solid Substrates for Biobarriers*

From a functional point of view, any solid material that's able to release fermentable organic compounds under a subsurface environment and contains no toxic chemicals is suitable

for being the solid substrate for bioremediation of PCE/TCE by reductive dechlorination. Because of the massive amount of material needed in every site application, materials with low market price are favorable. Commonly, mulch and compost are chosen. Mulch is the shredded and chipped pieces of trees or shrubs, mainly containing cellulose and lignin, while compost can come from many different ways, including from composted plant materials. Among all the mulch materials, bark mulch is the easiest to obtain, and is found to have the characteristics to support the bioremediation process. From a study that compared cypress, eucalyptus, pine bark, pine needle, melaleuca, and a utility-trimming mulch (GRU), pine bark mulch was found to be highest in lignin content (about 50%) but average for nitrogen content and carbon : nitrogen ratio (Duryea, et al., 1999). Lignin has higher adsorption capacity than common soil organic compounds (Garbarini & Lion, 1986). Pine bark mulch was also found to have overall the best adsorption capacity for PCE and its daughter products compared with hardwood and cypress mulch (Wei & Seo, 2010).

During the bioremediation process, pine bark mulch (refer to as "mulch" in this thesis) generates many compounds from hydrolysis, and the resulting monomers can be further fermented to a variety of compounds including alcohols, fatty acids, hydrogen, carbon dioxide and methane (Shen & Wilson, 2007). The resulting fermentation products can then support various dechlorinators (including DMC and *Geobacter*).

Besides mulch's potential for slowly and continuously releasing electron donor for the dechlorination process, it has been found to be a good biofilm-forming bed (Seo & Bishop, 2008). Because mulch has a good sorption capacity for organic contaminants, it can induce

biofilm formation (Seo & Bishop, 2008). The extracellular polymeric substance (EPS) of biofilm also has strong affinity for hydrophobic organic compounds, such as chlorinated ethenes (Moretti & Neufield, 1989) (Ebihara & Bishop, 2002). Hence, the formation of biofilms further rises the potential for contaminant sorption, and more sorption enhances the formation of biofilms of contaminant-utilizing microbes.

In a mulch column study treating naphthalene (Seo & Bishop, 2008), the abiotic sorption capacity was tested under no inoculation (previous growth bacteria were killed by the addition of sodium azide), and the breakthrough of naphthalene happened in ten days. The sorption capacity under biotic conditions (with the growth of naphthalene-degrading microorganism in column) was hard to quantify because it was hard to distinguish between the portion of naphthalene biodegraded and the portion adsorbed, but biofilm formation was definitely shown based on the observation of increasing mass of biofilm (phospholipid /dry mulch, w/w) in the biotic condition compared to the abiotic condition. More biofilm was formed in the first half of the column, indicating the positive correlation between biofilm formation and concentration of organic contaminants (Seo & Bishop, 2008).

It has been reported that the polarity, organic carbon content, cation exchange capacity (CEC) and surface area all affect the adsorption capacity of sorbents (Chen, et al., 2005; Zytner, 1992). Mulch with a mid to low polarity tends to adsorb overall the most PCE, TCE and *cis*-DCE. An increase in organic carbon content increases the adsorption capability of TCE (Wei & Seo, 2010). To determine the sorption capacity, researchers have fit adsorption data to various sorption models including Freundlich isotherm, and a found linear relationship between the

adsorption capacity (mg sorbate/kg sorbent) and aqueous concentration of contaminant at equilibrium (Wei & Seo, 2010). The adsorption capability of mulch for treating PCE and its daughter products is in the order of PCE>TCE>*cis*-DCE (Wei & Seo, 2010).

### *2.5 Previous Research Studies on the Application of Mulch Permeable Reactive Barriers to TCE Remediation*

Several mulch biobarrier research studies have been performed previously by others. Four studies focused on TCE bioremediation are summarized below.

In a column study conducted by Shen and Wilson (Shen & Wilson, 2007), the removal of TCE was studied in a column filled with mulch (50% v/v), cotton gin trash (10% v/v) and sand (40%). The column was constructed to simulate the biowall at the SS-17 site at Altus, Air Force Base in Oklahoma. It had a hydraulic residence time of 17 days, and was operated for 800 days with 2 mg/L (15 μM) of TCE in an anaerobic influent. The columns received real site groundwater amended with TCE, but with no bioaugmentation. The groundwater taken from the site was sealed in Teflon bags with minimum headspace, but no information about whether the DO level of the groundwater was monitored or not, although according to their result, a reducing environment was established in the column. As a result, less than 1% of TCE removal was associated with reductive dechlorination, according to *cis*-DCE and VC levels reported. Ethene was never detected above its detection limit of 0.07 μM. Over 793 days of operation, the columns effluent TCE concentration varied from 0.1 to 2% of the influent, and 80-90% TCE

removal was from abiotic degradation by FeS minerals which formed, due to high concentration of sulfur in local groundwater. The main product of FeS based TCE reduction was acetylene.

In a follow-up study done by Shen and coworkers, the same column and operational conditions from their 2007 study was used, but this time the column was inoculated with an enrichment culture from a monitoring well at the Altus Air Force Base (Shen, et al., 2010). With a residence time of 17 days and influent TCE of 12 mg/L, the effluent was composed of 10 µg/L of TCE and *cis*-DCE, and 1 µg/L of VC, since reduction by FeS minerals was still the dominant TCE destruction mechanism in the columns, due to high level of sulfate existing in groundwater. No data for complete dechlorination to ethene was shown, even though their microcosms completely transformed TCE to ethene. The capacity of their mulch biobarrier was estimated using methane production from microcosm tests, since methane is one of the final products of mulch anaerobic digestion. Using a Monod-like kinetic equation with kinetic parameters tuned for anaerobic digestion (Chin, 1981), and a biodegradability estimation of mulch (42% of total mass of mulch) and cotton gin trash (36% of total mass of cotton gin trash) from the equation developed by Richard (Richard, 2005), each gram of tree mulch (wet or dry not stated) could yield 71 mg of methane, the longevity of their column was found to be around 11 to 15 years. This longevity study conducted may have ignored the existence of methanotrophs, which could potentially consume methane, as well as the dissolved oxygen level in groundwater, which could cause more mulch degradation aerobically.

A study by Lu and coworkers (Lu, et al., 2008) examined the performance of a pilot scale mulch biobarrier under natural attenuation with detected *Dehalococcoides*. The contaminant

site (operable unit 1 (OU-1)) is also located at Altus Air Force Base in Oklahoma, USA. The mulch biobarrier (139 m long, 7 m deep and 0.46 m wide) had a hydraulic residence time of 7.7 days. Though no dissolved oxygen data were provided, it was stated that the upgradient groundwater dissolved oxygen level was low enough to be considered anoxic. After one month of operation of the biobarrier, TCE concentration was reduced from 46 µM to 0.4 µM, but TCE rebounded to 15 µM 30 meters down gradient of the biobarrier, for unknown reasons. *Cis*-DCE concentration tended to increase downstream of the biobarrier, while VC tended to decrease. No information was provided on the production of ethene, even though *Dehalococcoides* DNA was present in the biobarrier area.

A fourth study, a mulch column study, focused on treating influent water with a TCE concentration of 1.1 mg/L (8.4 µM) with eucalyptus mulch in an upflow column that was bioaugmented with a TCE-degrading enrichment culture (Oztürk, et al., 2012). With a hydraulic residence time of 7.2 days, the column was operated for 183 days. The dechlorinating culture used for bioaugmentation was first grown on TCE in basal medium with methanol as the primary electron donor. After inoculation, TCE was rapidly converted to VC, followed by a slow conversion to ethene. The *Dehalococcoides* population was at $1.21 \times 10^8$ cells/µg mulch sample (authors did not report wet or dry weight). In the column effluent, ethene was first observed on Day 120, but due to their instrument detection limit, no quantified data were shown. After reducing the flow rate by half, VC concentration dropped from 7.49 to 1.3 µM, and since VC was the main chlorinated ethene in the column, this was used to estimate ethene production. (The authors assumed complete mass balance of all chlorinated compounds.) Overall, after 183

days of operation, the authors calculated the dechlorination process had an efficiency of 74%, by taking the ratio of ethene produced to influent TCE concentration.

To date, there are no mulch biobarrier studies in lab or in field applications that have performed complete PCE/TCE dechlorination, and most of them were conducted with anaerobic natural or synthetic groundwaters, ignoring the mg/L-range DO level in shallow groundwaters (Rose & Long, 1988; Gómez, et al., 2002; Baker, et al., 2000). The inocula used in the columns or field biobarriers were either water and soil samples from TCE-contaminated wells that showed natural attenuation of TCE, or enrichment cultures that have not been commercialized and, therefore, the experiments cannot be replicated easily.

This thesis research used pine bark mulch filled columns and KB-1$^{TM}$ culture inoculum to treat oxygenated, TCE-contaminated water. The dechlorination process and dissolved oxygen concentrations were monitored along the length of the columns. The objectives of this thesis research were: 1) To find out if complete dechlorination of TCE can be achieved in mulch biobarrier columns receiving aerobic waters; 2) Try to find the longevity of the mulch biobarrier in terms of dechlorination performance; and 3) Monitor the distribution and quantities of the KB-1 dechlorinator populations.

# CHAPTER 3 MATERIALS AND METHODS

## *3.1 Chemicals*

TCE (99.5%, Fisher Scientific), *cis*-1,2-DCE (97%, Sigma-Aldrich), methane (chemically pure compressed methane from Airgas), and ethene (ultra high purity compressed ethylene from Airgas) were used to prepare standards for analysis. High purity compressed nitrogen (Airgas) was used as carrier flow in GC and other applications where anaerobic environment is required.

## *3.2 Stock Solutions*

### *3.2.1 Saturated TCE Stock Solution*

Four to five hundred μL of neat TCE (99.5%, Fisher Scientific) was added to 140 mL tap water in a 160-mL glass serum bottle to make a saturated TCE solution, which served as stock solution for the column experiment. The serum bottle was then placed on an orbital shaker at 100 rpm for at least a week, and then sat quiescently for three to five days before use. The sign of a saturated solution is the visual appearance of a spherical droplet of TCE on the bottom of the bottle after one week of orbital shaking, due to the fact that TCE is a dense non-aqueous phase liquid (DNAPL). During the entire preparation and use of the saturated TCE stock solution, the bottle was never inverted or vigorously shaken, to avoid breaking of neat TCE droplets and splashing of little droplets that might stay on the solution surface or suspended in solution. Such small TCE droplets have a chance to be picked up by injection syringes and thus

cause huge error. The saturated TCE solution was prepared and stored under room temperature of 22°C.

### *3.2.2 Methanol Carried TCE and cis-DCE Stock Solutions*

To effectively analyze TCE and *cis*-1,2-DCE via GC FID, methanol was used as the solvent in preparation of a stock solution that was then injected to serum bottles for creating calibration standards gravimetrically (Gossett, 1987). The reason to use methanol as a solvent rather than water is because the solubility of TCE and *cis*-1,2-DCE in methanol is infinite and much higher stock-solution concentrations can be created. The effect of methanol on Henry's Law Constant has been shown to be negligible when used at concentrations less than 5% (v/v) (Gossett, 1987). The methanol-carried TCE and *cis*-DCE solution was prepared and stored under room temperature of 22°C.

## *3.3 Mulch Column Setup*

Six glass columns (5-cm diameter, 60-cm height) were chosen to simulate sections of a mulch biobarrier receiving TCE-contaminated groundwater. Tap water (with DO of around 8 mg/L, pH between 6.5 and 7.5, dechlorinated for five days) was pumped in (pumping detail explained in *Water Reservoir and Pump Setup*), and TCE stock solution (200 mg/L) was pumped into the columns from the bottom (pumping detail explained in *Syringe Pump Setup*), at respective rates to achieve a desired influent TCE concentration. Thus the bottom of the

column mimicked the front face of a biobarrier, and the top its rear face. A column schematic is presented in Section 4.1 in Chapter 4. Each column had seven sampling ports, with 8-cm spacing between adjacent ports 1, 2, 3 and 4, and 10-cm spacing between adjacent ports 4, 5, 6 and 7. There were 2-cm heights of mulch below port 1 and above port 7.

Pine bark mulch (purchased from Agway in Ithaca, NY) was added to the six columns as the medium for bioremediation. The moisture content of the mulch was found to be 0.42 grams of water per gram of ambient mass of mulch) (following ASTM D4442: standard test method for direct content measurement of wood and wood-based materials). This moisture content was used for estimating porosity and hydraulic residence time (HRT) of the columns.

During fermentation of organics including mulch, pH and alkalinity may decrease due to production of organic acids and carbon dioxide. To prevent excessively low pH, Brennan et al. (2006) applied limestone chips in a one-to-one ratio by weight with chitin in their column study of tetrachloroethene biodegradation. In this thesis study, limestone chips (Fisher Scientific Cat. S25201A) were applied as 40% by weight of dry mulch to neutralize pH and provide alkalinity to the system. The pH of the column liquid was monitored every month (from the liquid taken for GC FID sampling), and found the pH stayed stable in a narrow range of 6.6 to 7.0 (data not shown). Without a comparative column of only mulch added and no limestone, we cannot conclude that the stable pH reading was from the contribution of the limestone, but for the purpose of this thesis research, a stable pH was attained with the use of limestone chips. Together, the porosity of the column with mulch and limestone was found to be 0.78, with

methods explained in Appendix G, which is much higher than typical subsurface soil porosity of between 0.4 to 0.5 (Rawls, et al., 1982).

To minimize TCE adsorption and corrosion to tubing and column walls, Teflon® PTFE film (0.01" thick), Teflon screw caps, Viton®Fluoroelastomer O-Rings, stainless steel, and glass were used where there was any direct exposure with TCE. Column operations and sampling were conducted under room temperature of 22°C.

### *3.4 Water Reservoir and Peristaltic Pump Setup*

A 10-L, open-air glass tank was used as the reservoir of the air-saturated tap water which was pumped into the columns. The tank was refilled every two days (about 4 liters every two days, based on the flow rate). Since the water tank was open to the atmosphere, no TCE could be added to it prior to entering the column; thus TCE was added separately using a syringe pump, which is explained in the next section. The tap water filled to the 10-L tank was not pre-dechlorinated, but with an average hydraulic residence time of 5 days in the tank, the chlorine residual reaching the column was undoubtedly very little. Besides, the chlorine residual would react very rapidly with mulch at front end of the columns. Three peristaltic pumps (Cole-Parmer Instrument Company 7523-70) were employed to deliver tap water into the six columns, meaning that each pump carried two pump heads that ran at the same rotational speed. The flow rate was set to 0.2 mL/min, which gave a flow rate of 287 mL/day to each column, and an expected hydraulic residence time of 3.3 days, based upon void volume. The tubing used within the peristaltic pumps was Masterflex 06508-1313 PharMed tubing, and

Masterflex 6404-14 tubing was used for connections between the peristaltic pumps and the water tank, as well as the columns.

### *3.5 Syringe Pump Setup*

A Cole-Parmer syringe pump was used to deliver TCE solution prepared by dilution of TCE-saturated solution to 200 mg/L before drawing it up into gas-tight syringes (Cole-Parmer, Cat. EW-07939-84). Syringes were then loaded onto the syringe pump. To determine the desired TCE concentration in the syringes, we first needed to know the flow ratio between the peristaltic pumps and the syringe pump. For a syringe volume of 10 mL each, and a refill rate of once per week, the flow rate was 10/7 mL/day, while the peristaltic pump's flow rate was set to 287 mL/day. Thus the flow rate of the syringe pump was 1/200 of that of the syringe pumps. Therefore, to achieve an influent TCE concentration of 1 mg/L, the concentration in the syringes should be 200 mg/L. Accounting for partitioning to headspace in the 35-mL serum bottles used (unitless Henry's Law Constant for TCE at 22°C of 0.331), 3.9 mL of TCE-saturated water (1.1 mg/mL) was injected together with 11.1 mL water into each 35-mL serum bottle, capped (Kimble-Chase, PTFE-faced, 20 mm), and aluminum crimp-sealed (Supelco Inc, 200 mm), to achieve 15 mL of 200 mg/L TCE solution. This achieved 15 mL of 200 mg/L solution was used in refilling the syringes. The bottles were inverted on orbital shaker at 120 rpm overnight at 22°C and then set quiescently for two days before use in refilling syringes.

Due to the fact that TCE adsorbs heavily to, passes readily through, and corrodes commonly used rubber tubing and plastic tubing connections

(http://www.coleparmer.co.uk/Chemical-Resistance)

(http://www.silicone.jp/e/catalog/pdf/rubber_e.pdf), the piping system from TCE containing syringes to the columns as well as connections and valves were 316 stainless-steel material. A schematic design of the system is attached in Appendix E.

### *3.6 Gas Chromatography / GC Calibration / Sampling*

Ethene and chlorinated ethenes were quantified on a Perkin Elmer Autosystem gas chromatograph (GC) with an FID (flame ionization detector), with the method modified based on previous studies done on the same GC (Distefano, et al., 1991; Smatlak, et al., 1996). The limits of detection (LoDs) for TCE, cis-DCE, VC and ethene were found by taking three times the minimum peak area that should be counted (it was found to be three times 50 µV*s, which gave 150 µV*s in this thesis research), and corresponding to the calibration curve of each compound. Thus, the LoDs for TCE, cis-DCE, VC and ethene were found to be 0.001, 0.002, 0.0008, and 0.006 µM, respectively. The detection limit for methane was 7.9 µM, as the noise level at the methane-appearing time was high.

Oxygen was quantified with a GC using a thermal-conductivity detector (TCD). For DO measurements, the sampling process as well as standard curve creation in this research aimed to minimize human error. DO is often measured with the use of a DO probe. Due to the low flowrate simulating groundwater flow (287 mL/day) and other design constraints (biofilm accumulation on probes, gas/liquid leak from probe insertion and removal), this method was not chosen. Instead, a GC TCD was used to measure DO by injecting headspace gas above an

equilibrated liquid sample. The GC was equipped with a 3-ft x 1/8-in. column packed with 60/80 Molecular Sieve 5A (Supelco, Inc.), held isothermally at 30$^{o}$C. The GC settings were the same as used by Gossett in a previous study (Gossett, 2010).

The sampling procedure for this column study – for both oxygen and chloroethenes – was to remove 5 mL of liquid from each column sampling port, inject it into a 9-mL glass serum vial which was previously purged with nitrogen, capped with a PTFE-faced serum stopper, and sealed with aluminum crimp. The 9-mL serum bottle was then vigorously shaken by hand for five minutes to reach gas-liquid equilibration at 22°C (required time verified in this thesis research) before two GC headspace injections: the first into the GC TCD for oxygen; and the second into the GC FID for methane, ethene and chlorinated ethenes. The GC injection volumes were each 500 µL.

During the process, every time the needle end came in contact with room air, there was a chance for oxygen to sorb and/or to enter the needle, which can affect the accuracy of the reading, since the level of dissolved oxygen was expected to be measured to a very low level. Furthermore, room air contacting the syringe barrel on the top side (above/behind the plunger) can sorb to the barrel walls and be subsequently introduced into the sample when the plunger is pulled back into that area as new sample is acquired. Thus, the goals for the DO measurement process were: first, to minimize introduction of oxygen into samples and syringe during liquid and gas transfer; second, since human error is unavoidable, try to keep the sampling and analytical movements consistent.

To achieve these two goals, 9 steps were taken to obtain a relatively stable and sensitive DO measurement:

1. Fully purge 9-mL serum bottles and seal with PTFE stoppers and aluminum crimps before use.
2. Purge the 5-mL sampling syringe with nitrogen gas before injecting into mulch columns, by slowly extracting nitrogen gas directly from nitrogen tank and pushing out, repeating three times.
3. Uptake about 1 mL of nitrogen gas in the sampling syringe, and quickly walk to the target sampling port, push out the nitrogen gas before immediately pushing the needle into the sampling port for sampling.
4. Take about 5.5 mL liquid sample, and move the syringe into a fume hood. Push out the extra 0.5 mL liquid into a beaker, and quickly inject the 5 mL liquid into the 9-mL serum bottle.
5. Invert the serum bottle so when pulling out the needle, only a small amount of liquid will squirt out instead of a larger volume of headspace gas, as the pressure inside the 9-mL serum bottle will be about one atmosphere above ambient pressure, after liquid sample has been added.
6. Keep the bottle inverted during the shaking process to avoid headspace gas escaping through the wound on stopper caused by the liquid injection.
7. Load the first 500 µL of headspace gas to GC TCD for oxygen measurement, because after each puncture on the stopper, the high bottle pressure will lead to a short-term

gas or liquid leakage. Since the oxygen measurement required more sensitivity, its measurement took place first.

8. Load the second 500 µL of headspace gas to GC FID for chlorinated compound, methane and ethene measurement.
9. Between sampling events, flush the 5-mL sampling syringe and GC injection syringe in nitrogen gas 10 times, and open, and leave in fume hood for drying.

### *3.7 GC Calibration for Vinyl Chloride (VC)*

During the period of this research, the lab had no pure vinyl chloride tanks with which to calibrate GC readings for VC. Therefore, an estimated VC calibration factor was determined, with details presented in Appendix A.3. For all other analytes, calibration curves were made using standards prepared from the methanol-carried stock solutions, and are shown in Appendix A.

### *3.8 TCE and cis-DCE Sorption Assays*

The sorption capacity of pine bark mulch for TCE and *cis*-DCE was determined by batch experiments. 10 grams of ambient-moisture mulch (natural shape, not ground or washed) was put into 160-mL serum bottles, and 100 mL of tap water was added. Knowing the moisture content of mulch (42% w/w), and assuming the density of mulch being the same as water (1 g/mL), the actual water in each bottle was 104.2 mL (100 mL plus 4.2 mL). The headspace in

each bottle was 50 mL (taking 160 mL total bottle volume and subtracting 100 mL added water and 10 mL mulch). After crimping with aluminum caps, 500 to 2000 micrograms of neat TCE and *cis*-DCE were added using gastight syringes. The sorption tests were conducted separately for TCE and *cis*-DCE, and bottles were incubated for at least 3 days under 25°C to achieve presumed equilibrium (the bottles were monitored after three days of orbital shaking, and again after nine days, using GC to make sure headspace concentrations had stabilized; data not shown). Headspace GC measurements were conducted for each bottle to measure the remaining total amounts of TCE and *cis*-DCE unsorbed, and after being subtracted from the initial total amount of the two compounds added, the amount sorbed was determined. Then, the value of $Qe$ corresponding to each $Ce$ in each bottle can be calculated, based on dry weight of mulch added (5.8 gram in each bottle). The adsorption test results are shown in Section 4.2.

### *3.9 Column Inoculation*

The KB-1™ enrichment culture used for this column study was provided by SiREM Lab of Guelph, Ontario, Canada. It is capable of dechlorinating a range of chlorinated solvents and recalcitrant compounds such as: chlorinated ethenes, chlorinated ethanes, chlorinated methanes, chlorinated propanes, RDX (Royal Demolition Explosive), and chlorofluorocarbons (SiREM: www.siremlab.com/products/kb-1). This mixed culture contains multiple *Dehalococcoides* strains, and also other bacterial groups such as *Geobacter*, fermenters, and methanogens.

A bottle of KB-1$^{TM}$ culture was obtained in July 2013 and was inoculated to the columns in October 2013. With an inoculation ratio of 1:1000 and an original DMC population density of 1.5 x $10^8$ cells/mL (Heavner, 2013), the column had a population density of 1.5 x $10^5$ cells/mL to start up with. To perform 1:1000 dilution to each column having a pore volume of 956 mL, around 1 mL of culture was needed. However, to avoid inaccuracy when evenly distributing this 1-mL culture among seven sampling ports, the culture was first diluted into 10 mL of anaerobic tap water. In this way, the volume of inoculum delivered to each sampling port was around 1.4 mL instead of 0.14 mL. On Day 133, a set of inoculation events was again performed on columns 4 and 5, where the 1-mL culture was mistakenly diluted into 10 mL of aerobic tap water, which was then distributed into each sampling port of the two columns. Thus, instead of being an inoculation, this became an event where 10 mL of aerobic water containing (we presume) dead dechlorinator cells was injected to the two columns. Although the volume injected was only 1/100 of the total column volume, and that mulch was known to have strong and fast removal of dissolved oxygen, this could still have had a negative effect on the dechlorination performance of the two columns, 4 and 5.

### *3.10 Molecular Biology Tools*

#### *3.10.1 DNA Extraction*

Column liquid samples were taken either from sampling ports using 10-mL disposable syringes, or collected from column effluents. 0.5 grams of wet solid mulch samples were taken

from column sampling ports, after the columns were taken offline, lying in a fume hood and with the sampling port stopper removed.

For liquid samples, depending on the sample volume, different times were allowed for centrifugation at maximum speed (7400 *x g*) to pellet the microbial cells. For 10-mL samples, 25 minutes was given, and for 20-mL samples, 40 minutes was given. Supernatant was discarded and pellets suspended with a certain volume of DNA-free water (advised by protocol from DNA Extraction Kit) were stored at -20°C until DNA was extracted. The DNA extraction was done according to the PowerSoil® DNA Isolation Kit instructions (Mo Bio Laboratories).

### *3.10.2 DNA Quantification Method*

DNA samples were quantified using NanoDrop 2000c Uv-vis Spectrophotometer (Thermo Scientific).

### *3.10.3 Primer Design*

A primer set for targeting the *Geobacter* KB1 pceA gene was designed using NCBI Primer Design Tool (http://www.ncbi.nlm.nih.gov/tools/primer-blast/) and was ordered from Integrated DNA Technologies. Primers are shown in Table 3.1 below.

**Table 3.1: Primer sets used in PCR and qPCR, and long amplicon primer sets for qPCR standards, both with sequence and melting temperature shown. Primers in the top half of table are designed for qPCR, and primers in the bottom half were used to create long amplicon standards for qPCR assays.**

| Strains Targeted | Gene ID | Gene Abbreviation | Annotation | qPCR/PCR Primer Sequence (5' - 3') | Melting Temp.(°C) | Amplicon Length(bp) | Reference |
|---|---|---|---|---|---|---|---|
| *Geobacter lovleyi* strain KB1 | glpce1 | PceA | PCE Reductive dehalogenase | TAATGTTGGCGTCATCACTCG (sense) CCCATGTATGAAAGCCTGGGA (anti-sense) | 56 | 233 | this study |
| All DMC strains | DET_DE16S | 16S rRNA | 16S ribosomal RNA | GGAGCGTGTGGTTTAATTCGATGC (sense) GCCCAAGATATAAAGGCCATGCTG (anti-sense) | 58.5 | 270 | Fung, et al., 2007 |
| DMC strains VS and GT; *Dehalococcoides* containing mixed cultures KB-1 and ANAS | DCKB1_96900 | VcrA | VC Reductive dehalogenase | GAAAGCTCAGCCGATGACTC (sense) TGGTTGAGGTAGGTGAA (anti-sense) | 56 | 205 | Waller, et al., 2005 |
| **Strain Targeted** | **Gene ID** | **Gene Abbreviation** | **Annotation** | **Long Amplicon Primer Sequence (5' - 3')** | **Melting Temp.(°C)** | **Amplicon Length(bp)** | **Reference** |
| *Geobacter lovleyi* strain KB1 | glpce1 | PceA | PCE Reductive dehalogenase | GGAGCAAGATGAATTTCCGT (sense) CCATAGCATCGTACGTCATC (anti-sense) | 53 | 626 | this study |
| All DMC strains | DET_DET16S | 16S rRNA | 16S ribosomal RNA | GATGAACGCTAGCGGCG (sense) GGTTGGCACATCGACTTCAA (anti-sense) | 50 | 1377 | Hendrickson et al., 2002 |
| DMC strains VS and GT; *Dehalococcoides* containing mixed cultures KB-1 and ANAS | DCKB1_96900 | VcrA | VC Reductive dehalogenase | CTATGAAGGCCCTCCAGATGC (sense) GTAACAGCCCCAATATGCCAAGTA (anti-sense) | 50 | 1482 | Müller et al., 2004 |

### *3.10.4 End-Point Polymerase Chain Reaction (End-Point PCR)*

The setup of the end-point PCR included the use of 5X Green or Colorless Gotaq® Buffer, PCR Nucleotide Mix, GoTaq® G2 Hot Start Polymerase (all from Promega) and forward and reverse primers (shown in Table 3.1), and followed the general PCR recipe suggested by the manufacturer. Mastercycler gradient thermal cycler (Eppendorf) was used to amplify the PCR products. PCR programs included an initial melt at 95°C for 2 minutes, followed by 40 cycles of 95°C for 45 seconds, annealing temperature for 45 seconds, and 72°C for 1 minute. After the 40$^{th}$ cycle, samples were held at 4°C. Annealing temperatures were optimized for individual primer sets. Positive and negative controls were used in every PCR test. The positive control used KB-1 extracted DNA to ensure positive results, and the negative control used DNA free water to replace DNA in the protocol.

### *3.10.5 Quantitative PCR (qPCR)*

Quantitative PCR was used to quantify the genes of interest (i.e. *Geobacter lovleyi* strain KB-1's *pceA* gene; *vcrA*, the VC reductive dehalogenase from DMC; and the 16S rRNA gene specific to DMC populations). The iQ™ SYBR® Green Supermix (BIO-RAD) was used, and the qPCR took place on the iCycler iQ® Multicolor Real-Time PCR Detection System. The qPCR amplification program set on the computer varies from each activity, but in general, 40 cycles of amplification was followed by a melting curve analysis. To quantify the amplified qPCR product, standards with known DNA concentrations were created using long amplicon standards. These long amplicon standards were generated by the primers in Table 3.1 and they

contain the qPCR target sequences. The qPCR and PCR products were then quantified using NanoDrop (see Section 3.11.2). Three to four standards were placed into each qPCR run, with the concentration range covering the concentration of samples of interest. A standard curve was drawn using the qPCR result of the standards, and all the samples were compared to the standard curve for a quantification of the initial DNA concentration before amplification, which is called starting quantity (SQ, in copies/µL). Unlike End-Point PCR where a gel test was usually followed to examine the amplicon length, at the end of qPCR run, a melting curve analysis was conducted, and, theoretically, DNA segments with similar length and sequence will melt at the same temperature. The melt curves for standards were used for comparison with the melting curve of the samples. If a sample melts at a much lower temperature than standards, primer dimers may have been formed, and if it melts at a higher temperature, non-specific amplification may have happened.

### *3.10.6 Gel Electrophoresis*

For the gel electrophoresis process, a 2% Agarose 0.5xTBE gel was used, and the gel box was connected to the Accu Power power source (VWR Scientific Products) for gel electrophoresis at 100 V. To determine the size of PCR products, low mass DNA ladder (ranging from 2000 bp to 100 bp) was loaded alongside samples. The gel was electrophoresed and then stained using ethidium bromide and imaged on a UV transilluminator (Fisher Scientific).

### *3.10.7 PCR/qPCR product Cleanup*

Before being sent to the DNA sequencing facility, both PCR and qPCR products were cleaned up to remove residual primers and nucleotides and any colored reagents. Two kits were used: USB® ExoSAP-IT® PCR Product Cleanup from Affymetrix,Inc and QIAquick® PCR Purification Kit from QIAGEN. The latter was required to remove SYBR green stain from qPCR products and greendye from the GoTaq Green PCR buffer.

### *3.10.8 DNA Sequencing*

Following cleanup, amplicons were combined with a single primer and submitted to the Cornell DNA Sequencing facility for DNA sequence determination by Sanger sequencing, according to the sequencing facility's instructions. Finch TV software was used to view and trim DNA sequences obtained from the sequencing facility. Trimmed DNA sequences were analyzed using BLAST (http://blast.ncbi.nlm.nih.gov/Blast.cgi) with either the entire nucleotide database (nr) or a database constrained to *Dehalococcoidetes*-associated sequences.

# CHAPTER 4 RESULTS AND DISCUSSION

## *4.1 Column Set-up and Operation*

Six columns were set up vertically, with up-flowing tap water (DO of 7.986 mg/L, pH between 6.5 and 7.5) containing 1 mg/L (7.6 μM) TCE. The detailed design is as described in the Materials and Methods Chapter, and Figure 4.1 is a Google SketchUp model of the column set-up. The columns were labeled 1 to 6 from left to right, with 1 and 2 serving as control columns (never inoculated), and columns 3 to 6 as experimental columns. The entire column experiment, from column operation to GC sampling, was all conducted at room temperature of 22°C.

The timeline of the column operation in Table 4.1 shows major events. Column sampling was done approximately weekly for chlorinated compounds (over the whole experiment) and DO was conducted weekly until anaerobic conditions were confidently established. Sampling for biomass DNA (suspended or planktonic) was conducted five times throughout the experiment. Re-inoculation was conducted (twice, one failed and one successful) to enhance the dechlorination performance by increasing the concentration of the dechlorinators in the columns. Day 212 is the last day of column monitoring for columns 3 and 6. After that, the two columns were taken offline for mulch DNA extraction, and the other two experimental columns kept operating. On Day 297, another round of sampling was performed on columns 4 and 5. The operation of control columns was terminated after the sampling on Day 130, due to pump malfunction.

**Table 4.1: Timeline for column operation.**

| Date | Days | Events |
|---|---|---|
| 11-Sep | 0 | Water flow started through mulch columns. |
| 14-Sep | 3 | TCE additions started. |
| 21-Oct | 40 | Inoculate columns 3, 4, 5, and 6 with 1:1000 KB-1$^{TM}$. |
| 19-Jan | 130 | Control columns were taken offline. |
| 22-Jan | 133 | Unsuccessful re-inoculation to columns 4 and 5. |
| 27-Feb | 169 | Re-inoculated columns 4 and 5 at port 4 with 1:1000 KB-1$^{TM}$. |
| 11-Apr | 212 | Last column GC sampling for columns 3 and 6. |
| 14-Apr | 215 | Took columns 3 and 5 offline for sampling attached growth DNA on mulch. |
| 5-Jul | 297 | Sampling of columns 4 and 5 for chlorinated ethenes and ethene level. |

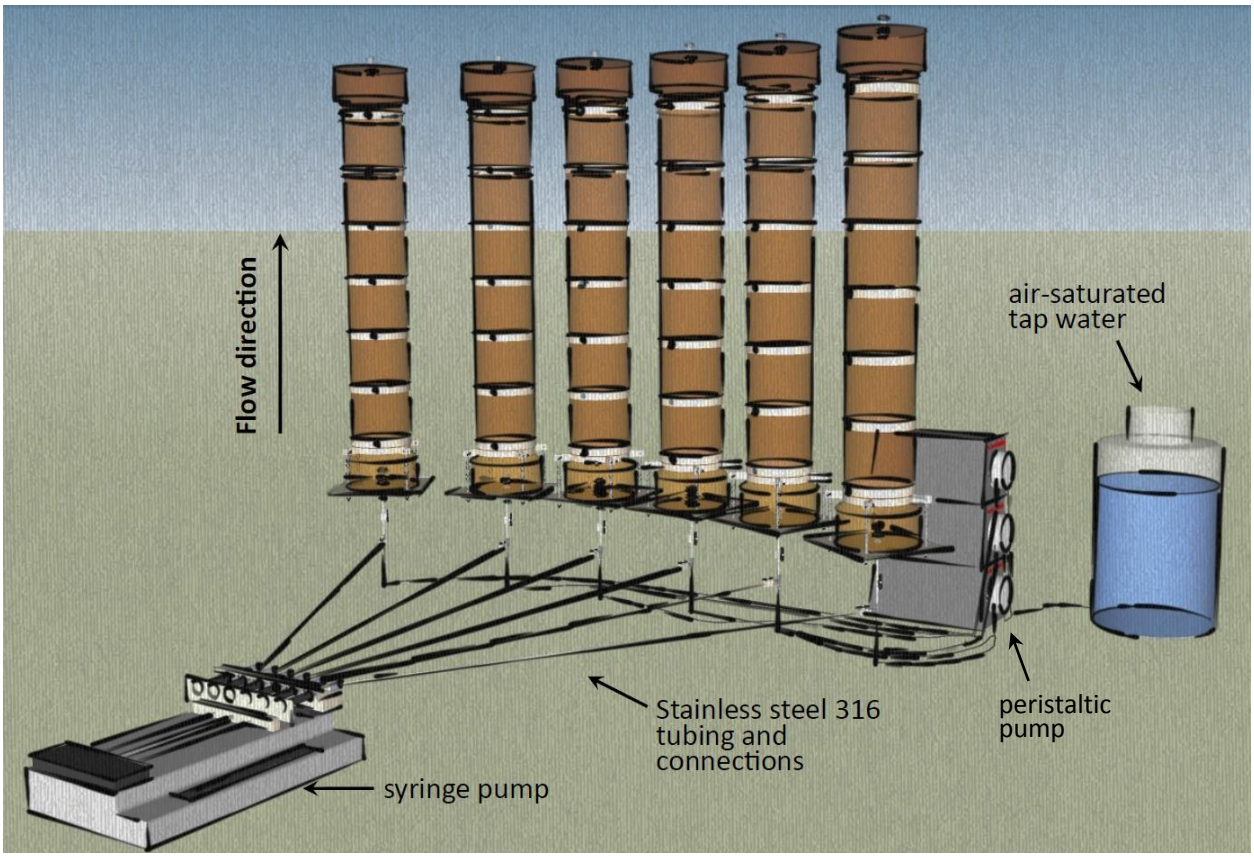


**Figure 4.1: The schematic of the column experiment drawn with Google SketchUp. The mulch placed in the columns is represented by the brown color. The effluent tubes were not drawn, but they were 6 separate tubes that connected the effluent ends of the columns and an opened collection tank sitting in a fume hood.**

### *4.2 Adsorption Assays*

The adsorption capability of mulch for TCE and *cis*-DCE is an important aspect to consider in mulch biobarriers. It retards the mobility of chloroethenes in groundwater, but it also potentially causes problems in data interpretation (i.e., in differentiating chloroethene losses from solution by sorption from losses by biological transformation). High sorbed-TCE concentrations can encourage the attached growth of dechlorinators, which can potentially enhance TCE dechlorination (Seo & Bishop, 2008). The sorption capacities of mulch for TCE and *cis*-DCE were experimentally determined in this study, and compared with published results.

#### *4.2.1 Adsorption Studies with TCE and cis-DCE*

The adsorption assays for TCE and *cis*-DCE were both performed in 160-mL glass serum bottles capped with PTFE-faced serum stoppers and sealed with aluminum crimps. Chunks of pine bark mulch, without any pretreatment (i.e. autoclaving, washing, or grinding) were put into bottles. The experimental method was presented in Section 3.8.

The Freundlich Isotherm was used to fit the adsorption curves (Freundlich, 1906). The Freundlich Isotherm is shown below as Equation 4.1:

$$Q_e = K_f {C_e}^{1/n_f}, \qquad \textbf{Equation 4.1}$$

where $Q_e$ is the ratio of the mass of sorbate and the mass of the sorbent at equilibrium (mg of sorbate/kg of sorbent);

$K_f$ is the Freundlich isotherm constant indicating the tendency of sorption (L/kg);

$C_e$ is the equilibrium concentration of sorbate in the aqueous phase (mg/L);

and $n_f$ is the adsorption intensity constant (unitless).

In circumstances where the concentration of sorbate is low, $Q_e$ is often observed to be directly proportional to $C_e$, thus converting the equation to the linear form $Q_e = K_f C_e$. The results of TCE and *cis*-DCE adsorption assays are shown in Figures 4.2a and 4.2b. The data showed a good fit to a linear isotherm over the sorbate concentrations assayed. As the slope (= the constant $K_f$) for the *cis*-DCE adsorption isotherm (36.4 L/kg) is greater than that of TCE (16.8 L/kg), the adsorption tendency for *cis*-DCE is greater than that of TCE, which is same as reported in Wei and Seo's work (Wei & Seo, 2010). This result is surprising, given that *cis*-DCE has a higher polarity index and is more soluble in water than TCE, and thus should have less affinity for low-polarity organic material, such as mulch.

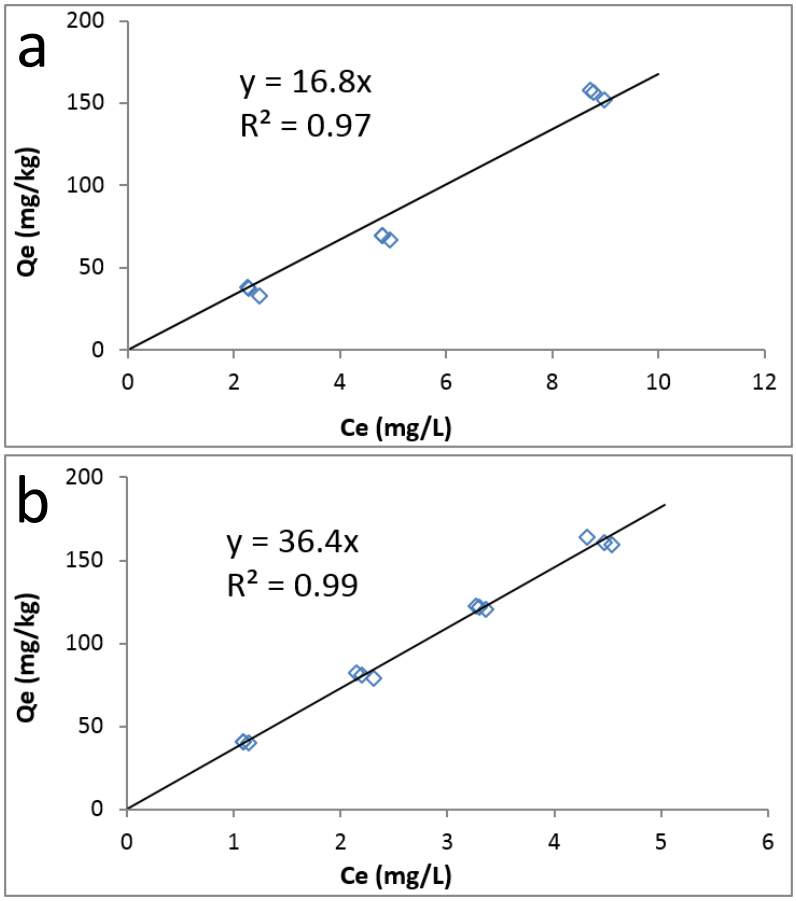


**Figure 4.2: The measured pine bark mulch adsorption isotherms for TCE (a) and *cis*-DCE (b). The blue diamonds are experimental measurements, which are fitted by a first-order adsorption isotherm model. Slopes are equal to the adsorption tendency ($K_f$). Hence, the adsorption tendency for *cis*-DCE is greater than that of TCE.**

### *4.3 Comparison of TCE Adsorption Isotherm with Other Studies*

Several column studies by previous researchers have also included assays for TCE adsorption and the retardation of TCE. Shen and Wilson (Shen & Wilson, 2007) found the $K_f$ of plant mulch with TCE to be 21 L/kg. Their assay was based on a TCE concentration range of around 0.3 to 2 mg/L (2.28 to 15.2 µM), which was in the low range and was fit with a linear

isotherm. Wei and Seo (Wei & Seo, 2010) used 50 mg/L TCE (380 µM) for conducting an adsorption assay, and found $K_f$ of 0.292 L/kg for pine mulch. Since Wei and Seo's test was undertaken in a high TCE concentration range, it was not fit as a linear Isotherm ($n_f$ found to be 1.26) and cannot be directly compared to this thesis study. Öztürk et al. (Oztürk, Tansel, Katsenovich, Sukop, & Laha, 2012) used eucalyptus mulch as their biobarrier medium and reported $K_f$ to be 10.6 L/kg, across a TCE concentration range between 0.3 to 0.8 mg/L (2.28 to 6.08 µM). The $K_f$ of 16.8 L/kg from this thesis study is between the two reported values from Shen and Wilson's study (21 L/kg) and Öztürk et al.'s study (10.6 L/kg).

### *4.4 Breakthrough of TCE in a Pine Bark Mulch Biobarrier Column*

#### *4.4.1 Predicted Breakthrough*

Once the adsorption isotherms for TCE and *cis*-DCE were determined, the adsorption capacity of the designed mulch biobarrier could then be estimated, as could the speed of the adsorption front in the columns and the time to TCE-breakthrough. The speed of the adsorption front is the speed at which the constant pattern of the adsorption front (see Figure 4.3) moves through the column. The *time of breakthrough* is defined by the time it takes for 50% of the influent sorbate concentration to reach the end of the column. Equations 4.2 and 4.3 *are the speed of the adsorption* front and *time of breakthrough* equations, respectively. Figure 4.3 is the conceptual presentation of the adsorption front in a column.

$$S = \frac{U_{superficial} C_0}{\varepsilon C_0 + \rho_b Q_e}, \qquad \textbf{Equation 4.2}$$

where $S$ = speed of the adsorption front (cm/day);

$U_{superficial}$ = superficial velocity of the approaching groundwater (cm/day);

$C_0$ = contaminant concentration in groundwater entering the column (mg/L);

$\varepsilon$ = biobarrier porosity;

$\rho_b$ = bulk density of adsorbent in the biobarrier (kg/L);

and $Q_e$ = sorbed concentration in equilibrium with $C_0$ (mg/kg).

$$T = \frac{X}{S}, \qquad \textbf{Equation 4.3}$$

where $T$ = time of breakthrough (days);

$X$ = column height or biobarrier thickness (cm);

and $S$ = speed of the adsorption front (cm/day).

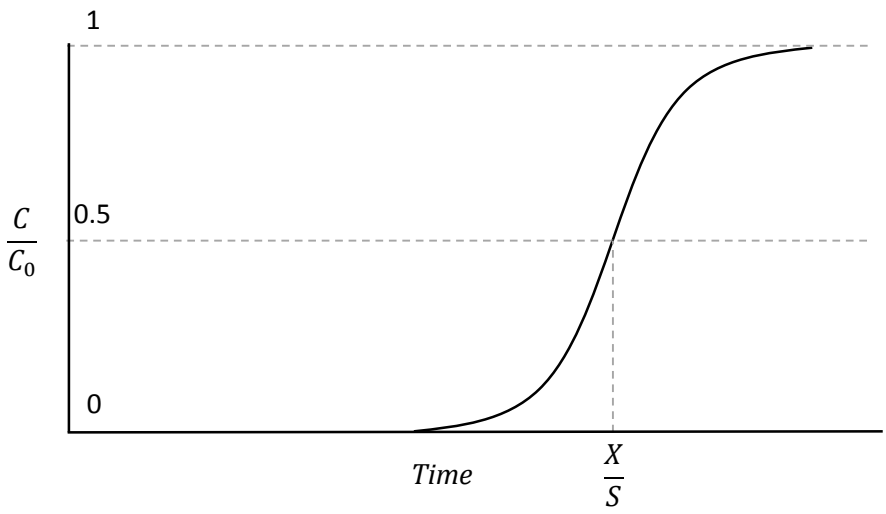


**Figure 4.3: A conceptual presentation of the adsorption front. The time of breakthrough is shown as X/S, where X is the height of the column, and S is the speed of the adsorption front. C is the aqueous phase concentration leaving the column at any given time.**

Using the superficial velocity of 14 cm/day, porosity of 0.78, TCE concentration of 1 mg/L, an assumed bulk density of mulch of 1 kg/L (since mulch has high void ratio, and was soaked with water), and the adsorption capacity ($Q_e$) of 16.8 mg/kg per 1 mg/L of TCE, the speed of the adsorption front for TCE is calculated via Equation 4.4:

$$S = \frac{U_{superficial} C_0}{\varepsilon C_0 + \rho_b Q_e} == \frac{14\frac{cm}{d} \times 1\frac{mg}{L}}{0.78 \times 1\frac{mg}{L} + 1\frac{kg}{L} \times 16.8\frac{mg}{kg}} = 0.80\,\frac{cm}{d} \qquad \textbf{Equation 4.4}$$

The predicted time of breakthrough can then be calculated via Equation 4.5:

$$Time\ of\ breakthrough = \frac{column\ height}{speed\ of\ adsorption\ front\ (S)} = \frac{60cm}{0.80\frac{cm}{d}} = 75\ days \qquad \textbf{Equation 4.5}$$

### *4.4.2 Observed TCE Breakthrough*

Prior to inoculation, water with 1 mg/L TCE was pumped through the columns and TCE in the column pore water at different depths was monitored with time, with results shown in Figure 4.4. Note that the peristaltic pump delivering tap water to column 2 malfunctioned on Day 15, and as a result the TCE concentration built up. Thus, the data from column 2 were not taken in consideration when finding the observed time of breakthrough. Note that in Figure 4.4, the TCE concentration never reached the calculated influent concentration of 7.6 µM (in another words, the $C/C_0$ never reached 1, in Figure 4.3), except for the first sampling port on column 3 on Day 43. Besides this, an "S" shaped adsorption front was not formed in the columns. These two observations imply that the sorption mechanism in the mulch column is a very slow and complex process. Due to time limitation, the sorption test was only given 40 days, before an estimation of the speed of the adsorption front was made. If the predictions were correct, half the influent concentration of TCE (half of 7.6 µM is 3.8 µM) should be seen exiting the column at Day 75. However, the actual speed of the adsorption front was faster. For example, the effluent concentration (represented by the values from sampling port 7, which is 1 cm from the end of the column) for the four experimental columns all exceeded the expected breakthrough concentration by Day 43 (the two control columns were not sampled on Day 43), indicating a faster actual speed of the adsorption front. Besides the complex diffusion processes in the column, another reason could be short circuiting in column flow, where the flow chose a preferred pathway instead of using the entire cross-sectional area. This would increase the superficial velocity in some regions, and increase the speed of the adsorption front.

The observed time of breakthrough can be determined by selecting a distance into the column (a sampling port) and determining the time it took for the TCE concentration at this point to reach half of influent concentration. Sampling ports 5 on all the columns were chosen, and found that by Days 36, 39.5, 43, 43, and 32.5, columns 1, 3, 4, 5 and 6 reached half TCE influent concentration. Day 39.5 on column 3 and Day 32.5 on column 6 were average values since no data point directly fell on the dashed line. Averaging across columns, it took 38.8 days for the concentrations at port 5 (37 cm into the columns) to exceed 3.8 µM TCE.

With an averaged time of breakthrough of 38.8 days from TCE entering the column to passing sampling port 5 (37 cm into the column), the actual speed of adsorption front was estimated to be 0.95 cm/day using Equation 4.5 compared to the theoretically calculated 0.80 cm/day. Then, the actual time of breakthrough for the full length of the columns was found using Equation 4.5 to be 63 days. The retardation factor calculated using Equation 4.6 below was 14.7.

$$Retardation\ Factor = \frac{superficial\ velocity\ of\ water}{speed\ of\ adsorption\ front} = \frac{14\,^{cm}/_{day}}{0.95\,^{cm}/_{day}} = 14.7 \qquad \textbf{Equation 4.6}$$

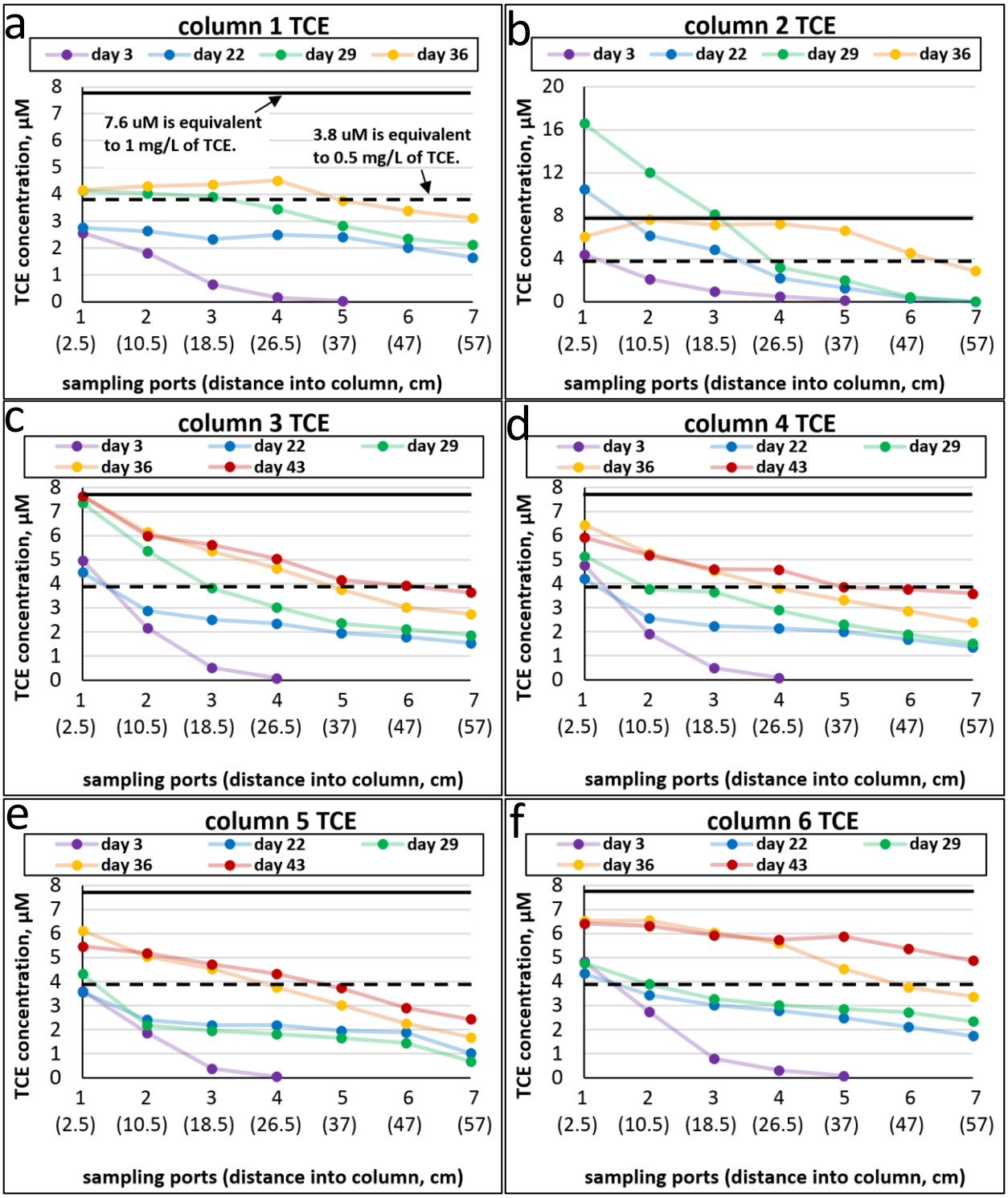


**Figure 4.4: TCE concentration profiles over time in the six columns following introduction of TCE. The connected dots with colors of purple, blue, green, yellow and red correspond to Days 3, 22, 29, 36 and 43 measurements of TCE concentration in pore water from each sampling port of the six columns. The bold black horizontal line indicates the influent TCE concentration of 7.6 µM, and the dashed line indicates 50% of influent TCE concentration of 3.8 µM.**

### *4.5 Dissolved Oxygen Levels in Columns*

#### *4.5.1 GC Calibration Curve for Dissolved Oxygen*

Following the methods described in Section 3.6, a GC TCD oxygen calibration curve was created (see Figure 4.5). As can be seen in Figure 4.5, this method had a high LoD, which was not caused by the sensitivity of the instrument for oxygen, but the amount of oxygen introduced into the 9-mL bottles during the sample preparation. The TCD was sensitive enough that the readings of pure nitrogen gas injected had peak heights between 18 to 26 (shown in Table B.1 in Appendix B.1). The background readings for supposed, zero-oxygen-added bottles were significant (Peak heights had an average of 63.9 µV and a standard deviation of 14.5 µV). This was due to the limitation of the experimental design. The detection limit was calculated to correspond to a peak height of 107.5 µV (as shown by dashed line in Figure 3.3, and calculation shown in Appendix B.2), which corresponds to a rather high DO concentration of around 5 mg/L – not low enough to be of much use in determining anoxia in columns.

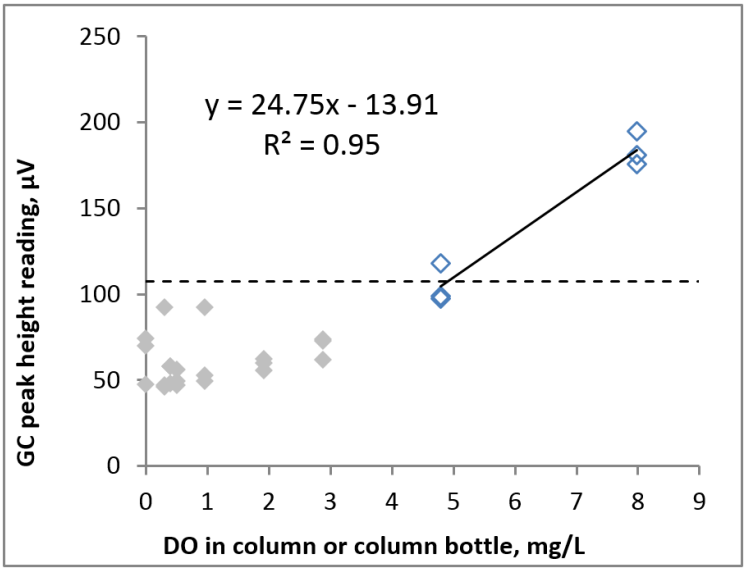


**Figure 4.5: Calibration curve for dissolved oxygen levels constructed with the consideration for the GC-TCD method's detection limit (shown as dashed line). The straight line only fits the blue diamonds, and the grey diamonds are values below detection limit, which were not used for the calibration curve.**

### *4.5.2 Dissolved Oxygen Level in Columns*

DO levels were monitored using the method described in Section 3.6. Table 4.2 contains the GC peak height readings for DO monitored in columns. Based on the detection limit of 107.5 µV (ca. 5 mg/L DO), most readings were below the detection limit. The readings above the detection limit were labeled either with red text or with a star, as shown in Table 4.2. The values labeled with a star were considered measurement errors, as they either exceeded the oxygen solubility limit of 7.986 mg/L (calculated using local atmospheric pressure and room temperature of 22°C), or they were measurements in the middle of the columns with lower readings upstream from them (It is assumed that the DO can only decrease along the column due to oxygen consumption.). In this way, the only real measurement value that isn't excluded as erroneous was on Day 43 for the first sampling port of column 6 (highlighted in red text).

As shown in Table 4.2, the majority of samples had oxygen levels below the detection limit of the method (corresponding to approximately 5 mg/L of oxygen). Since the detection limit was quite high, the establishment of anaerobic conditions could not be confirmed from GC TCD readings alone. However, it is known from Runtian Yang's research (Yang R. , 2014) that aqueous DO gets consumed quickly after coming in contact with pine bark mulch. Given that DO levels in sampling port 1 measured below detection limits in the majority of measurements, for all columns, and that DO levels would only decrease from sampling port 1 onward, we felt confident that anaerobic conditions were established in at least the latter portions of the columns. Therefore, inoculation of four of the columns was performed on Day 40.

**Table 4.2: Column DO measurements as peak height (corresponding DO concentration if peak height above 107.5 µV) from Days 3 to 43. Sampling ports 1 to 7 are consecutive ports located from influent end to effluent end. The only credible measurement obtained was column 6 port 1 reading on Day 43 shown labeled in red. The readings shown as "-" mean that the DO samplings were not taken.**

| Column no. | Sampling port no. | GC peak height reading in µV (DO concentration in mg/L) | | | | |
|---|---|---|---|---|---|---|
| | | Day 3 | Day 15 | Day 22 | Day 29 | Day 43 |
| 1 | 1 | 34.7 | 79.8 | 80.5 | 44.3 | - |
| | 2 | 36.3 | 48.4 | 37.5 | 159.7 (6.8)* | - |
| | 3 | 36.6 | 51.4 | 38 | 49.3 | - |
| | 4 | 42.1 | 70.9 | 48.8 | - | - |
| | 5 | 47.6 | 308 (14.0)* | 43.2 | - | - |
| | 6 | 43.7 | 49.1 | 42 | - | - |
| | 7 | 45 | - | - | - | - |
| 2 | 1 | 34.2 | 225.5 (10.0)* | 46.7 | 41.3 | - |
| | 2 | 46.3 | 62.9 | 79.5 | 111.4 (4.5)* | - |
| | 3 | 43.1 | 61.7 | 44.2 | 43.3 | - |
| | 4 | 39.6 | 56.3 | - | - | - |
| | 5 | 51.1 | 70.7 | - | - | - |
| | 6 | - | 65.9 | - | - | - |
| | 7 | - | - | - | - | - |
| 3 | 1 | 212.6 (9.4)* | 58.5 | 97.9 | 65.8 | 53.8 |
| | 2 | 63.1 | 94.7 | 49.4 | 69 | 80.4 |
| | 3 | 36.6 | 52.8 | 59.7 | 242.7 (10.8)* | 66.9 |
| | 4 | 65.7 | 107.4 (4.3)* | - | - | 46.5 |
| | 5 | 35.4 | 184.3 (8.0)* | - | - | 53.1 |
| | 6 | - | 50.3 | - | - | - |
| | 7 | - | - | - | - | - |
| 4 | 1 | 35.1 | 45.3 | 183.3 (8.0)* | - | 95.9 |
| | 2 | 114.6 (4.6)* | 58.6 | 51.7 | - | 49.4 |
| | 3 | 40.5 | 72.5 | 68.2 | - | 47.2 |
| | 4 | 37.4 | 50.7 | - | - | - |
| | 5 | 39.3 | 246.6 (11.0)* | - | - | - |
| | 6 | - | 56.9 | - | - | - |
| | 7 | - | - | - | - | - |
| 5 | 1 | 37.5 | 56.7 | - | - | 54 |
| | 2 | 36.9 | 68.9 | - | - | 94.4 |
| | 3 | 37.3 | 57.4 | - | - | 58.9 |
| | 4 | 57.2 | 77.9 | - | - | 61.6 |
| | 5 | 41.7 | 81.7 | - | - | - |
| | 6 | 37.9 | 45.5 | - | - | - |
| | 7 | 37.1 | - | - | - | - |
| 6 | 1 | 42.1 | 56.8 | - | - | 177.2 (7.7) |
| | 2 | 40.4 | 51.4 | - | - | 57.6 |
| | 3 | 33.8 | 41.5 | - | - | 49.5 |
| | 4 | 38.5 | 40 | - | - | 45.9 |
| | 5 | 55.4 | 50.5 | - | - | - |
| | 6 | 45.5 | 76.7 | - | - | - |
| | 7 | 29.3 | - | - | - | - |

*Readings above the detection limit but suspected of error because either the calculated DO is above solubility limit or because an earlier port showed DO below detection.

### *4.6 Column Performance*

#### *4.6.1 Column Performance Shown at Important Time Points*

The experimental columns' dechlorination performances (columns 3 to 6) were continuously monitored following inoculation on Day 40. The control columns (columns 1 and 2) were suspected of contamination on Day 58 sampling, because *cis*-DCE was found in the effluent ends of the columns. The details are presented at the end of this section. Aqueous concentrations of TCE and its dechlorination daughter products (*cis*-DCE, VC and ethene) are shown in Figures 4.6 through 4.11, for selected, significant time points. The full concentration data are shown as 3-D plots in Figures 4.12 through 4.15.

Figure 4.6 presents the chlorinated ethenes' concentrations on Day 36 for all the six columns, 4 days before inoculation. Since no *cis*-DCE was observed on any columns within this 36 days, no natural attenuation appeared to be occurring.

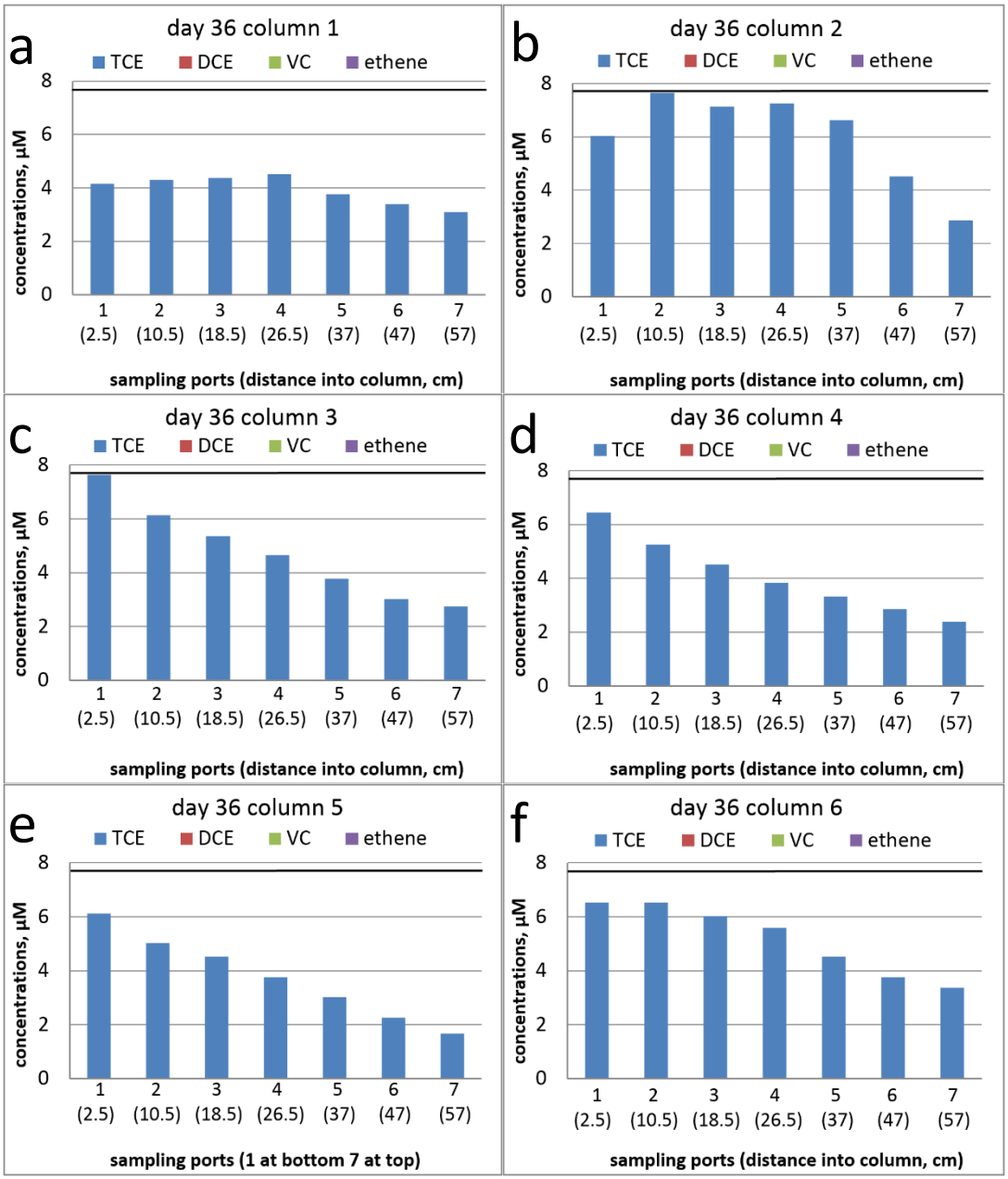


**Figure 4.6: Chlorinated ethene concentrations on Day 36, 4 days before inoculation of columns 3 to 6 on Day 40. Only TCE was observed, meaning no natural attenuation occurred. The black line indicates the influent TCE concentration at 7.6 µM.**

Three days after inoculation, *cis*-DCE was detected in inoculated columns, as shown in Figure 4.7. Note that the stacked-bar charts used in this section are intended to show dechlorination performance as well as chlorinated ethene mass balances (in µM), as the colored bars representing each chlorinated ethene are stacked onto one another. The appearance of *cis*-DCE at the second sampling port of column 3 and the third sampling port of columns 4, 5 and 6 reflect that the DO level was low enough for reductive dechlorination to occur, at least from the third sampling port on. Note that slightly more *cis*-DCE was produced from columns 3 and 6 than from 4 and 5. Possible explanations would be: 1) the DO in columns 4 and 5 was higher than in columns 3 and 6 during inoculation, which could kill a portion of the

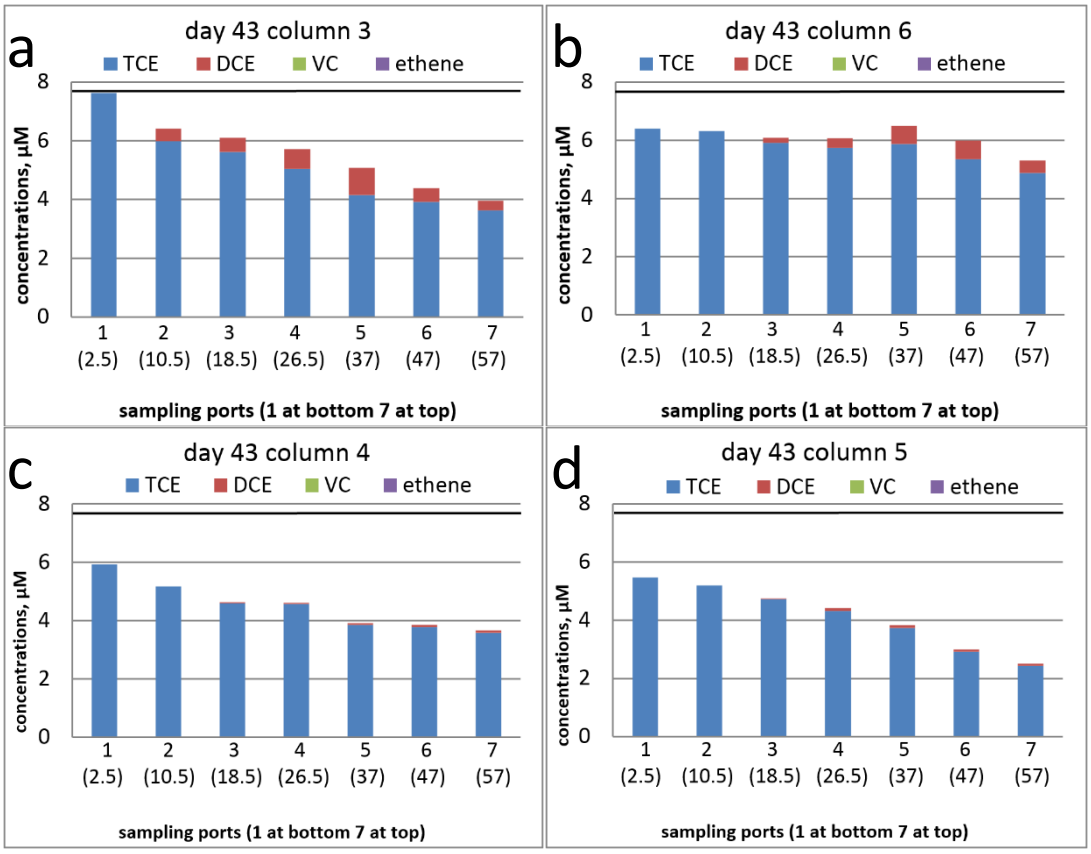


**Figure 4.7: Chlorinated ethene concentrations on Day 43 for the four inoculated columns. On Day 43, which was three days after inoculation, *cis*-DCE was detected in all inoculated columns. The blue bar is TCE and red is *cis*-DCE. No VC or ethene was detected at this time.**

dechlorinators in columns 4 and 5, and cause the slower start; 2) columns 4 and 5 had oxygen slowly leaking in from the seals or sampling ports; or 3) the KB-1$^{TM}$ culture inoculated to columns 4 and 5 happened to contain fewer robust cells.

Eight days after inoculation, low levels of VC were found in three of the four inoculated columns, as shown in Figure 4.8. The high *cis*-DCE concentration observed at the effluent ends of columns 3 and 6 (above 7.6 µM as depicted by Figure 3.7 (a) through (d)) may be because when the aqueous phase TCE was dechlorinated, the adsorbed TCE started to desorb, and also dechlorinated. As a result, *cis*-DCE concentrations higher than influent TCE were observed, but only for a short period of time, until all the TCE desorbed from mulch (data not shown, but the trend can be seen in 3-D, Figures 4.12 through 4.15).

From Day 48 on, the levels of VC in the four inoculated columns almost doubled by Day 102 (data not shown), from 0.01 to 0.02 µM, suggesting a very low growth rate or poor health of the *Dehalococcoides*. However, from Day 102 to Day 130 (Figure 4.9), the levels of VC in columns 3 and 6 increased from 0.02 to around 0.33 µM. The VC levels for columns 4 and 5 also increased from 0.01 to around 0.05 µM during this time. Also on Day 130, which was 90 days after inoculation, trace amounts of ethene were observed in all the four inoculated columns.

Note that from Figures 4.8 through 4.11, a line chart with the concentration of each chlorinated ethene was added next to every stacked-bar chart, to better display the trends of individual chloroethenes along the length of the columns.

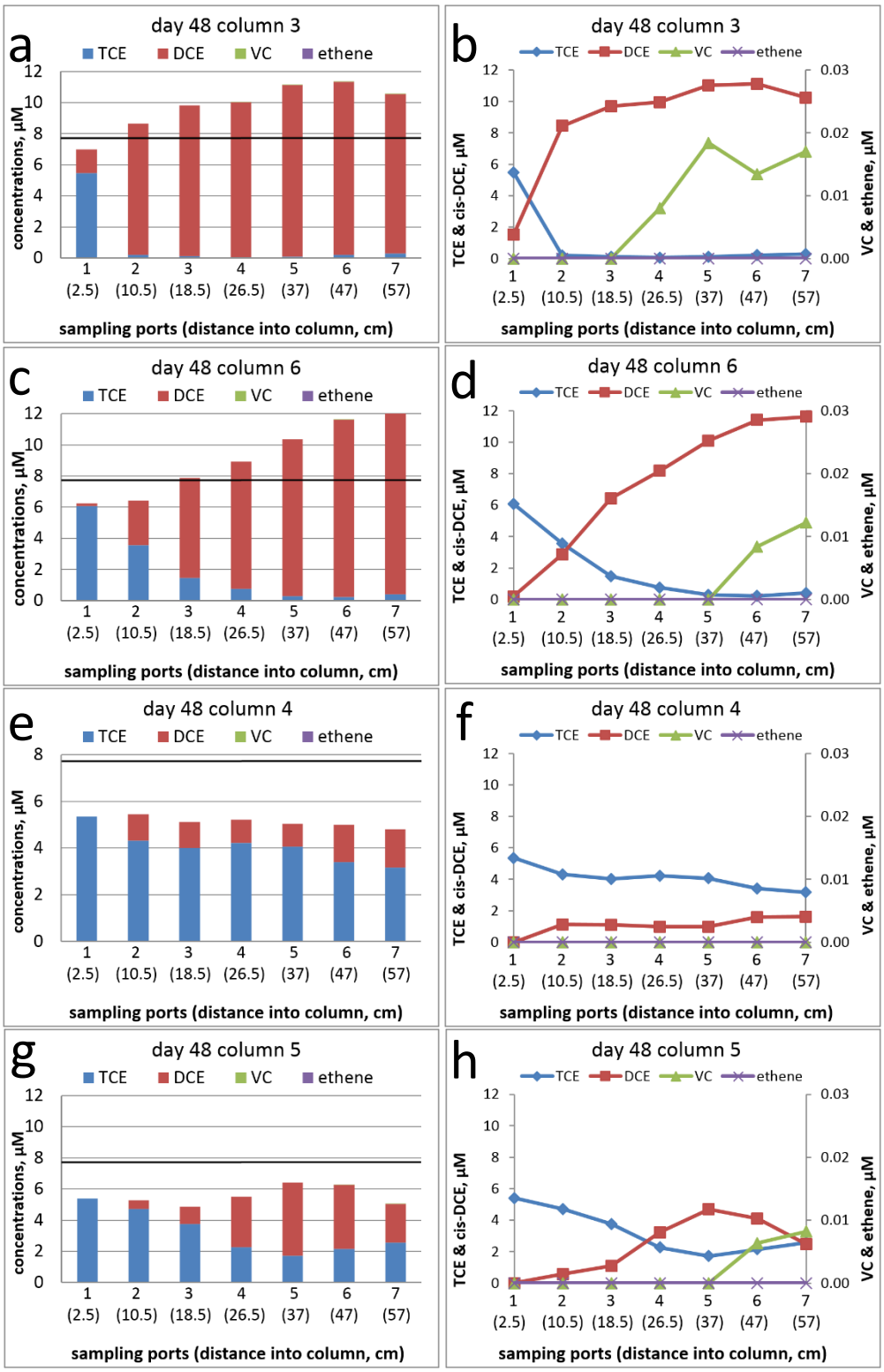


**Figure 4.8: Chlorinated ethene concentrations on Day 48 for the four inoculated columns 3 to 6. Eight days after inoculation, VC was detected for the first time in columns 3, 5 and 6. Column 4 showed VC on Day 51. Note that VC and ethene are plotted on a different concentration scale because their detected levels were very low compared to TCE and *cis*-DCE.**

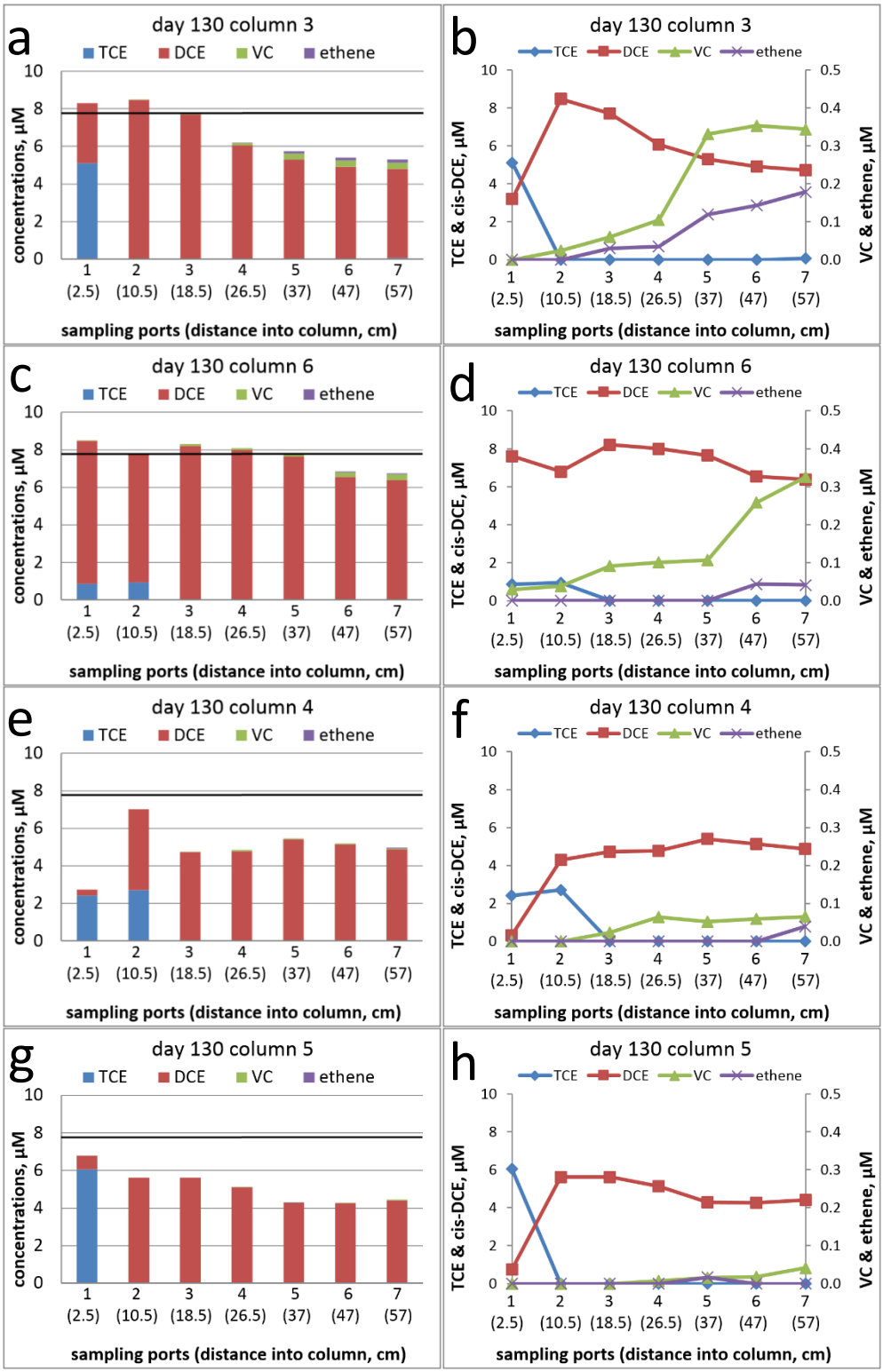


**Figure 4.9: Chlorinated ethene concentrations on Day 130 for the four inoculated columns 3 to 6. Columns 3 and 6 had better performances than 4 and 5, as more VC and ethene were produced.**

As seen in Figure 4.10, on Day 212, almost complete dechlorination (99% of the total amount of TCE and its daughter products at sampling port 7 was ethene) was achieved in column 3, and 73% was achieved in column 6. The other two inoculated columns 4 and 5 did not perform this well, with 29% and 4% dechlorination completion (ethene level) achieved, but the continuous improvement in performance was noticeable.

Although the performances of columns 4 and 5 were lower than those of columns 3 and 6 throughout the experiment, they started to produce VC and ethene about the same time as column 3 and, and the continuous increase in concentrations of VC and ethene was apparent. After the failed re-inoculation performed on Day 133 (as described in Section 3.9) which could potentially cause even poorer health to the dechlorinators in columns 4 and 5, another re-inoculation was made to columns 4 and 5 on Day 169, with a small volume of undiluted KB-1$^{TM}$ culture injected into sampling port 4 (in the middle of column, where anaerobic conditions were assumed to be well developed) to create another 1:1000 inoculation. A small boost of VC and ethene concentration was observed, even though they did not catch the pace of columns 3 and 6. The re-inoculation effect can be seen in Figures 4.14 and 4.15, the 3-D dechlorination progress charts for columns 4 and 5.

On Day 297, which is almost three months after the end of the continuous monitoring (ended on Day 212), another set of measurements was taken for columns 4 and 5. The two columns were continuously operated throughout the whole period. As shown in Figure 3.10, both columns 4 and 5 have achieved almost complete dechlorination in column effluents, with

99% and 95% completion, respectively. Overall, complete dechlorination (95% to 99%) was achieved in all inoculated columns within 10 months.

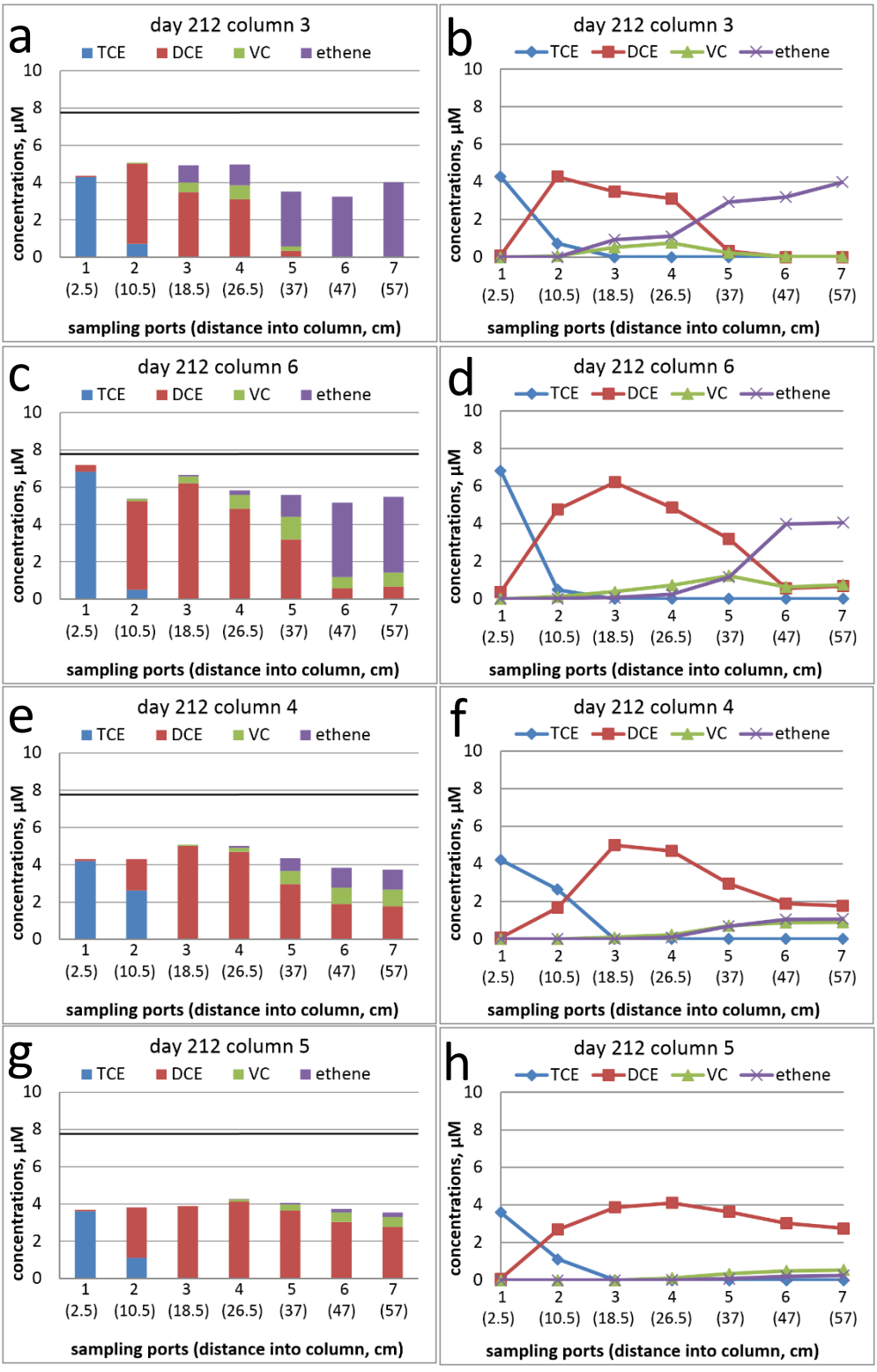


**Figure 4.10: Chemical concentrations on Day 212 for the inoculated columns 3 to 6. Almost complete dechlorination (99%) was observed in column 3, 73% achieved in column 6, 29% achieved on column 4, and 4% achieved in column 5.**

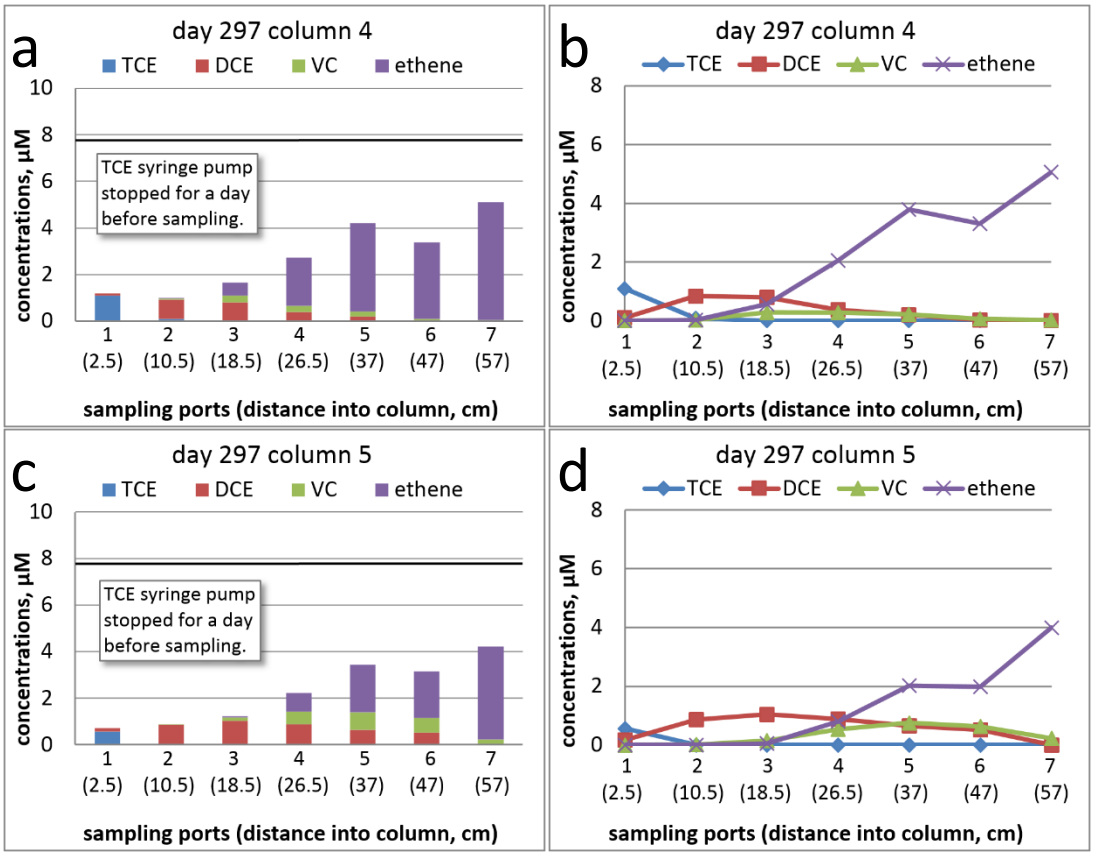


**Figure 4.11: Chemical concentrations for columns 4 and 5 on Day 297. The two columns achieved 99% and 95% completion in dechlorination, respectively. The poor mass balance at the front half of the columns was because the syringe pump for delivering TCE was stopped accidentally for a day.**

### *4.6.2 Mass Balance in TCE and its Daughter Products in Columns*

The stacked-bar charts from Figures 4.8 to 4.11 were used because they show the sum of moles of TCE and its daughter products at each sampling port. Theoretically, the summation of TCE and its daughter products should be close to influent TCE concentration of 7.6 µM for measurements of each sampling port, since the conversions of TCE to *cis*-DCE, *cis*-DCE to VC, and VC to ethene all occur as one-to-one molar ratios. However, this was not fully achieved. Even if taking sorption into account, a 7.6 µM of the summation of chlorinated ethenes should have been reached at least in the lowest few sampling ports, given a long operation time, such as 100 to 200 days. However, the mass balance became worse with time, as seen in Figures 4.8 to 4.11.

The most likely reason was that the actual TCE concentration entering the bottom of the columns was not the assumed, 7.6 µM, especially in later portions of the experiment. A possible explanation is that TCE in the syringe of the syringe-pump system partially escaped, although whether through evaporation from the syringes, or somewhere else in the stainless-steel piping system is unknown. This would explain why the mass balance got worse with time, since erosion of stainless steel and tightness of the tubing connections might have worsened with time.

The second reason for observed lack of mass-balance, which is particular for this thesis study, is that the calibration curve for VC was rather crudely estimated, with method shown in Appendix A.3. This could have caused a systematic under-estimation of the VC concentration in the column, which led to the lack of mass balance in stacked-bar charts, although this should

not be the only reason, as poor mass balance was found in many instances where VC was not produced. Additionally, aerobic pathways could be contributing to loss of the chlorinated ethenes. The products of aerobic degradation (e.g. $CO_2$ and $Cl^-$) were not monitored in our study. Aerobic VC oxidation has been shown by Gossett (Gossett, 2010) to be feasible even at very low oxygen levels. It is also possible that mulch contributes suitable substrates to support co-metabolic aerobic oxidation of TCE in the influent ends of the columns. Molecular-biological analysis of the communities in the aerobic, influent portions of the columns could have been designed to look for presence/expression of relevant markers of aerobic dechlorination.

### *4.6.3 The Overall Column Performance, as Shown in 3D Charts*

In this section, a 3-D view of dechlorination performance is presented for each of the four inoculated columns. This includes all the GC FID samples measured from each sampling port (1 at bottom, close to inflow, and 7 at top), from Day 3 to Day 212 for columns 3 and 6, and from Day 3 to Day 297 for columns 4 and 5. Figures 4.7 to 4.11 previously presented TCE and its daughter products' concentrations at selected time points, while this set of 3-D Figures presents a "full picture" of the entire column experiment.

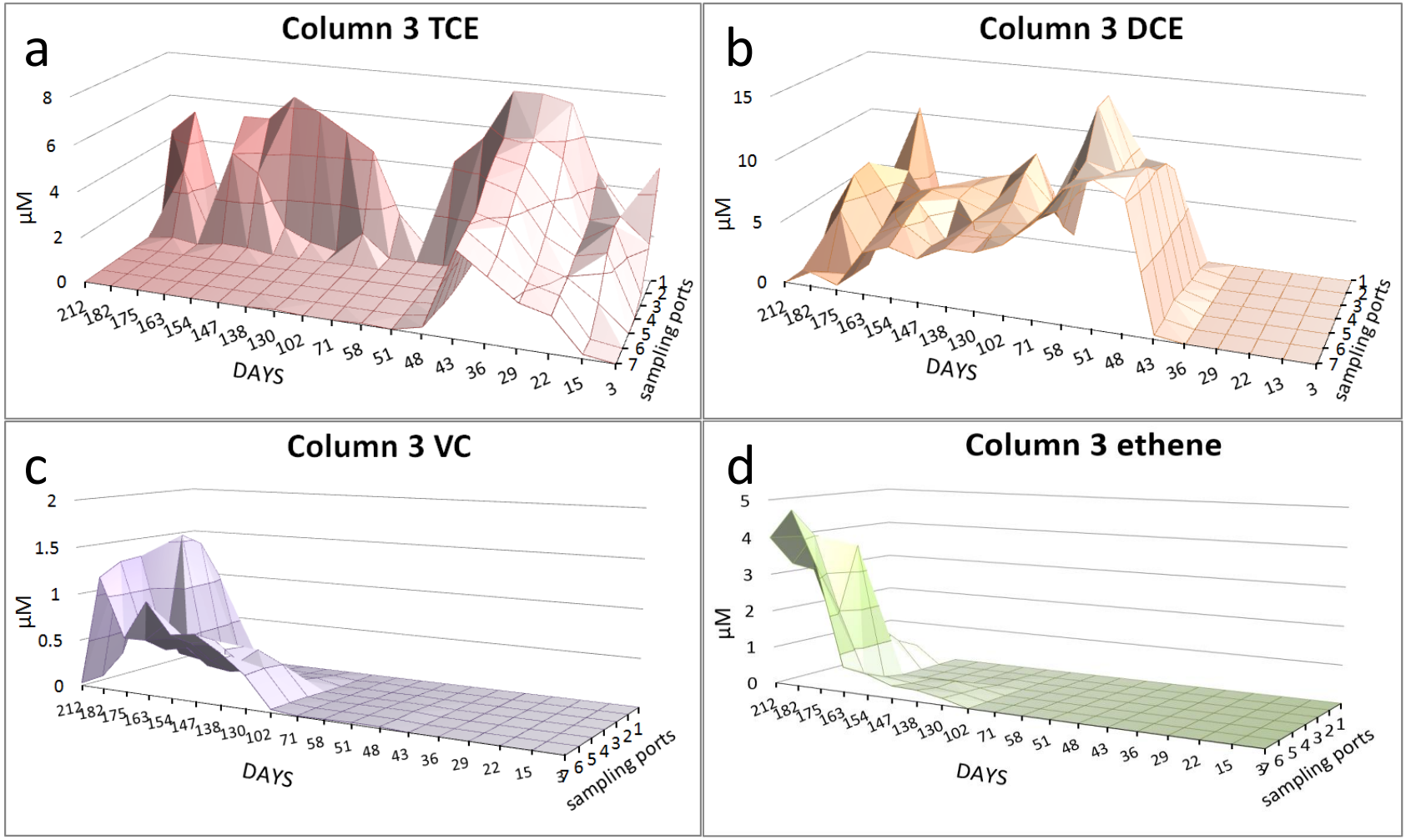


**Figure 4.12: The aqueous-phase chemical concentrations for column 3, starting from Day 3 (three days after TCE and water started to flow in) to Day 212. Column 3 was inoculated with KB-1™ on Day 40 at a dilution of 1:1000. After Day 102, VC and ethene were rapidly produced, and the column reached almost complete dechlorination (99%) by Day 212.**

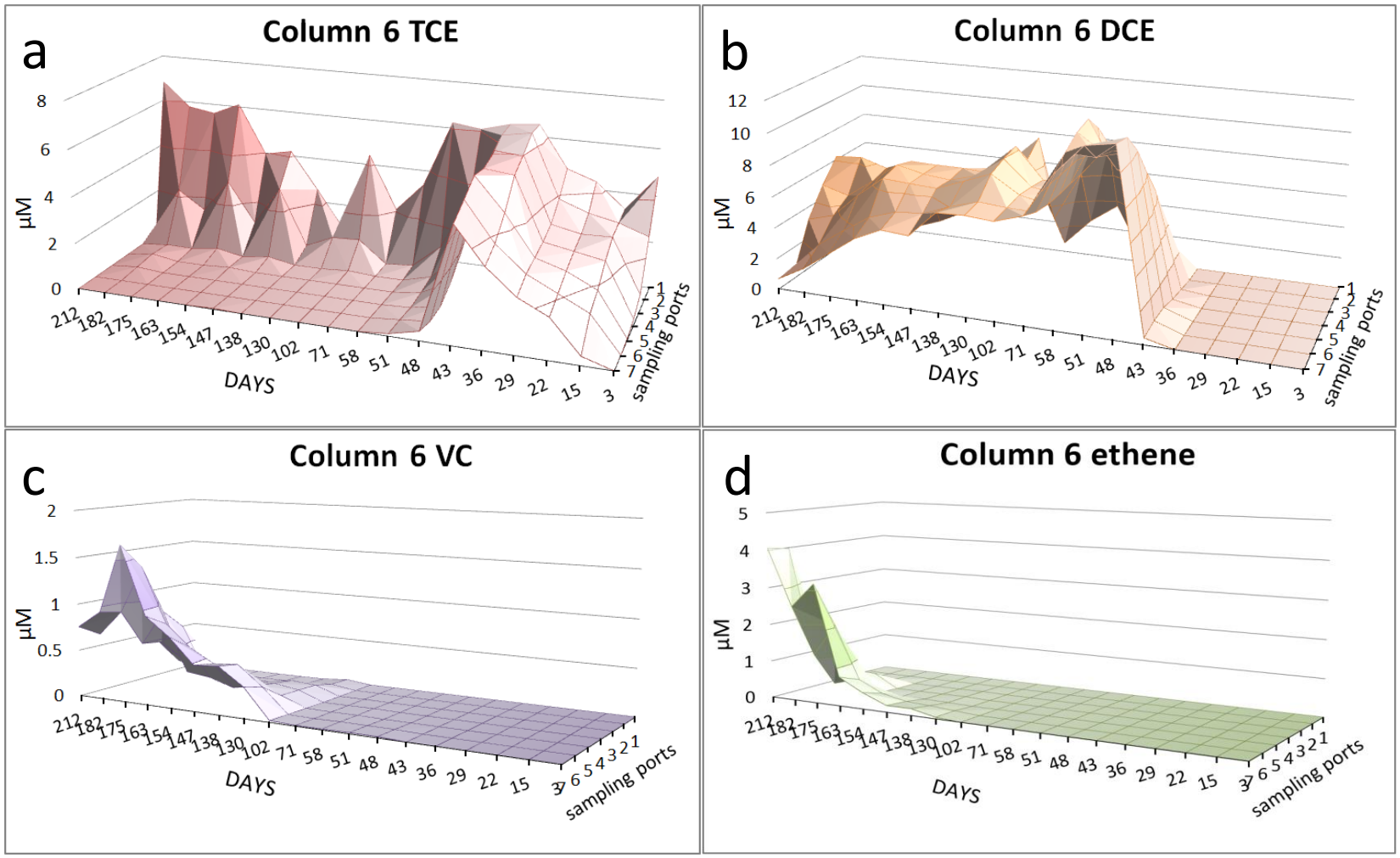


**Figure 4.13: The aqueous-phase chemical concentrations for column 6, starting from Day 3 (three days after TCE and water started to flow in) to Day 212. Column 6 was inoculated with KB-1™ on Day 40 at a dilution of 1:1000. After Day 102, VC and ethene were rapidly produced, and the column reached 73% complete dechlorination by Day 212.**

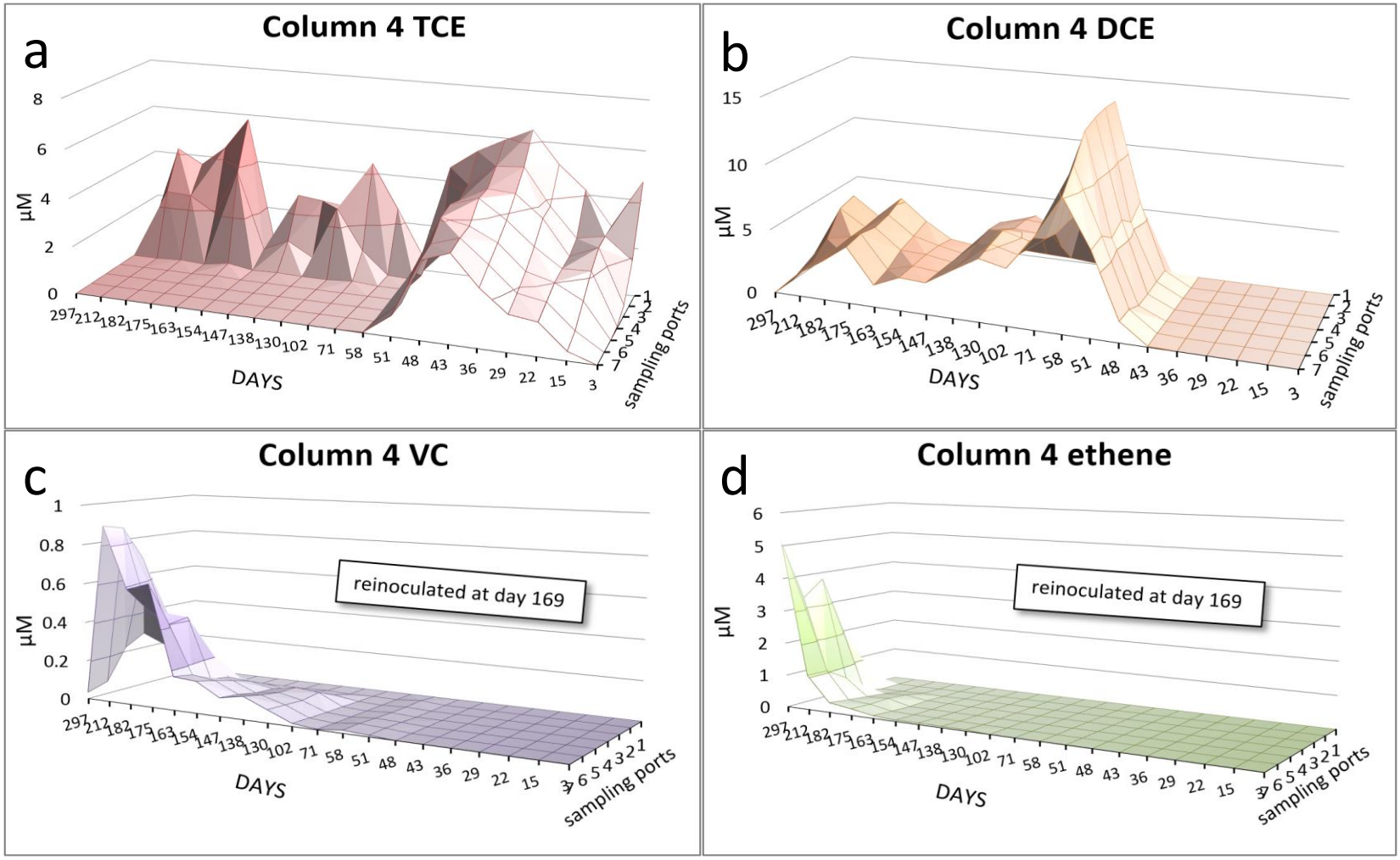


**Figure 4.14: The aqueous-phase chemical concentrations for column 4, starting from Day 3 (three days after TCE and water started to flow in) to Day 297. Column 4 was inoculated with KB-1™ on Day 40 at a dilution of 1:1000, and re-inoculated on Day 169. VC and ethene started to increase at Day 102, but really showed rapid production after re-inoculation on Day 169. 99% complete dechlorination was achieved by Day 297.**

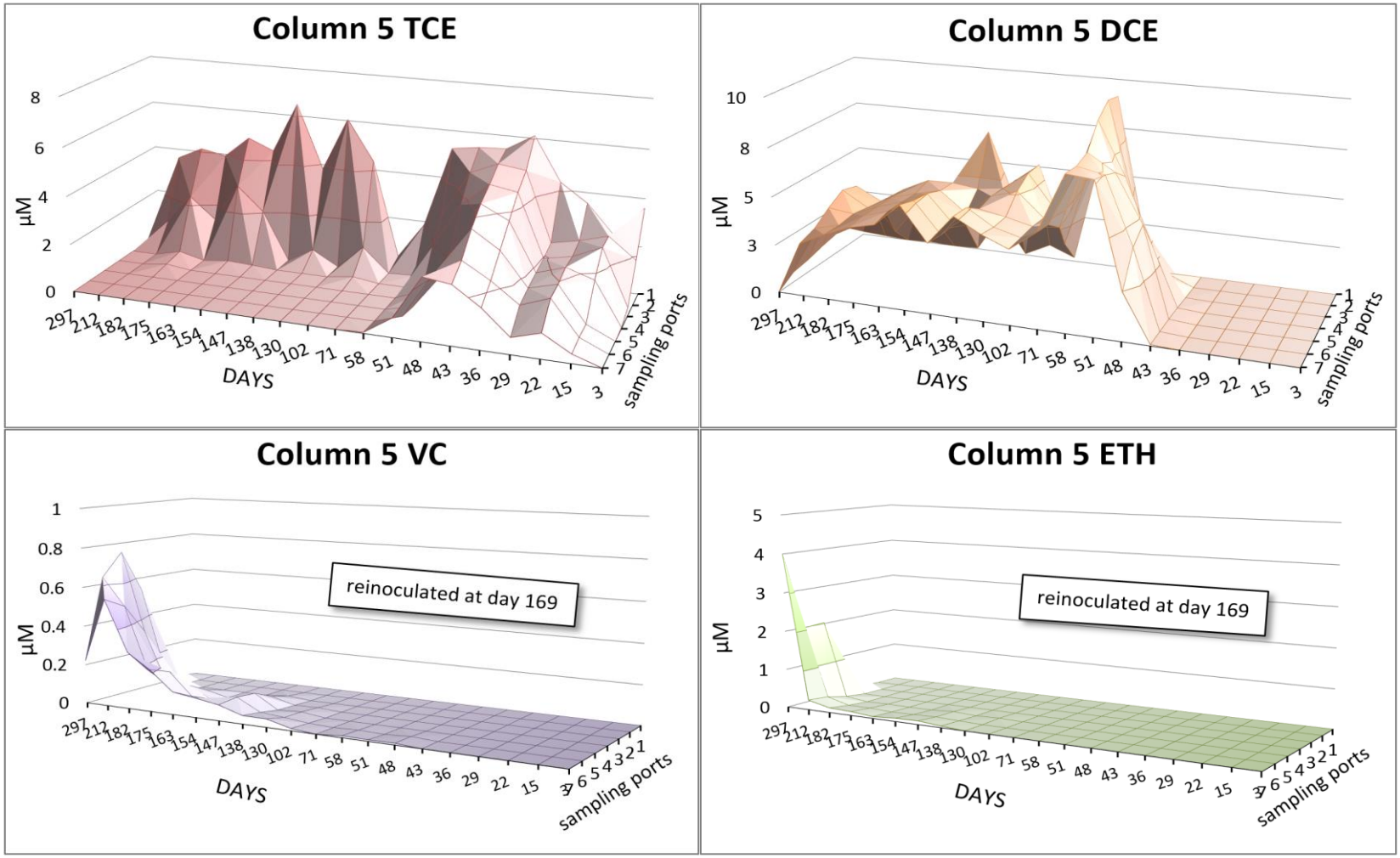


**Figure 4.15: The aqueous-phase chemical concentrations for column 5, starting from Day 3 (three days after TCE and water started to flow in) to Day 297. Column 5 was inoculated with KB-1™ on Day 40 at a dilution of 1:1000, and re-inoculated on Day 169. VC and ethene started to increase at Day 102, but really showed rapid production after re-inoculation on Day 169. 95% complete dechlorination was achieved by Day 297.**

### *4.6.4 Comparison with Other Column Studies*

Öztürk et al. investigated TCE removal with the use of mulch biobarriers (Öztürk, et al., 2012). With a longer hydraulic retention time of 7.2 days (ours was 3.3 days), a total operation period of nearly 300 days, controlled anaerobic conditions throughout the column experiments, and a TCE-degrading culture that was detected to have mostly a DCE dechlorinating consortium clone (DCEH2), the column dechlorinated 1mg/L TCE influent to a mostly VC-containing effluent. Ethene was detected at the end of the column but was not quantified. Therefore no sense of the completeness of dechlorination can be gained. Unlike this thesis research, their column did not have *cis*-DCE predominately in the column for very long, but mostly VC after roughly day 100. The difference in the relative abundance of chlorinated-ethene daughter products depends on the inoculated culture, and obviously their culture contained more DCE-dechlorinating strains, while the culture used in this thesis research apparently had more VC-dechlorinating strains. In terms of application, the KB-1$^{TM}$ culture used is better, for being able to quickly convert VC to ethene instead of producing the more contaminated compound VC. However, in our study, VC accumulated more than reported for the full-strength KB-1 culture in other studies (Kovacich, et al., 2007) (Duhamel, et al., 2002).

Kovacich et al. (Kovacich, et al., 2007) applied KB-1$^{TM}$ culture to a field biobarrier test, although the biobarrier consisted of two to three layers of recirculating wells instead of a low-maintenance mulch biobarrier. The TCE to be treated ranged from 0.5 to 4 mg/L, which was not too far from concentrations in this thesis research, but their groundwater flow rate was 60 cm/day, 4 times faster than what was used in this thesis research. The electron donor used was

EOS that contains lactate and soybean oil that serve as short-term and long-term electron donors and carbon sources for dechlorination. At sections of the biobarrier where only two layers of recirculating wells were used, ethene started to appear after 9 months of operation, and complete dechlorination was achieved after a year. At sections where three rows of recirculating wells were used, ethene started to show in 2 to 4 months, but complete dechlorination was not achieved after 1 year of operation. Thus, the performance of the biobarrier system coupled with the use of EOS (continuous injection) did not perform as well as the mulch biobarrier studied in this thesis research.

### *4.6.5 Contamination in Control Columns*

During Day-58 sampling of columns 1 and 2, *cis*-DCE was found in both towards the effluent ends of the columns. While this could have resulted from rise in indigenous populations in mulch, it is more likely the result of cross-contamination from inoculated columns. The effluent ends of all columns were interconnected. Since no sampling was done on columns 1 and 2 between Day 36 and Day 58, and that the four experimental columns were inoculated on Day 40, contamination would have to have occurred after Day 40, with dechlorinators entered the two control columns from the interconnected effluents via bacterial motility — i.e., that the dechlorinators traveled from the effluents of the other four inoculated columns to the two control columns. A very close relative of *Geobacter lovleyi* strain KB1, (*Geobacter lovleyi* strain SZ) was found to have flagellar motility (Sung, et al., 2006), so *Geobacter lovleyi* strain KB1 is suspected to have motility as well. No DMC strains have been

shown to possess motility. It is possible that the *Geobacter* in the column effluents of columns 3 to 6 sensed the TCE from control columns and migrated up the control columns. The fact that only *cis*-DCE was produced as the dechlorination product from TCE in the control columns suggests (but certainly does not prove) that only *Geobacter* became active in the control columns, as the *Geobacter* strain only dechlorinates TCE to *cis*-DCE. However, given adverse environmental conditions, dechlorinating bacteria that have the ability to fully dechlorinate TCE can also stall at *cis*-DCE.

On top of the fact that the two control columns were found contaminated on Day 58 sampling, the sampling process on Day 58 itself could have caused additional contamination, as a total volume of around 35 mL column liquid was drawn out of each control column for GC FID analysis, and thus pulling in from the combined effluents 35 mL liquid, which contained dechlorinators flowing out of the four inoculated columns. The effluent tubing system was modified on Day 59, so that the six columns' effluents were all separated. It is possible that DMC contamination also took hold and generated VC and ethene, but lack of chloroethene sampling in control columns after Day 58 prevents us from drawing any conclusions.

To verify that the dechlorination activity in the control columns was due to contamination, rather than from the indigenous dechlorinators in mulch, DNA level assays would be needed to determine whether the genetic fingerprints of the dechlorinators in the control columns are a match to those in KB1.

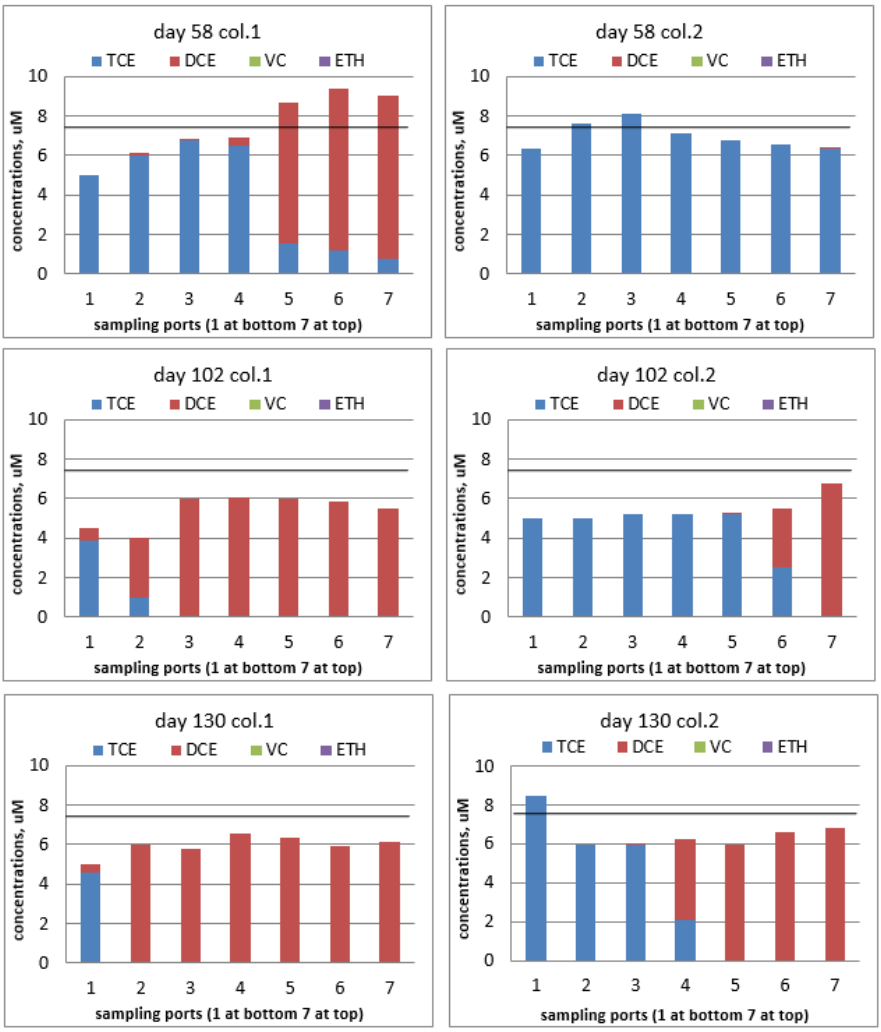


**Figure 4.16: What is presumed to be contamination of control columns (columns 1 and 2) was evident on Day 58. Up to Day 130, only *cis*-DCE was observed as the dechlorination product, indicating the possible contamination by *Geobacter lovleyi* strain KB1 only.**

### *4.6.6 Methane Production*

During the dechlorination process, methane was also produced from methanogens possibly including those native to the mulch as well as from the KB-1$^{TM}$ culture. Methanogens are strict anaerobes that produce methane either from carbon dioxide and hydrogen (for hydrogenotrophic methanogens), or from acetate (for acetotrophic methanogens) (Demirel & Scherer, 2008). The formation of methane can be used as evidence of a suitable anaerobic environment for dechlorinators such as *Dehalococcoides* (Freedman & Gossett, 1989). As shown in Figure 4.18 below (the 3-D figure), methane started to form on Day 43 in the inoculated columns (columns 3 to 6), and experienced a rapid increase from Day 43 to Day 130 before slowly decreasing until Day 212. Prior to inoculation, methane was not found in any of the six columns. Unfortunately, no sampling for the control columns was taken between Day 36 sampling and Day 58 sampling. On Day 58 sampling, methane was found in the two control columns as well as *cis*-DCE. Although it is not known exactly when methane started to form in the control columns, the methane levels in the control columns were surprisingly similar to the levels in the inoculated columns on Day 58, as shown in Figure 4.17. Methanogens may naturally exist in mulch, and the appearance of methane in the control columns may not necessarily indicate contamination. However with the appearance of *cis*-DCE and the high level of methane produced, the control columns were assumed to be contaminated by the methanogens present in the KB-1 inoculum. Some methanogens have flagellar motility (Jarrell, et al., 1996).

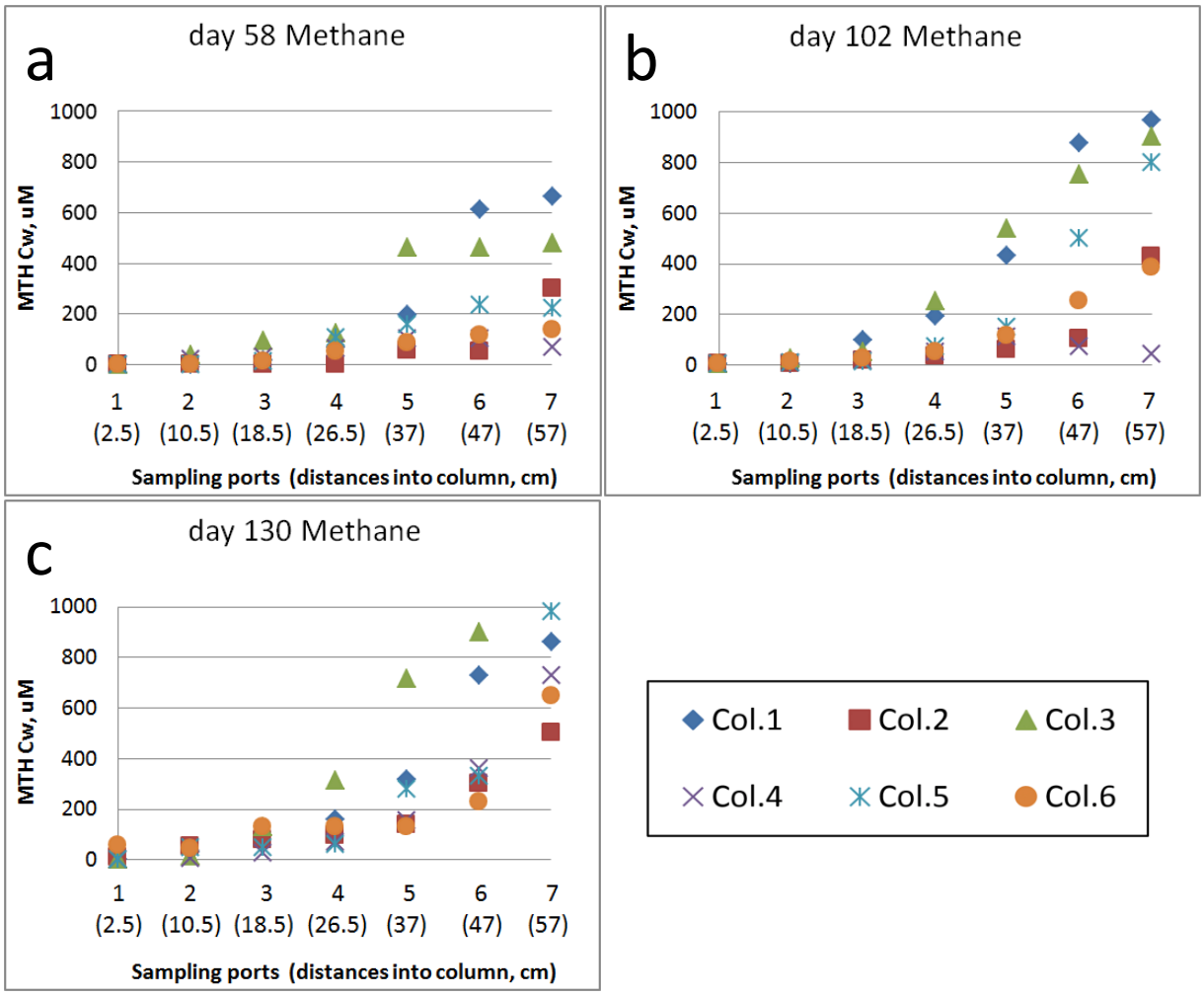


**Figure 4.17: The methane concentrations of columns 1 and 2, compared to the inoculated columns (3 to 6). Columns 1 and 2 had around the same level of methane produced as the inoculated columns.**

Figure 4.18 below illustrates the methane production from inoculated columns 3 to 6, and the trend of the methane level first increased from Day 43 to Day 130, and then experienced a gradual decrease from Day 130 to Day 212. One explanation for the increase of methane up until Day 130 was that initially, the biodegradable organic matter in mulch was abundant, and thus was able to produce enough hydrogen and acetate to support the growth of methanogens and dechlorinators.

The decrease of methane production later on may be explained by the following. After the most rapidly degradable organic matter in mulch was depleted, the production of hydrogen and acetate slowed, and since the threshold hydrogen concentration for dechlorinators (*Dehalococcoides*) was found around 2 nM (Smatlak, et al., 1996; Yang & McCarty, 1998), and around 11 nM for methanogens (Yang & McCarty, 1998), the dechlorinators were able to depress the hydrogen level low enough to slow the activity of hydrogenotrophic methanogens. Meanwhile methane could still be produced by acetotrophic methanogens, but these also experienced a slower activity due to less acetate produced because of the depletion of rapidly degraded mulch substrates.

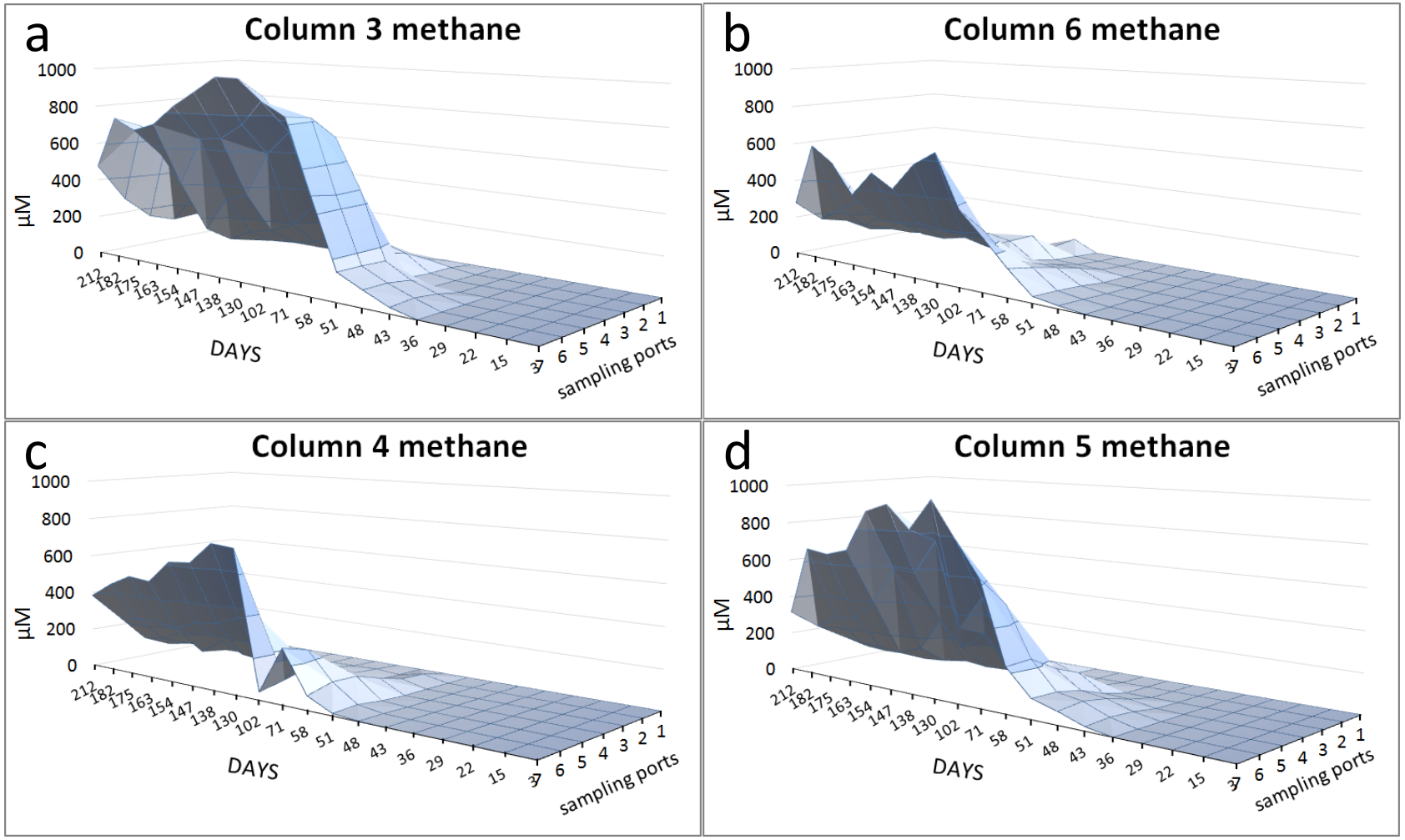


**Figure 4.18: Aqueous methane concentrations in the four inoculated columns. The inoculation occurred on Day 40, and the first appearance of methane was on Day 43, which was three days after the inoculation. In general, the methane concentrations increased from Day 43 to Day 130, and then slowly decreased to the end of the experiment at Day 212.**

### *4.7 Estimating the Longevity of the Mulch Column*

It is important to estimate the longevity of such a mulch biobarrier. In the case where high-DO water is flowing into the mulch, this DO is the main electron acceptor that will be coupled with oxidation of the electron donors released by mulch. Unfortunately, the high detection limit for DO in this study makes it difficult to determine how far oxygen is penetrating into the column over time. However, we can use other evidence to estimate column longevity. Figure 4.19 shows the TCE concentration in each inoculated column from Day 58 to Day 212, for the purpose of showing a TCE concentration rebound over time. As can be seen from the Figure, the blue lines which represent earlier days are generally lower than green and yellow, which represent the middle and late periods of column operation, respectively. In columns 4 and 5, the later timepoints (yellow lines) show TCE levels penetrating further into the columns than the middle timepoints (green lines). This trend is not present however, in columns 3 and 6. Overall the blue lines are lower than the green and yellow lines. This indicates a TCE concentration rebound in the front end of the column, which likely corresponds to the intrusion of DO further into the columns. This can affect dechlorination directly (by killing the strictly anaerobic dechlorinators). Additionally, the consumption of the mulch's electron donating capacity will deprive the dechlorinators of their electron donors as well. The capacity of pine bark mulch to remove DO has been studied by Runtian Yang (Yang R. , 2014). He found that 1 gram dry weight of pine bark mulch can consume 31.2 milligrams of DO.

With this DO consumption capacity, the equivalent volume of column consumed (the pine bark mulch in it) in 212 days was estimated to be a 5 cm height segment at the front end of the column (equal to a penetration speed of 0.7 cm/month) (for calculation detail, go to

Appendix F). This estimation assumed rapid DO removal upon contact with mulch. The longevity of the column can be estimated using solely the DO consumption, as the TCE entering the column was significantly lower than the DO level. Considering only oxygen consumption capacity, the 60 cm mulch column could last for almost 7 years, but some length of column is needed for achieving complete dechlorination in the column effluent, therefore more study is needed to set a safety factor for the estimation of the longevity of the mulch biobarrier system.

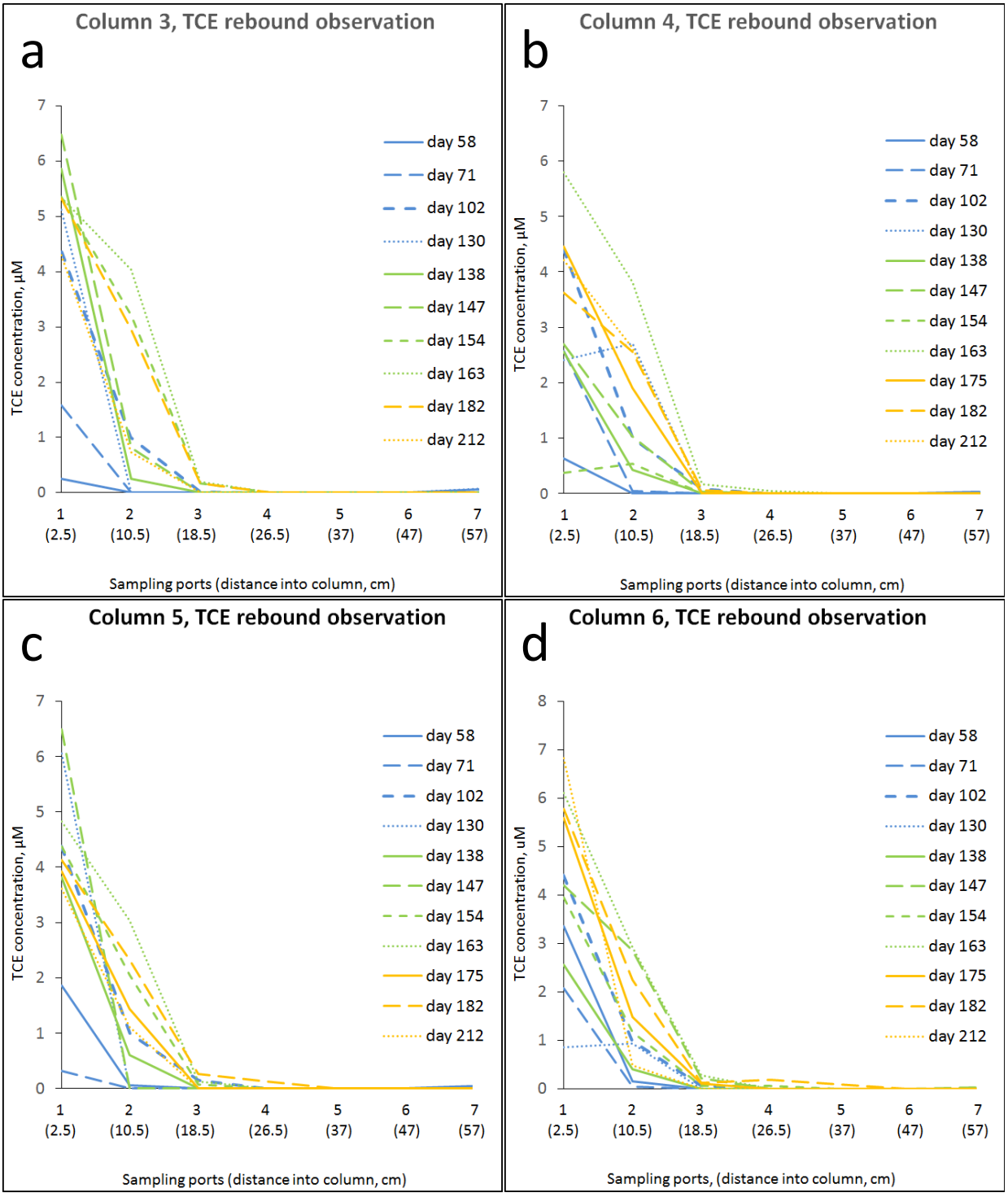


**Figure 4.19: The TCE concentrations in all inoculated columns suggest increased TCE penetration over time at the front end of the columns. In general, blue lines (representing earlier days of experiment) are located lower than green lines (middle time points) and yellow lines (latest time points).**

### *4.8 Detection and Quantification of Dechlorinating Microorganisms Using Molecular Biology Techniques*

#### *4.8.1 DNA Extraction along the Time Course of the Column Operation*

Along with dechlorination performance monitoring, DNA from column liquid samples were extracted at several timepoints, in order to identify the dechlorinators' distribution in the columns, and, ideally, to quantify their populations. Table 3.3 is the overall timeline of this study with DNA sampling and analysis events incorporated.

**Table 4.3: DNA sampling events along the entire timeline of study and analyses performed on extracted DNA.**

| Date | Days | Events* | Endpoint PCR (PCR)/qPCR performed | | |
|---|---|---|---|---|---|
| | | | glpce1 | DMC 16S rRNA | vcrA |
| 11-Sep | 0 | water flow started through mulch columns | | | |
| 14-Sep | 3 | TCE additions started | | | |
| 15-Sep | 4 | 20 mL column effluent DNA sampling | Attempted** (PCR) | | Attempted** (PCR) |
| 21-Oct | 40 | Inoculated columns 3, 4, 5, and 6 with 1:1000 KB1 | | | |
| 14-Dec | 94 | 10 mL column top and bottom DNA sampling | | | |
| 5-Jan | 116 | 20 mL column effluent DNA sampling | Yes (PCR) | Yes (PCR) | |
| 19-Jan | 130 | Control columns were taken offline | | | |
| 22-Jan | 133 | 1 mL oxygenated KB1 added into each sampling ports of column 4 and 5 | | | |
| 27-Feb | 169 | Re-inoculated col. 4 and 5 on port 4 with 1:1000 KB1 | | | |
| 27-Mar | 197 | 10 mL column port DNA sampling, column 3 to 6, port 1 to 7 | Yes (PCR) Yes (qPCR) | Yes (qPCR) | Yes (PCR) |
| 11-Apr | 212 | Last chlorinated compound sampling | | | |
| 14-Apr | 215 | Terminated the operation of column 3 and 6, and took mulch samples | Yes (qPCR) | Yes (qPCR) | |

* Events labeled in green are biomass sampling processes.
** The gel tests following the PCR failed, therefore labeled as "attempted."

### *4.8.2 End-Point PCR Tests Conducted*

End-point Polymerase Chain Reaction (End-Point PCR or PCR) was conducted to verify the existence of certain genes and dechlorinator strains. Gel electrophoresis and imaging under UV light were done on the PCR products to see if the products were appearing with the right amplicon size (which is determined by the primer set used in PCR). To further confirm the PCR product was the target gene, a subset of amplicons was then sent for DNA sequencing using the Sanger sequencing method, to get the actual sequence of the amplicon. The amplicon sequence was then BLASTed against the NCBI nr database to determine the most closely related sequence. Table 4.4 below summarizes the PCR tests conducted in this study.

**Table 4.4: PCR performed for the column experiment, with associated DNA sequencing results.**

| PCR Date | DNA sampling date | Primer(s) used | PCR program used | annealing Temp (°C) | DNA sample locations | gel electrophoresis test result | Sanger DNA Sequencing of PCR product | | | |
|---|---|---|---|---|---|---|---|---|---|---|
| | | | | | | | Original column location | Sequence No. | Result* | Best match from BLAST |
| 2-Jan | day116 20ml Column Effluent | DMC 16S; GeopceA | T52C40 G2 | 53.5; 51 | column 1 to 6 effluent | positive (see Figure 4.20) | ----------not performed---------- | | | |
| 31-Mar | day197 10mlport Liquid | GeopceA | T51C40 | 51 | column 3 to 6, port 1 to 4 | positive (see Figure 4.21) | Column 3 and 4, port 7 | 10318683 | good | *GeopceA* gene |
| 2-Apr | day197 10ml port Liquid | vcrA; GeopceA | T51C40 | 51 | column 3 to 6, port 1,4&7 | positive (see Figure 4.21) | Column 3 port 7 | 10314337 | good | *Dehalococcoides* sp. KB1 vcrA gene |

*Sanger DNA Sequencing results are shown in Appendix D.

Gel electrophoresis images of PCR reactions are shown in Figures 4.20 and 4.21. In Figure 4.20, both *Geobacter pceA* gene (*GeopceA*) and DMC 16S rRNA gene amplicons were clearly visible on the gel, corresponding to DNA from the Day 116 effluent of all 6 columns—both controls and inoculated columns. Figure 4.21 shows the result of the gel test of vcrA and *GeopceA* PCR amplicons from DNA extracted from column ports on Day 197. The *vcrA* amplicon bands appeared in all samples, from sampling ports 1, 4 and 7 on columns 3, 4 and 6 (column 5's PCR samples were lost), although higher light intensity was found on later ports, suggesting a higher abundance of *vcrA* genes in the ports corresponding to *cis*-DCE and VC dechlorination. Bands for *GeopceA* amplicon were observed for DNA from all inoculated column samples (sampling ports 1, 3, 4, and 7 on columns 3 to 6). However, but the band intensity was very low on sampling port 1, suggesting a low abundance of *Geobacter* at the column entrance. This corresponds very well with the GC data which shows that TCE dechlorination as either absent or slow in port 1 (e.g. Figure 4.19). It is interesting that the *vcrA* band intensities from port 1 DNA were higher than for the *GeoPceA* bands from the same DNA samples. However, without a quantitative method it is difficult to draw any conclusions about relative quantities of the two biomarker genes. It does suggest, however, that the *vcrA*-containing DMC population is distributed throughout the columns.

As indicated in Figure 4.21, the PCR product from DNA of sampling port 7 of column 3 was sequenced using Sanger sequencing, and the existence of the *vcrA* gene was verified (see Appendix D). Also, the *GeopceA* gene amplicon was verified for sampling port 7 of columns 3 and 4 (see Appendix D). Sanger sequencing was not conducted for all the PCR samples. However, given that the four inoculated columns are achieving dechlorination of TCE to ethene,

the existence of the *Geobacter* and *Dehalococcoides* strain KB-1 (the strain with a *vcrA* gene) can be safely assumed. Future work is needed to confirm from Day 3 column liquid DNA samples that the biomarkers were not present in the mulch itself.

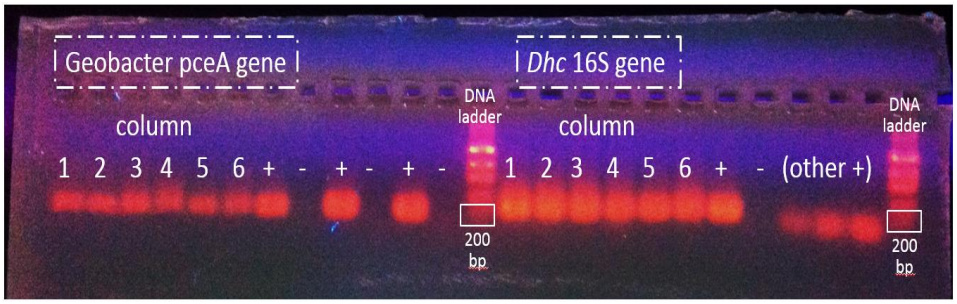


**Figure 4.20: Gel electrophoresis of the PCR result from Day 116 DNA extracted from column effluents, with *GeopceA* genes and DMC 16S rRNA genes targeted. The gel result showed that all columns contained both genes, however, DNA sequencing was never successfully run to confirm. Positive (+) and negative (-) controls consisted of KB-1 DNA and DNA-free water, respectively. The band of the DNA ladders corresponding to 200 bp is highlighted. Expected amplicon sizes are 233 bp and 270 bp for the GeopceA and DMC 16S, respectively.**

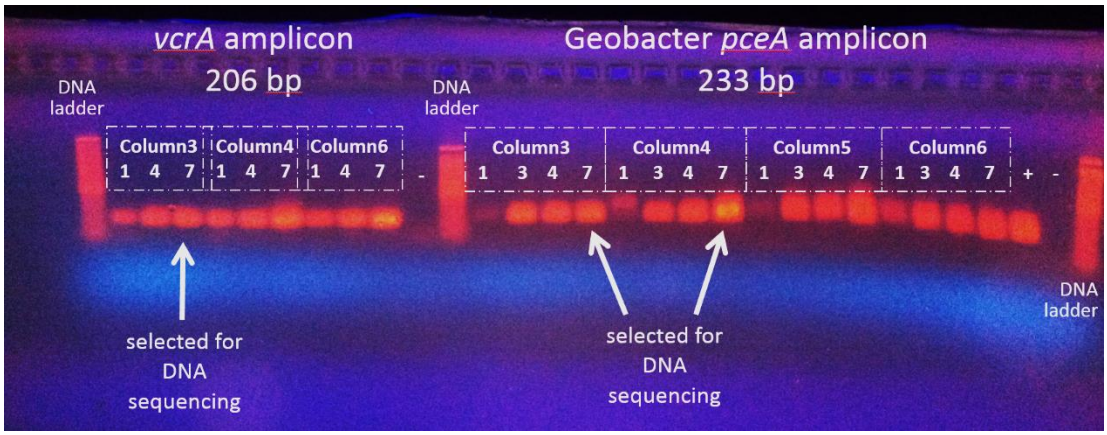


**Figure 4.21: Gel electrophoresis of the PCR products from Day 197 DNA extraction, with *vcrA* gene and *GeopceA* gene targeted. The expected sizes were found for the *vcrA* and *GeopceA* amplicons (205 bp and 233 bp, respectively). Positive (+) and negative (-) controls consisted of KB-1 DNA and DNA-free water respectively. *VcrA* gene and *GeopceA* gene were verified with Sanger Sequencing for selected samples (as shown in figure). Compared to Figure 4.10 of Day 212 column sampling, little TCE was converted into cis-DCE on sampling port 1, which agreed with this gel test, where *GeopceA* band on port 1s were weaker in light intensity than port 3, 4 and 7. Again from Figure 4.10, dechlorination from *cis*-DCE to VC and ethane mainly happened starting sampling port 3, but this gel test showed visible bands on port 1s for vcrA amplicon. This could due to DNA means there's cells, not mean activity. But *vcrA* gene dominated throughout the column.**

### *4.8.3 Quantitative PCR Tests Conducted*

Quantitative PCR (qPCR) was employed to attempt to quantify the dechlorinators' populations at different locations of the columns. DNA from liquid samples (extracted on Day 197) and mulch samples (extracted on Day 215) were used. Table 4.5 is a summary of all successful and attempted qPCR assays performed. The definition of a successful qPCR run includes successful amplification of the qPCR products, correct melting curve (of the qPCR amplicon) and successful validation with DNA sequencing. For convenience, each qPCR assay was given a name (see column "qPCR Assays" in Table 4.5), which was used throughout the thesis. In the following pages, two sets of discussions will be presented: one for the two GeopceA qPCR assays and one for the two DMC 16S qPCR assays.

**Table 4.5: Summary of qPCR assays with melt curve and DNA sequencing results.**

| Date | qPCR Assays | DNA used | Annealing Temp ($^{o}$C) | Biomarkers | Most samples above detection limit? | Correct Melt Curve? | wells selected for sequencing** (result*) | Result from BLAST hit† |
|---|---|---|---|---|---|---|---|---|
| 4/25 | qPCR: DMC 16S No.1 | Day 197 columns 3 and 6 sampling port liquid DNA and Day 215 mulch DNA | 54 | DMC 16S rRNA | yes | yes | bottom mulch from column 3 (+) | non-specific amplification |
| | | | | | | | column 3 port 3 (+) | non-specific amplification |
| 4/27 | qPCR: GeopceA No.1 | Day 197 columns 3 to 6 sampling port liquid DNA | 52 | *GeopceA* | no | no | long amplicon standard(+) | *Geobacter lovleyi* strain KB1 |
| | | | | | | | column 4 port 2 (late melt curve peak) (-) | |
| 5/4 | qPCR: GeopceA No.2 | Day 197 columns 3 and 6 sampling port liquid DNA, and Day 215 mulch DNA | 54 | *GeopceA* | yes | no | column 3 port 6 | non-specific amplification |
| | | | | | | | Column 6 port 5 | non-specific amplification |
| 7/7 | qPCR: 16S DMC No.2 | Day 197 columns 3 and 6 sampling port liquid DNA and Day 215 mulch DNA | 56 | DMC 16S rRNA | yes | yes | Mulch from column 6 port 3 (-) | |
| | | | | | | | column 3 port 3 (+) | non-specific amplification |

* The symbol "-" means sequencing failed; "+" means the sequencing was successful, but does not mean we obtained the right product.

** The corresponding column locations can be found in Table D.1, using the well number.

† For detailed sequencing result, please refer to Appendix D.

### *4.8.3.1 qPCR Analysis for GeopceA Gene*

Two qPCR assays were conducted for quantifying *GeopceA* genes in the columns. The gene is carried by the *Geobacter* strain in the KB-1$^{TM}$ culture inoculated. The existence of the gene was confirmed from a PCR reactions (see section 4.8.2 and Figure 4.21 for PCR details, and Appendix D for sequencing result).

The First GeopceA qPCR, named qPCR: *GeopceA No.1* was done on column port liquids from columns 3 to 6, taken from Day 197. Most samples were below the amplification threshold of 2.29E+02 copies/µL (shown in Appendix C, Figure C.1). For column samples, even for the few samples that were above the amplification threshold, the melt curves were different than for the qPCR standards (shown in Figure 4.22 and Appendix C, Figure C.2). Figure 4.22 below shows the melt curves for several samples that were selected as representatives of: standards (the center purple high peak), a sample with an early peak (dark red peak to the left),

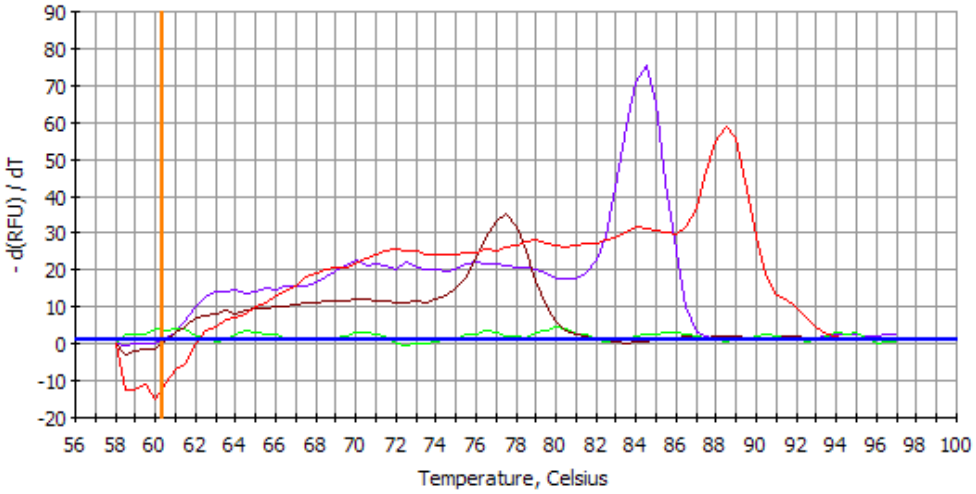


**Figure 4.22: The melt curves selected from qPCR: *GeopceA No.1*. The center purple peak (centered around 84°C) was from one of the standards; the dark red peak to the left (centered around 78°C) represents an early peak likely from a primerdimer; the red peak to the right (centered around 88°C) represents a late peak. The light green curve below the 3 curves represent a blank sample.**

a sample with a late peak (red peak to the right) and blank (the light green curve below the 3 peaks). As can be seen from Figure C.2 in Appendix C, all the standards peaked at around 84$^{o}$C, while all the column samples showed peaks that peaked at a different temperature. The sample giving the late peak shown in Figure 4.22 was sequenced using *GeopceA* reverse primer, and the sequencing result showed a failed sequencing reaction (sequencing results summarized in Table 4.5).

The suspected reason for the low amplification and wrong melt curves was a low annealing temperature used (52$^{o}$C) which may be allowing primer dimers or nonspecific amplification. Therefore an end-point PCR test followed by gel imaging was done to find out if a higher annealing temperature could be used. In Figure 4.23, end-point PCR amplicons were visible on the gel for all annealing temperatures tested (51$^{o}$C to 54.7$^{o}$C). PCR amplicons from reactions annealed at 51 and 54.7$^{o}$C were sent for Sanger sequencing and were confirmed to be the *GeopceA* gene.

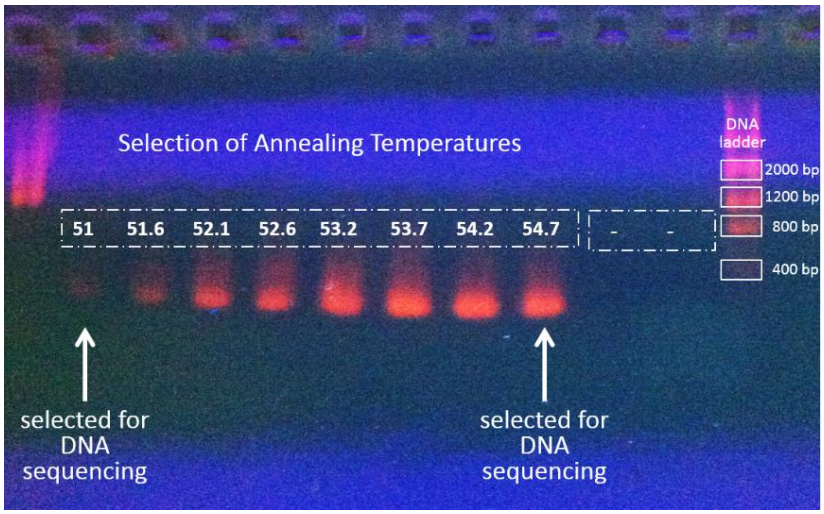


**Figure 4.23: Gel elecgtrophoresis of the temperature gradient PCR run for the *GeopceA* primer set. The DNA used was extracted from KB-1™ culture, not column liquid samples. The PCR product from the two wells pointed out in the figure were sent for DNA sequencing (result not shown), and both returned perfect matches with the *GeopceA* gene. Therefore, in the next qPCR run, annealing temperature of 54°C was used.**

Therefore, in the next qPCR run conducted on May 4th (named qPCR: *GeopceA No.2*, with details in Table 4.5 and Appendix C.2), the annealing temperature used was 54°C. In this qPCR, both liquid and mulch DNA from columns was analyzed. The higher annealing temperature resulted in better amplification (Figure C.3), but the melt curve analysis still showed significant non-specific amplifications (Figure C.4). The sequencing of two of the column samples that showed late peaks (centered above 88°C) did not correspond to *GeopceA* genes. One sequence gave 100% match of only the forward primer used for sequencing, and the other gave imperfect hit of random results (shown in Table D.1 in Appendix D). This suggests that non-specific amplification still happened despite the higher annealing temperature. The annealing temperature of 54°C should not be raised because it cannot be higher than the melting temperature of 56°C. However, improvements on the qPCR assay can still be made, with two possible solutions: (1) allow more cycles, and (2) decrease primer concentration to eliminate primer dimers, in order to increase correct amplification.

The reasons for the different results from endpoint versus quantitative PCR are not clear. Both assays were allowed 40 PCR cycles and used the same annealing temperatures and DNA samples. It is possible that the PCR buffer chemistry differences between the endpoint PCR and qPCR reaction solutions are causing the discrepancies. It can be seen that many of the qPCR reactions for column samples are still in the exponential increase phase at 40 cycles. These issues will be investigated by future students.

#### *4.8.3.2 qPCR Analysis for DMC 16S rRNA Gene*

The April 25th qPCR test (named *DMC 16S No.1*) aimed to quantify DMC 16S rRNA genes in DNA extracted from mulch (attached bacteria) and aqueous (planktonic) bacteria. Columns 3 and 6 were sacrificed on Day 215 for mulch DNA extraction. The qPCR test resulted in good melt curve and good amplification, with results shown in Appendix C.3.1. However DNA sequencing results (see Table 4.5 and Table D.1) suggested that the dominant amplicons were related to uncultured *Chlamydia* 16S rRNA genes, not *Dehalococcoides* (see Appendix C3.2). The fact that the DMC 16S rRNA primers are not perfect matches for the *Chlamydiales* sequence suggests that raising the annealing temperature may effectively reduce the nonspecific amplification of these non-target 16S rRNA sequencing.

To avoid non-specific amplification, a higher annealing temperature of 56°C was used (this destabilizes mismatches between the primers and the non-target genes). End-Point PCR was performed to confirm amplification at 3 different annealing temperatures with DMC 16S primer: 52.7, 55.7 and 58.7°C, as shown in Figure 4.24. The second qPCR conducted on DMC 16S rRNA with the same mulch and column liquid DNA used for *DMC 16S No.1* but with 56°C annealing temperature, is named *DMC 16S No.2*, with details shown in Table 4.5 and Appendix C.4. As shown in Figure C.10 and C.11, the qPCR resulted in good amplification and melt curves, very similar to *DMC 16S No.1*. However, from the DNA sequencing result, non-specific amplification was observed again. For one sample, the best hit turned out to be *Chlamydia*-16S rRNA genes, just like for *DMC 16S No.1* (see Table D.1 in Appendix D for detailed sequencing results). This population is likely native to the mulch. It is not found in the KB-1™ culture.

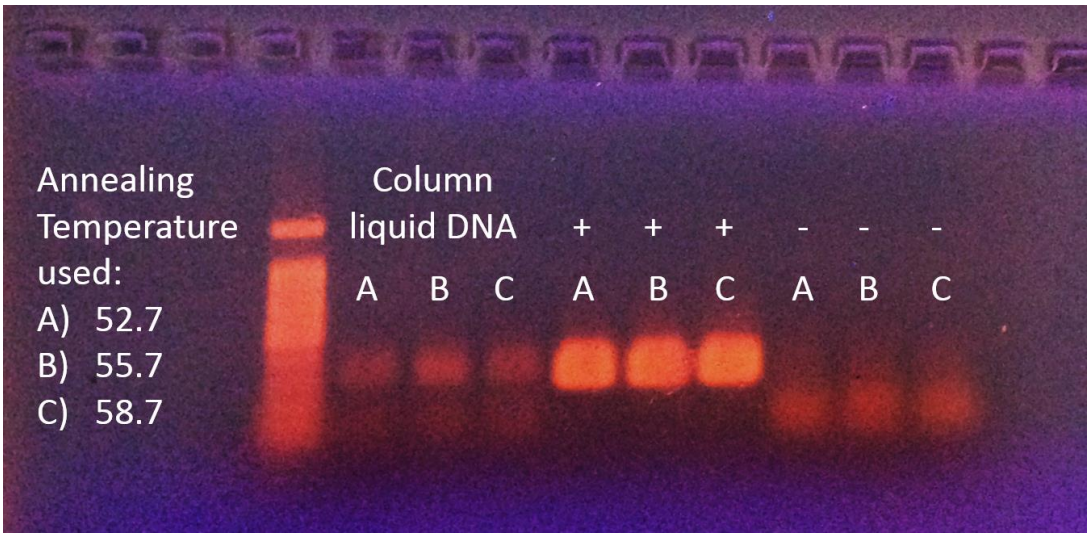


**Figure 4.24: The gel test of the PCR test conducted using Day 197 column 3 port 3 liquid extracted DNA with three different annealing temperatures, aiming to find the ideal annealing temperature for the DMC 16S rRNA primer set. The PCR products with all the 3 annealing temperatures showed bands in the gel, and sequencing is needed to confirm the right product. The 3 middle bands with "+" signs were positive controls which used DNA extracted from KB-1™ enrichment culture, and the 3 bands labeled "-" were negative controls.**

The sequencing of the two 16S qPCR assays confirmed non-specific amplification, but all amplifications were 16S rRNA genes from different microorganisms. Therefore, the quantities reported in Figure 4.25 and 4.26 for mulch and planktonic populations cannot be ascribed to DMC specifically. The data used to construct these two Figures can be found in Appendix C.5. The data suggest much higher (100 to 100,000) populations of bacteria on mulch versus as planktonic cells in pore water. No trend in populations was seen across the length of the columns.

A PCE-dechlorinating lab-scale column study (30 cm long) was done by Behrens and coworkers (Behrens, et al., 2008). Instead of using mulch as column packing material and

electron donor, they used aquifer material (mostly sand and gravel with only 0.001% organic matter), and continuously added lactate as the electron donor and carbon source. The PCE containing (0.09 mM) anaerobic groundwater (purged to anaerobic state prior to use) was pumped into the column to allow a hydraulic residence time of 1.3 days. The column was inoculated with an enrichment culture called Evanite, which contains *Dehalococcoides* strains, and genes like *pceA*, *tceA*, *vcrA* and *bvcA* were all detected in the column. By the end of the run of 170 days, the column had the ability to dechlorinate PCE to VC and ethene, with roughly 70% ethene and 30% VC in the column effluent on Day 170 (Azizian, et al., 2008). The column was then sacrificed, with segments of column solid material taken out. DNA was extracted for further molecular biology analysis.

By performing 16S rRNA qPCR analysis to DMC 16S and all bacteria 16S, they found that the *Dehalococcoides* population decreased in samples further along the column, dropping from (3.6 ± 0.6)E+6 copies/gram column material to (5.6 ± 0.4)E+5 copies/gram column material. The *Dehalococcoides* population was 1% to 3% of the total Bacteria community. For DNA samples, the *tceA* level was found to be similar to *vcrA* and *bvcA* at the front end of the column, which was around 4.4E+5 copies/ gram column material, and decreased significantly, and could not be detected in the second half of the column. This was because after Day 80, the level of PCE and TCE in the effluent stayed low and *cis*-DCE and VC were the dominant daughter products in the column until Day 170, which lowered the "need" for *tceA* gene, especially in the second half of the column. The *vcrA* gene level was slightly more abundant in the front half of the column, but *bvcA* was the dominant gene in the second half of the column. Examining transcript level in the

RNA pool, *tceA* and *vcrA* levels peaked at around 7 cm into the column and decreased at 25 cm. The *bvcA* transcript level was low at 3 cm into the column, but stayed high throughout the rest of the column. Since the column material was taken out for DNA and RNA extraction on Day 170, when the effluent contained 70% ethene and 30% VC, a portion of the column, especially the second half may contain only VC and ethene, although this is a prediction because no sampling ports were built on the side of their column. Although no qPCR was conducted for *vcrA* and *bvcA* gene in the current Master's thesis research, we might suspect that *vcrA* and/or *bvcA* level to be higher deeper into our columns as well.

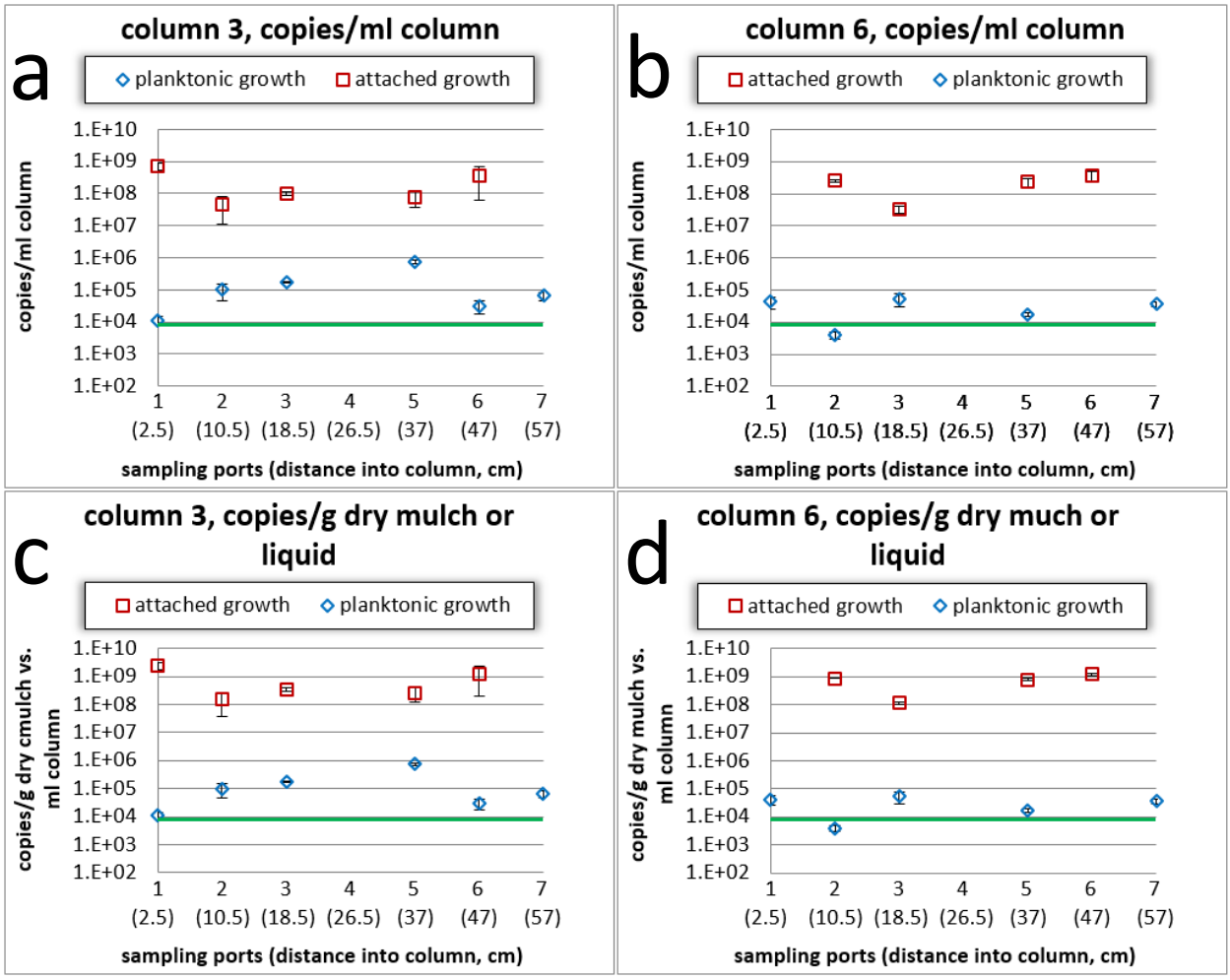


**Figure 4.25: The 16S rRNA quantification of qPCR: DMC 16S No.1 (with annealing temperature of 54°C) shows roughly 100 to 100,000 times more 16S rRNA gene copies detected on mulch than in planktonic phase. Note that the 16S genes amplified and quantified here were not only DMC. The green horizontal line is the lowest concentration of the standards used in this qPCR. (a) and (b) show gene copies per mL of column, whether mulch (wet) or liquid for columns 3 and 6 respectively. (c) and (d) show gene copies per gram of dry mulch and copies per mL of column liquid for column 3 and 6 respectively. The error bars represent standard deviation of triplicate qPCR reactions.**

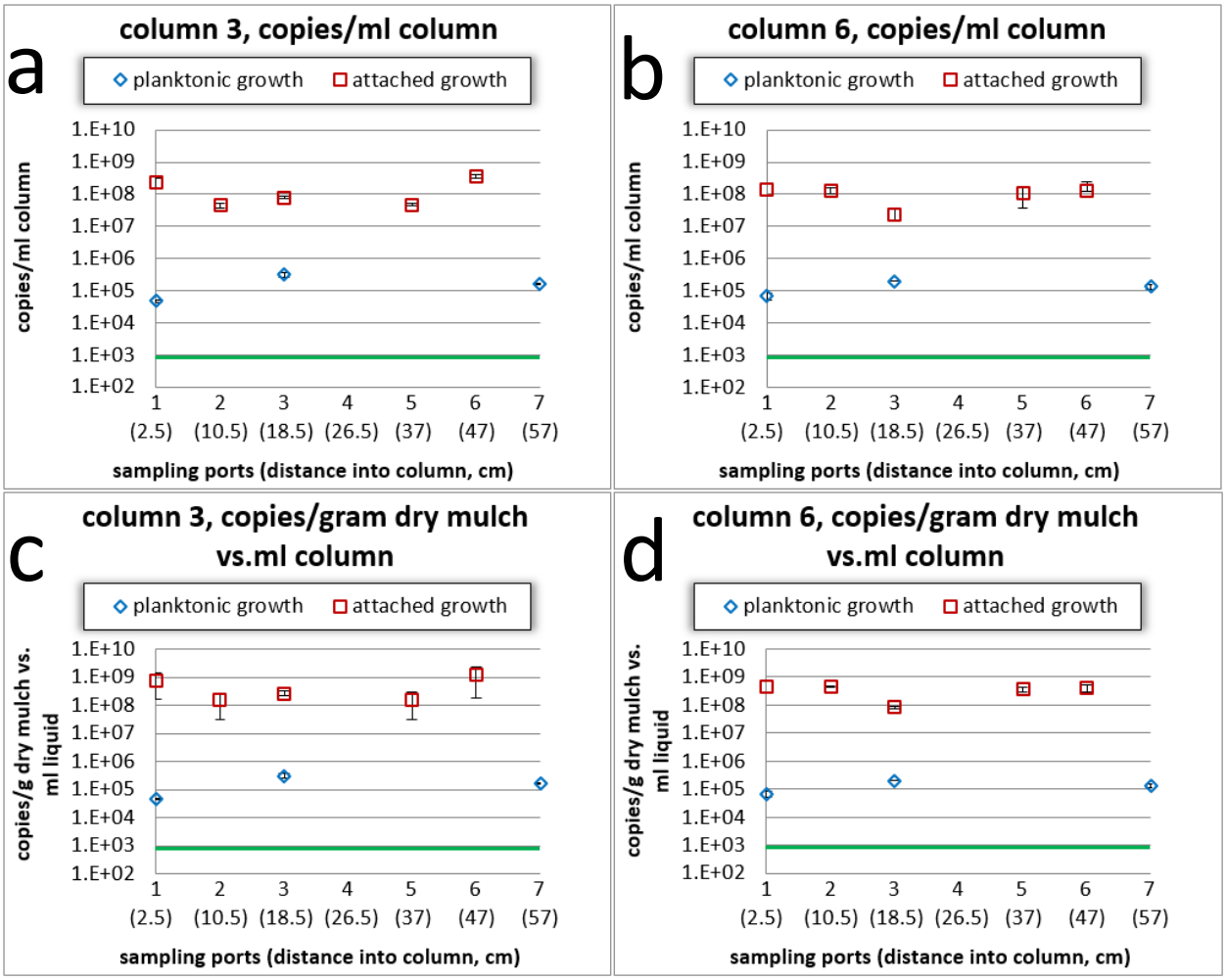


**Figure 4.26: The 16S rRNA quantification of qPCR: DMC 16S No.2 (with annealing temperature of 56°C) shows roughly 100 to 100,000 times more 16S rRNA gene copies detected on mulch than in planktonic phase. Note that the 16S genes amplified and quantified here were not only DMC. The green horizontal line is the lowest concentration of the standards used in this qPCR. (a) and (b) show gene copies per mL of column, whether mulch (wet) or liquid for columns 3 and 6 respectively. (c) and (d) show gene copies per gram of dry mulch and copies per mL of column liquid for column 3 and 6 respectively. The error bars represent standard deviation of triplicate qPCR reactions.**

# CHAPTER 5 CONCLUSIONS AND SUGGESTIONS FOR FUTURE WORK

***The following conclusions were drawn from the result of this study:***

1. The mulch biobarrier inoculated with 1:1000 KB-1$^{TM}$ enrichment culture was able to achieve 73% to 99% complete dechlorination of oxygenated water contaminated with 1 mg/L of TCE, within 172 to 257 days following inoculation. The HRT in the columns was 3.3 days.

2. Within 3 centimeters of the column inlet (port 1), mulch reduced the DO level of incoming groundwater flow from 7.9 mg/L and generated an environment that is anaerobic enough for TCE dechlorination to occur (as seen by the appearance of *cis*-DCE and other daughter products).

3. The dechlorinators inoculated into the column on Day 40 (both DMC and *Geobacter*) were still found in the column (both suspended in water and attached to mulch) more than 5 months later. Based on the dechlorination performance, the mulch columns provided a good habitat for the dechlorinators at least 8 months after inoculation.

4. The qPCR analyses detected 100 to 100,000 times more 16S rRNA gene copies in the attached phase (on mulch) than in planktonic phase on a per mL of column basis. The qPCR products were dominated by a non-DMC sequence (a *Chlamydia*-like organism) which was nonspecifically amplified with the DMC 16S primers.

5. Based on the findings of another Cornell researcher (Runtian Yang), the equivalent volume of column consumed (i.e., the pine bark mulch in it) after the 212 days of column operation was estimated to be a 5-cm segment at the influent ends of the columns. Considering

only oxygen consumption capacity, the 60-cm tall mulch column should last almost 7 years, but an additional length of column is needed for achieving complete dechlorination in the column effluent. Therefore more study is needed to set a safety factor for the estimation of the longevity of the mulch biobarrier system.

***The following investigations are suggested for future work:***

*1. For improving dechlorination performance:*

The rapid increase in concentrations of VC and ethene did not happen until Day 130 and Day 182 for columns 3&6 and 4&5, respectively, indicating a long lag phase for the DMC populations in the KB-1$^{TM}$ enrichment culture used as inoculum. To shorten the lag-time and achieve earlier complete dechlorination, future researchers could try to inoculate the column at a higher concentration (i.e. 1:100 instead of 1:1000), or try amending the columns with some soluble organic compounds such as lactate or butyrate to "jump start" dechlorination in the columns.

*2. Treatment of groundwater containing other possible electron acceptor content (other than DO):*

Mulch barriers are also commonly used for treating nitrate containing groundwater around agricultural lands to prevent eutrophication in lake and rivers when high concentrations of nitrate enter (Su & Puls, 2007). Therefore, if the mulch biobarrier were used to treat a TCE contaminated groundwater which also had a significant concentration of nitrate, a new estimation of the longevity of the mulch biobarrier may be needed. Future researchers could

conduct experiments to investigate the effect of nitrate to the dechlorination performance of a mulch biobarrier.

*3. Future molecular biology assays:*

Since the existence of the DMC 16S gene could not be confirmed in the column by qPCR due to competing non-specific amplifications, future research should include DNA sequencing of End-Point PCR products. New primer sets may be designed to avoid non-specific amplifications when using qPCR to quantify DMC 16S rRNA genes. Future research should also confirm that the DNA extracted from columns prior to inoculation did not contain the dechlorinators' biomarkers.

For qPCR assays of *GeopceA* gene quantification, instead of further increasing the annealing temperature, other approaches should be taken: increasing the number of qPCR cycles (from 40 up to 45 or 50), and decreasing primer concentration to help eliminate primerdimers, in order to increase the efficiency of correct amplification. qPCR of the *vcrA* gene is also an important follow up assay for quantification of this gene biomarker throughout the columns.

# APPENDICES

## *Appendix A. Calibration Curves*

### *A.1 Calibration Curves for TCE and cis-DCE*

Two sets of calibration curves for TCE and *cis*-DCE were made: one for the mulch adsorption tests and one for column water sampling. Figure A.1 and A.2 show the calibration curves used for adsorption tests in 160-mL bottles for TCE and *cis*-DCE, respectively. Bottles containing 100 mL tap water and thus 60 mL headspace were injected with different concentrations of methanol-carried TCE and *cis*-DCE solutions. The aqueous and headspace volume were assumed unchanged, since the amount of solution injected were very small. The bottles were inverted on orbital shakers (100 rpm) overnight before GC sampling. The temperature of incubation was 25 °C. 250 µL of headspace was injected to GC FID with locking, gas tight syringes.

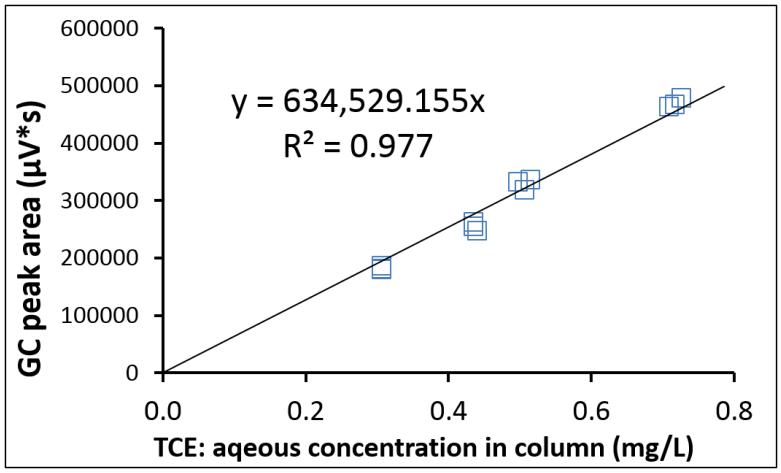


**Figure A.1: GC-FID Calibration curve of TCE for adsorption tests.**

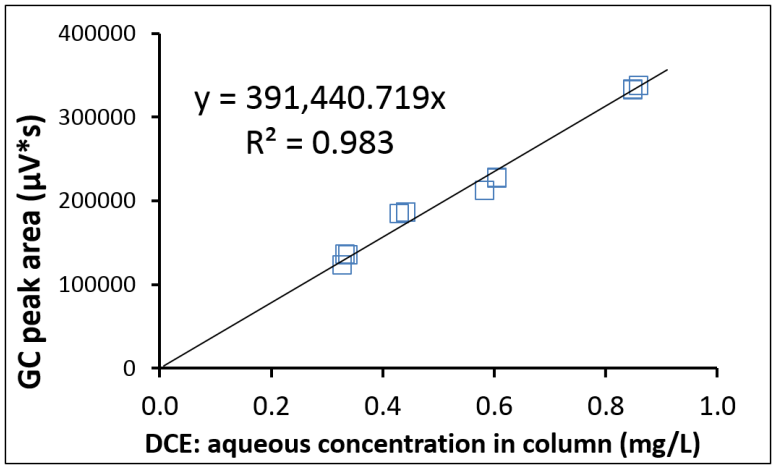


**Figure A.2: GC-FID Calibration curve of *cis*-DCE for adsorption tests.**

Figure A.3 shows the calibration curves for determining aqueous concentrations in column water samples. The first step of preparing this calibration was the same as preparing the calibration bottles for adsorption tests, as described above. Then, 5-mL of bottle liquid was taken using locking, gas tight syringes and injected into a 9-mL serum bottle. The sampling process from the 9-mL was described in Section 3.6. The LoDs for TCE and *cis*-DCE were found to be 0.001 and 0.002 µM, respectively (also shown in Section 3.6).

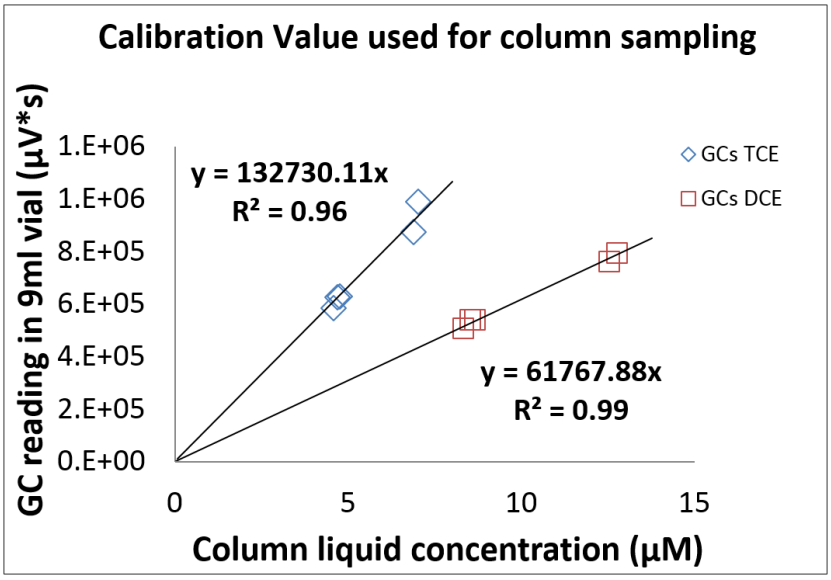


**Figure A.3: GC-FID Calibration curves for aqueous column samples for TCE and *cis*-DCE. The blue diamond represent TCE readings, and the red square represent *cis*-DCE readings.**

### *A.2 Calibration Curves for Ethene and Methane*

GC-FID Calibration Curves for ethene and methane were constructed for aqueous column samples. Figures A.4 and A.5 depict the calibration curves for ethene and methane, respectively. The preparations of the 160-mL and 9-mL calibration bottles were as described in Appendix A.1, for TCE and *cis*-DCE, with the only difference being that the ethene and methane were taken from gas cylinders and injected into 160-mL serum bottles, instead of using methanol-carried stock solutions. The sampling process from the 9-mL was described in Section 3.6. The LoDs for ethene and methane were found to be 0.006 and 7.9 µM, respectively (also shown in Section 3.6).

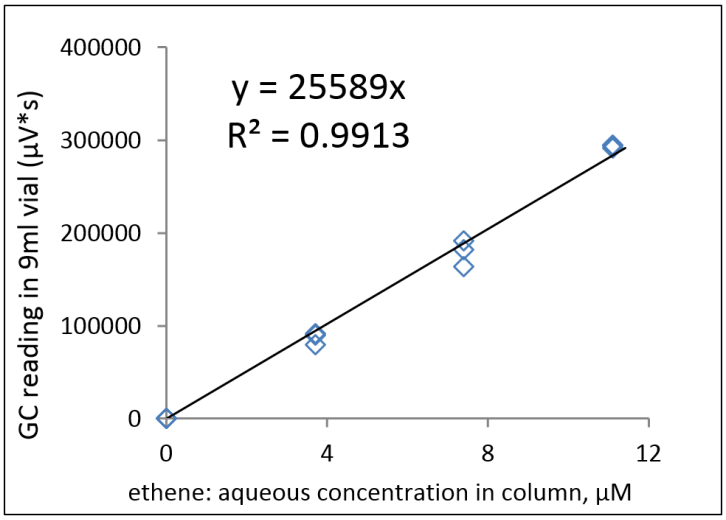


**Figure A.4: GC-FID Calibration curve for aqueous column samples for ethene.**

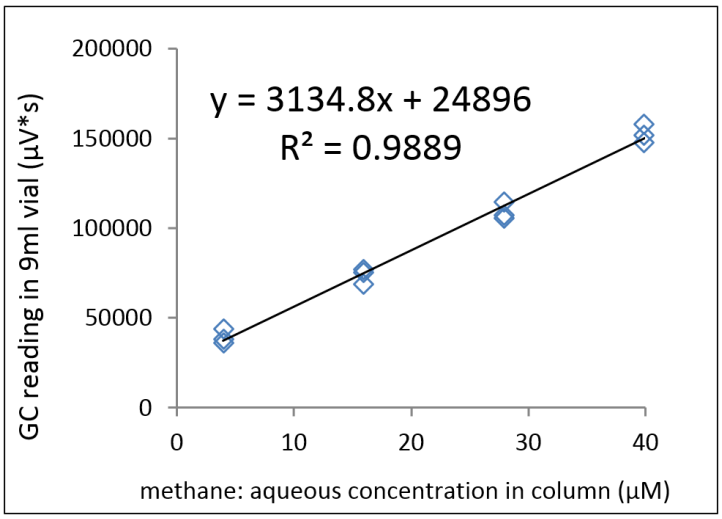


**Figure A.5, GC-FID Calibration curve for aqueous column samples for methane.**

### *A.3 Inferred Calibration Curve for VC*

The instrumental response factor (written as $\varphi$ in equations below) is the ratio of GC peak area and the mass of compound actually injected into GC. The calibration factor (written as ***F*** in equations below) is the factor used to convert GC readings to the units easy for researchers to use, such as total amount of a particular chloroethene in a serum bottle. Because no pure VC standards were available, VC calibration curves could not be constructed. Therefore, a calibration curve for VC was inferred by comparing calibration curves of all other chemicals to one another other and to a set of calibration curves (that included VC among them) from a previous researcher.

On one GC with the same column and running conditions (temperatures of injector, oven and detector; type of carrier gas; if FID, the ratio of air and hydrogen mixture), the response factor differs from compound to compound. On one GC and with the same column and running conditions, the response factor for one compound changes slightly with time. But fortunately, the rate of change of the response factor for one compound over time is similar to those of other measurable compounds. Thus, by acquiring a previous researcher's calibration factors and other related data (shown in equations below) for VC and other chlorinated compounds measured at that time (such as TCE, *cis*-DCE and ethene), the current-day response factor for VC can be estimated based on the ratio found using other compounds. Using this response factor a calibration factor for VC (relating peak area to aqueous concentration) can be predicted as well.

Parameters used in equations:

$PA$ = peak area from GC injection (μVs)

$\varphi$ = response factor (μVs / μmol of constituent injected into GC)

$C_g$ = volumetric concentration of constituent in gas phase of serum bottle standard (μmol/L)

$C_w$ = volumetric concentration of constituent in liquid phase of serum bottle standard (µmol/L)

$H_c$ = pseudo-dimensionless Henry's constant for conditions in the serum bottle standard

$F$ = calibration factor (µVs / total µmol of constituent in a serum bottle standard)

$M_T$ = total mass of constituent in a serum bottle standard

$v_s$ = volume of headspace gas injected to GC for calibration (L)

$V_g$ = volume of headspace in a serum bottle standard (L)

$V_w$ = volume of liquid in a serum bottle standard (L)

(1) Find $\varphi$ from one previous researcher's calibration factor (Heavner, 2013), *F,* data.

Since $F = PA/M_T$ **Equation A.1**

$PA = \varphi\, v_s\, C_g$, **Equation A.2**

$M_T = C_g V_g + C_w V_w$ , *and* **Equation A.3**

$C_g = CwH_c$ , **Equation A.4**

the relationship between calibration factor and response factor can be found as:

$$\varphi = F\left(\frac{V_g + \frac{V_w}{H_c}}{v_s}\right)$$ **Equation A.5**

Using this equation, the $\boldsymbol{\varphi}$ for TCE, *cis*-DCE, VC, ethene and methane were calculated from Heavner's calibration data. (column 5 in Table A1)

(2) Calculate *F* used in this study, as shown in Figure A.1 and A.2. (column 6)

(3) Use the equation in (1) to calculate $\boldsymbol{\varphi}$ in this study for all compounds. (column 7)

(4) Take the ratio of $\boldsymbol{\varphi}$ used in this study and Heavner's for all compounds. (column 8)

Theoretically, the ratio of $\boldsymbol{\varphi}$ for these compounds should be the same, however, due to several reasons (such as imperfection in conducting the experiments, and that Heavner recalibrated

some of the compounds at a different time point when $\varphi$ had already shifted), difference is unavoidable. Therefore, without taking methane into account (because it has less similarity with the other four compounds: single carbon, no C-C double bond), the average of the ratio of $\varphi$ is assigned to VC as 1.901, shown in table.

(5) Then the factor *F* is calculated for VC using the equation in (1), and is used in quantifying VC in this research. (1.25E+6 in column 6 row 4)

**Table A.1: Predict the calibration factor for VC.**

| (1) Compounds Compared | (2) *Hc* Heavner | (3) *Hc* This Study | (4) ***F*** Heavner | (5) $\varphi$ Heavner | (6) ***F*** This Study | (7) $\varphi$ This Study | (8) ratio of $\varphi$ |
|---|---|---|---|---|---|---|---|
| TCE | 0.488 | 0.392 | 1.25E+05 | 3.30E+08 | 6.04E+05 | 8.37E+08 | 2.536 |
| cDCE | 0.189 | 0.167 | 6.34E+04 | 3.74E+08 | 2.58E+05 | 7.84E+08 | 2.098 |
| VC | 1.257 | 1.137 | 2.75E+05 | 3.83E+08 | ***1.25E+06*** | ***7.29E+08*** | ***1.901*** |
| ethene | 8.511 | 8.696 | 6.88E+04 | 4.94E+07 | 2.45E+05 | 5.28E+07 | 1.070 |
| methane | 28.574 | 31.440 | 5.62E+04 | 3.57E+07 | 1.67E+05 | 2.93E+07 | 0.821 |

## *Appendix B. Oxygen Measurements using GC TCD*

### *B.1. "Zero" Level of Oxygen Measurement*

To make sure the GC TCD was performing consistently throughout the sampling process, 500 µL of nitrogen gas taken directly from a nitrogen tank (high purity) was injected to the GC before every sampling activity. The oxygen reading from this practice can reflect the level of $O_2$ contamination due to sampling and injection. Table B.1 below shows the peak height value obtained and the retention time of the peak from allegedly pure N2 injection. The peak height value can be seen as consistent, ranging from13.9 to 26.6 µV, and the narrow range of the retention time also indicated the consistent performance of the GC TCD. The mean represents the peak height that should be subtracted from all real samples' values – or alternatively, is an intercept on a standard plot of peak height vs. oxygen concentration.

**Table B.1: Background level of oxygen measurement using GC TCD.**

| Date of sampling | GC peak height reading | |
|---|---|---|
| | peak height (µV) | retention time (min) |
| 23-Aug | 22.3 | 0.61 |
| 24-Aug | 23.8 | 0.61 |
| 25-Aug | 22.7 | 0.6 |
| 26-Aug | 26.6 | 0.59 |
| 27-Aug | 21.2 | 0.58 |
| 29-Aug | 22.5 | 0.59 |
| 30-Aug | 18.9 | 0.59 |
| 12-Sep | 13.9 | 0.58 |
| 13-Sep | 15 | 0.59 |
| 14-Sep | 12.4 | 0.59 |
| 15-Sep | 20.7 | 0.59 |
| 3-Oct | 16.2 | 0.62 |
| 10-Oct | 20 | 0.59 |

### *B.2. Oxygen Calibration Curve and Detection Limit Calculation*

In Table B.2 below, the value obtained from zero oxygen bottles (labeled in bold Italics) were used to find the LoD. The LoD was calculated as mean value of measurements from blank samples (labeled in bold Italics) plus 3 times the standard deviation of those values (MacDougall, et al., 1980). With mean value of 63.9, µV and standard deviation of 14.54 µV, the LoD was found to correspond to a peak height of 107.5 µV.

**Table B.2: Oxygen calibration curve measurements. The 3 bold Italics data were used to find the limit of detection (LoD).**

| O2 inj. to column bottle, ml | Cw_b, mg/L | 250ul sampling for column bottle | | 500ul sampling for 9ml bottle | |
|---|---|---|---|---|---|
| | | GC_b peakheight (uV) | appear time (min) | GC_s peakheight (uV) | retention time (min) |
| | 0 | 16.2 | 0.60 | ***74.4*** | 0.57 |
| 0 | 0 | 16.8 | 0.60 | ***47.3*** | 0.57 |
| | 0 | 24.5 | 0.60 | ***70.0*** | 0.57 |
| | 0.297 | 95.2 | 0.60 | 46.2 | 0.56 |
| 0.31 | 0.297 | 98.6 | 0.60 | 92.5 | 0.57 |
| | 0.297 | 97.0 | 0.60 | 46.9 | 0.57 |
| | 0.402 | 120.7 | 0.60 | 58.1 | 0.57 |
| 0.42 | 0.402 | 133.2 | 0.60 | 58.1 | 0.57 |
| | 0.402 | 127.2 | 0.60 | 47.9 | 0.57 |
| | 0.498 | 148.3 | 0.60 | 46.9 | 0.56 |
| 0.52 | 0.498 | 149.7 | 0.60 | 49.4 | 0.57 |
| | 0.498 | 149.9 | 6.00 | 56.1 | 0.57 |
| | 0.958 | 300.6 | 0.60 | 52.6 | 0.57 |
| 1 | 0.958 | 290.1 | 0.60 | 92.2 | 0.57 |
| | 0.958 | 284.6 | 0.60 | 49.3 | 0.57 |
| | 1.916 | 543.3 | 0.60 | 59.8 | 0.57 |
| 2 | 1.916 | 569.6 | 0.60 | 55.6 | 0.56 |
| | 1.916 | 561.9 | 0.60 | 62.2 | 0.58 |
| | 2.873 | 742.2 | 0.60 | 61.6 | 0.57 |
| 3 | 2.873 | 780.5 | 0.61 | 72.6 | 0.57 |
| | 2.873 | 771.8 | 0.61 | 73.7 | 0.58 |
| | 4.789 | 1272.5 | 0.60 | 97.5 | 0.57 |
| 5 | 4.789 | - | - | 98.7 | 0.58 |
| | 4.789 | - | - | 117.7 | 0.58 |
| column | 7.986 | | | 175.5 | 0.58 |
| bottle | 7.986 | peak swamped | | 194.7 | 0.58 |
| open air | 7.986 | | | 181.1 | 0.57 |

## *Appendix C. qPCR Test Results*

### *C.1 April 27 qPCR Test for GeopceA Gene with DNA from Column Water Samples*

For convenience, this qPCR event is named "*qPCR: GeopceA No.1*." This qPCR event used GeopceA primers to target DNA column from port liquid samples obtained on Day 197 from column 3 to 6. The annealing temperature used was 52$^{o}$C, and most amplicons were below detection limit after 40 cycles of amplification, but the long amplicon standards were above detection limit, and the sequencing of the standard returned a perfect match of the *GeopceA* gene. Figure C.1 shows the amplification curves of the full qPCR plate, including standards, blanks and all samples (column 3 to 6, port 1 to 7 liquid). For details of all the qPCR runs, see Table 4.5. Figure C.2 depicts the melt curve of the full plate. All the standards showed up at 84 $^{o}$C, but the column samples did not. The peak appearing earlier than 84 $^{o}$C may be primer dimers, and the peak appeared later may be non-specific amplification due to low annealing temperature. The DNA sequencing of one of the column sample that had a late peak failed, as shown in Table D.1.

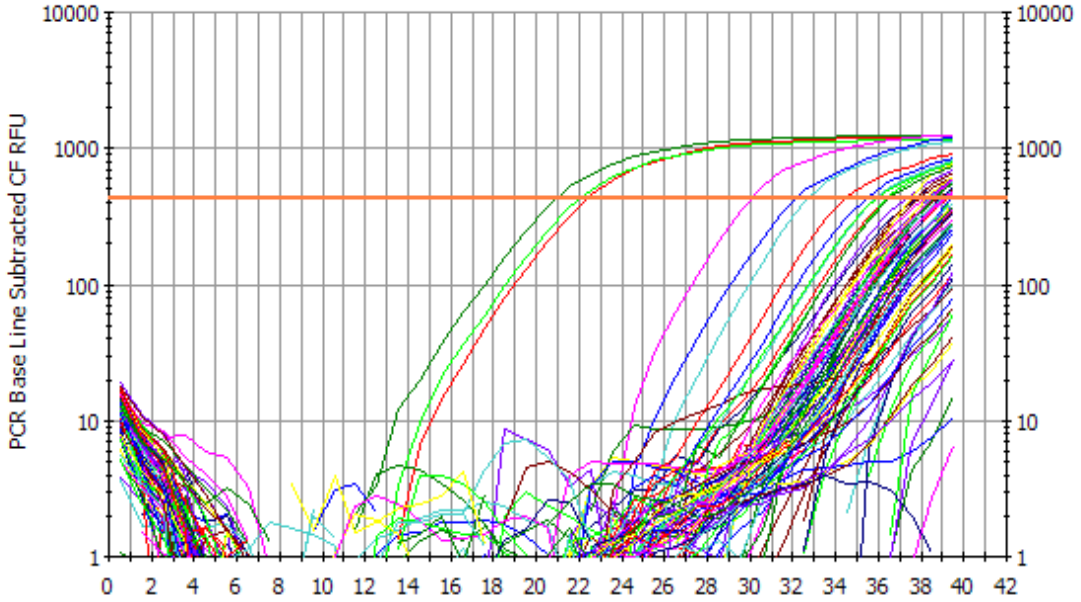


**Figure C.1: qPCR amplification curves for standards (long amplicons of the *GeopceA* gene), blanks and DNA samples from column water samples. Note that the fluorescence (RFU on y-axis) did not pass the threshold for most of the samples. The orange bold horizontal line is the threshold. This qPCR was done on April 27th, using *GeopceA* primers, with an annealing temperature of 52°C.**

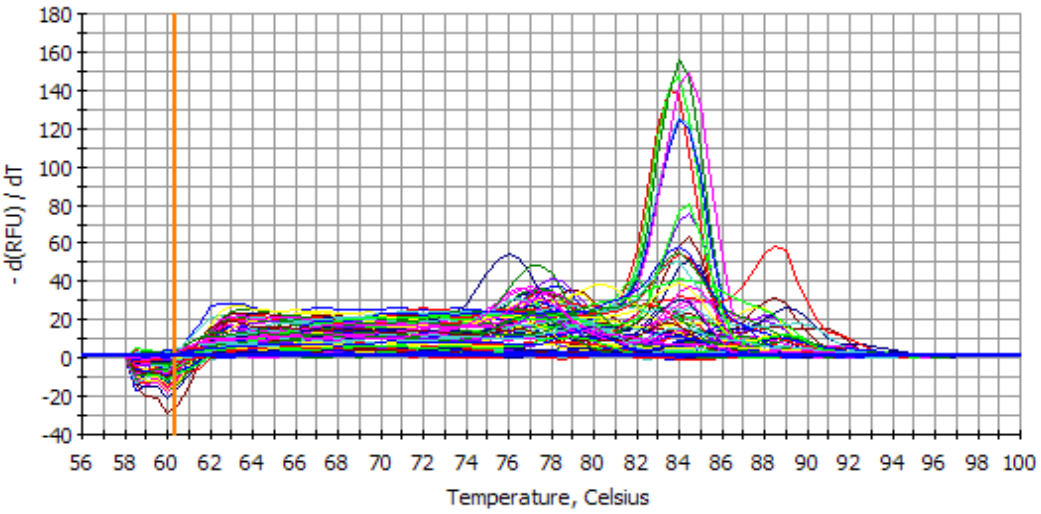


**Figure C.2: qPCR melt curves for April 27th qPCR test on *GeopceA* gene (including standards, blanks and experimental samples). qPCR melting curves that showed the "triple peaks", indicates the amplification of multiple products. Standards show a single peak centered around 84 °C. This qPCR was done on April 27th, using *GeopceA* primers, with an annealing temperature of 52°C.**

### *C.2. May 4th qPCR Test for GeopceA Gene with DNA from Column Mulch and Water Samples*

For convenience, this qPCR event is named "*qPCR: GeopceA No.2*." This qPCR event used GeopceA primers to target DNA from column mulch (obtained on Day 215) and water samples (obtained on Day 197) from column 3 and 6. The annealing temperature used was 54$^{o}$C instead of 52$^{o}$C on *qPCR: GeopceA No.1*. Figure C.3 and C.4 illustrate the amplification curve and melt curve for all the samples including standards, blanks and column samples. As shown in the melt curves (Figure C.4), the higher annealing temperature did not helped with eliminating the non-specific amplifications, as all the column sample melt curves had either early, or late, or multiple peaks. The peak for standards stayed at the same temperature of 84$^{o}$C. The DNA sequencing of one of the column samples that had a late peak did not return with any successful sequence.

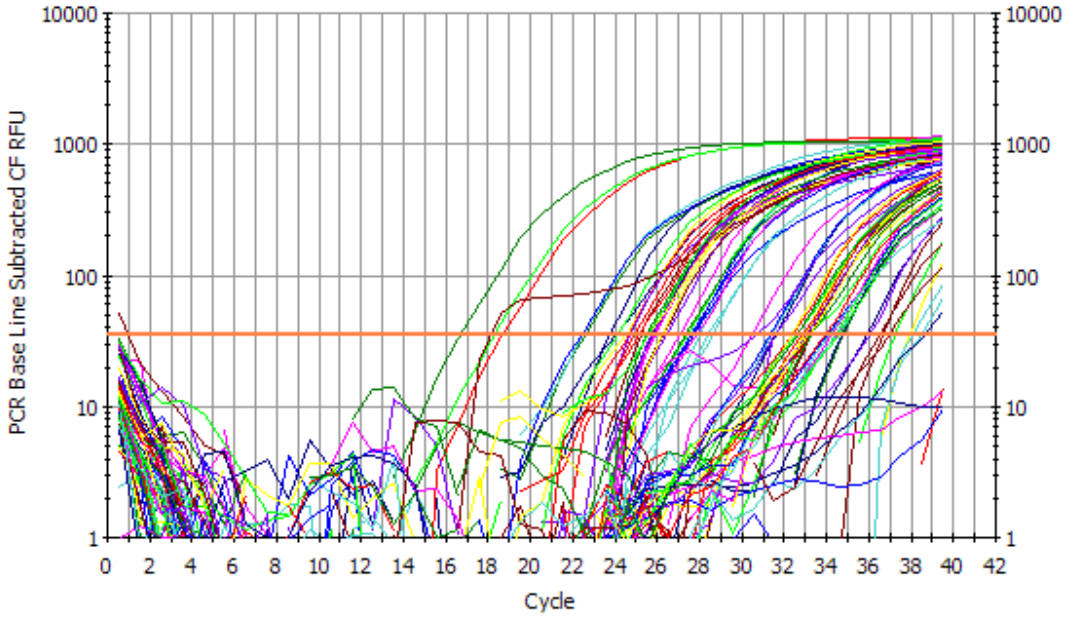


**Figure C.3: qPCR amplification curves for standards (long amplicons of the *GeopceA* gene), blanks and DNA samples from column 3 and 6 mulch and water samples. This time, the fluorescence (RFU on y-axis) passed the threshold for most of the samples. The orange bold horizontal line is the threshold. This qPCR was done on May 4$^{th}$, using *GeopceA* primers, with an annealing temperature of 54$^{o}$C.**

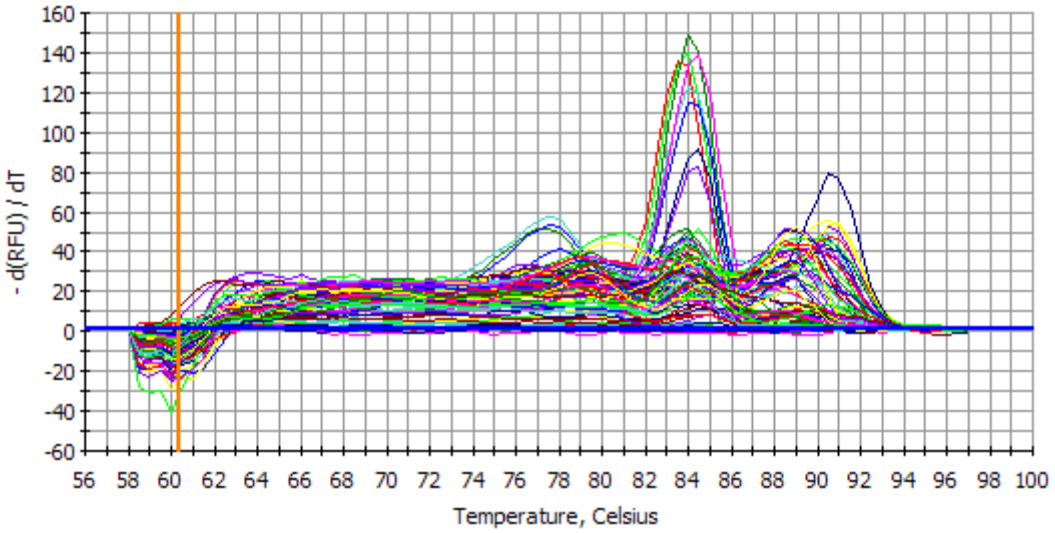


**Figure C.4: qPCR melting curves for April 25$^{th}$ qPCR test on *GeopceA* gene (including standards and experimental samples). qPCR melting curve that showed the "triple peaks" after rising the annealing temperature from52 to 54$^{o}$C. Standards show a single peak centered around 84 $^{o}$C.**

### *C.3. April 25th qPCR Test for DMC 16S rRNA Gene on Column Mulch and Water Samples*

#### *C.3.1 qPCR Result*

For convenience, this qPCR event is named "*qPCR: DMC 16S No.1*." This qPCR event used DMC 16S primers that were supposed to target only DMC strains. Samples included DNA from column mulch (obtained on Day 215) and water samples (obtained on Day 197) from column 3 and 6. The annealing temperature used was 54$^{o}$C. Figure C.5 and C.6 show the amplification curve and melt curve, respectively, Even though most of the samples were amplified, and the melt curve for the standards and column samples closely overlap at 88$^{o}$C, the DNA sequencing result showed that the amplicons were non-specific.

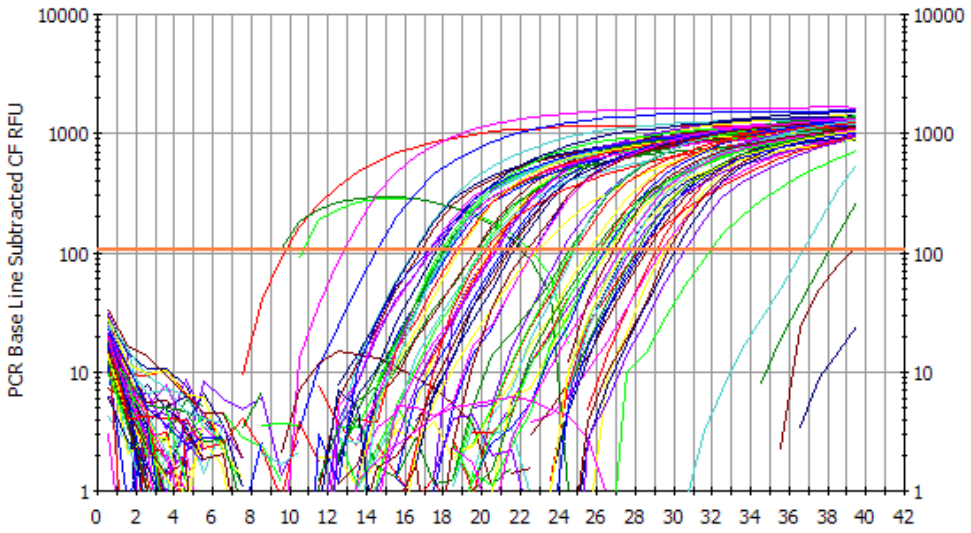


**Figure C.5: qPCR amplification curves for standards (long amplicons of the DMC 16S rRNA gene), blanks and DNA samples from column 3 and 6 mulch and water samples. The fluorescence (RFU on y-axis) passed the threshold for most of the samples. The orange bold horizontal line is the threshold. This qPCR was done on April 25$^{th}$, using DMC 16S rRNA primers, with an annealing temperature of 54$^{o}$C.**

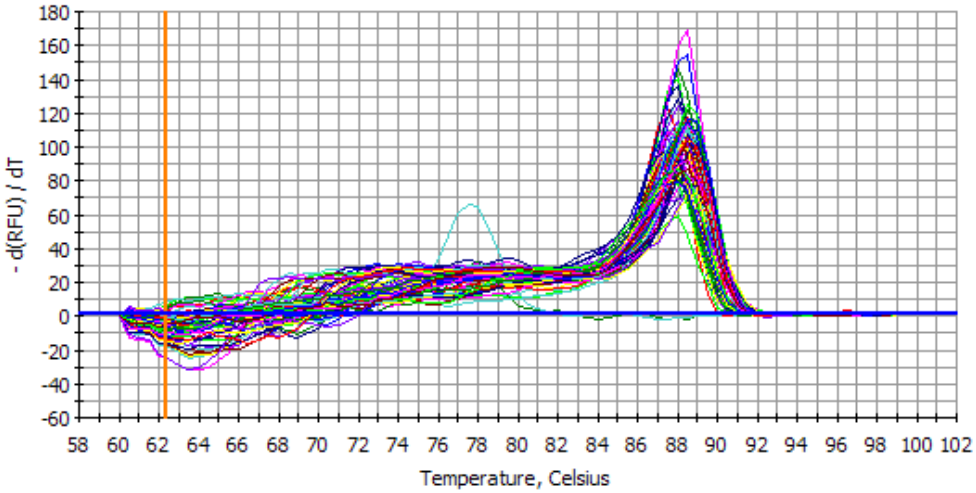


**Figure C.6: qPCR melt curves for April 25$^{th}$ qPCR test on DMC 16S rRNA gene (including standards, blanks and experimental samples). The good melt curves suggested that the correct amplicon was achieved, but the sequencing result (below) suggested nonspecific amplification of other organisms' 16S rRNA genes. The annealing temperature used was 54$^{o}$C.**

### *C.3.2 Discussion of Non-specific Amplification for qPCR: 16S DMC No.1*

Although the melt curves following qPCR were similar for all standards and samples, further verification of the correct amplicon was done by submitting selected qPCR products for Sanger DNA sequencing. For the qPCR products resulting from Column 3/port 3 and Col 3 mulch DNA, an uncultured *Chlamydia* 16S rRNA sequence (GenBank Accession number: EU403857) (not a *Dehalococcoides* sequence) and uncultured *Acidobacteria* 16S rRNA sequence (GenBank Accession number: KJ081620) (not a *Dehalococcoides* sequence) were the best hits after BLASTing the resulting sequence, respectively. The resulting BLAST result for column 3, port 3 DNA is shown in Figure C.3.7 below. The best hit resulting an unculured *Acidobacteria* 16S rRNA sequence had an identities of 96%, but following the similar discussion for the uncultured *chlamydia* below, the sequence was confirmed to be a non-specific amplification (result not shown).

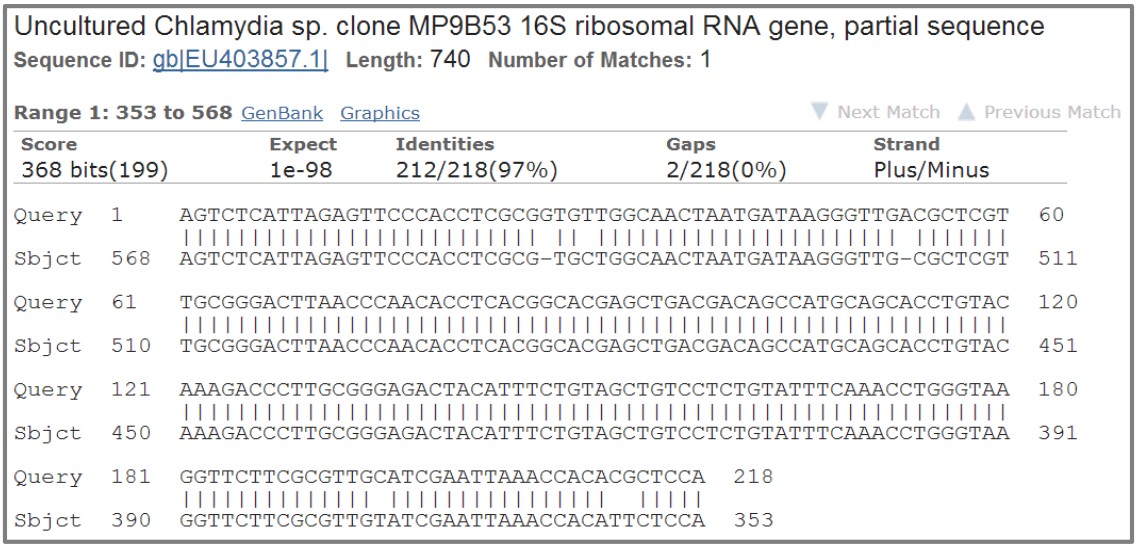
Uncultured Chlamydia sp. clone MP9B53 16S ribosomal RNA gene, partial sequence

**Sequence ID:** gb|EU403857.1| **Length:** 740 **Number of Matches:** 1

**Range 1: 353 to 568** GenBank Graphics ▼ Next Match ▲ Previous Match

| Score | Expect | Identities | Gaps | Strand |
|---|---|---|---|---|
| 368 bits(199) | 1e-98 | 212/218(97%) | 2/218(0%) | Plus/Minus |

```
Query  1    AGTCTCATTAGAGTTCCCACCTCGCGGTGTTGGCAACTAATGATAAGGGTTGACGCTCGT  60
           ||||||||||||||||||||||||| || ||||||||||||||||||||| |||||||
Sbjct  568  AGTCTCATTAGAGTTCCCACCTCGCG-TGCTGGCAACTAATGATAAGGGTTG-CGCTCGT  511

Query  61   TGCGGGACTTAACCCAACACCTCACGGCACGAGCTGACGACAGCCATGCAGCACCTGTAC  120
           ||||||||||||||||||||||||||||||||||||||||||||||||||||||||||||
Sbjct  510  TGCGGGACTTAACCCAACACCTCACGGCACGAGCTGACGACAGCCATGCAGCACCTGTAC  451

Query  121  AAAGACCCTTGCGGGAGACTACATTTCTGTAGCTGTCCTCTGTATTTCAAACCTGGGTAA  180
           ||||||||||||||||||||||||||||||||||||||||||||||||||||||||||||
Sbjct  450  AAAGACCCTTGCGGGAGACTACATTTCTGTAGCTGTCCTCTGTATTTCAAACCTGGGTAA  391

Query  181  GGTTCTTCGCGTTGCATCGAATTAAACCACACGCTCCA  218
           |||||||||||||| ||||||||||||||||   |||||
Sbjct  390  GGTTCTTCGCGTTGTATCGAATTAAACCACATTCTCCA  353
```

**Figure C.3.7: The best BLAST hit of the DMC 16S qPCR amplicon from DNA from Column 3, port 3, was an uncultured *Chlamydia*-like 16S rRNA sequence (GenBank accession number EU403857).**

The DMC 16S primers were aligned against EU403857 to see if there was perfect matching between the primers and the *Chlamydia*-like sequence. Only a portion of the primers aligned with the sequence, indicating that there was nonspecific annealing during the qPCR amplification, possibly due to low annealing temperature (54 $^{o}$C) used for the qPCR process. Figure C.3.8 shows the primers' alignment result.

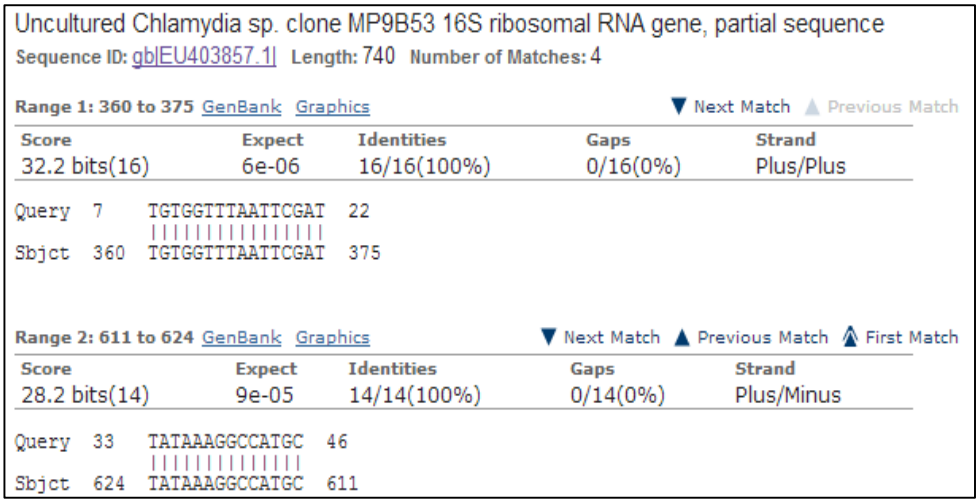


**Figure C.3.8: The alignments of the DMC 16S rRNA primers (forward and reverse) with EU403857 shows imperfect alignment, indicating partial annealing during the qPCR amplification, possibly caused by low annealing temperature. Alignment is perfect only across 15 of the 24 nucleotides of the forward primer (top) and 14 of the 24 nucleotides of the reverse primer (bottom).**

For comparison, the best BLAST hit of the qPCR amplicon among the *Dehalococcoidetes* (taxid: 301297) is shown below, in Figure C.3.9. There was only 86% identity in this alignment compared to 99% identity with the uncultured *Chlamydia*-like sequence. This suggests that the dominant amplified sequence from qPCR was not a *Dehalococcoides* gene segments. Though DMC 16S sequences may also be amplifying, they are not the dominant amplicons. This impacts interpretation of the gene copies data obtained for the column samples.

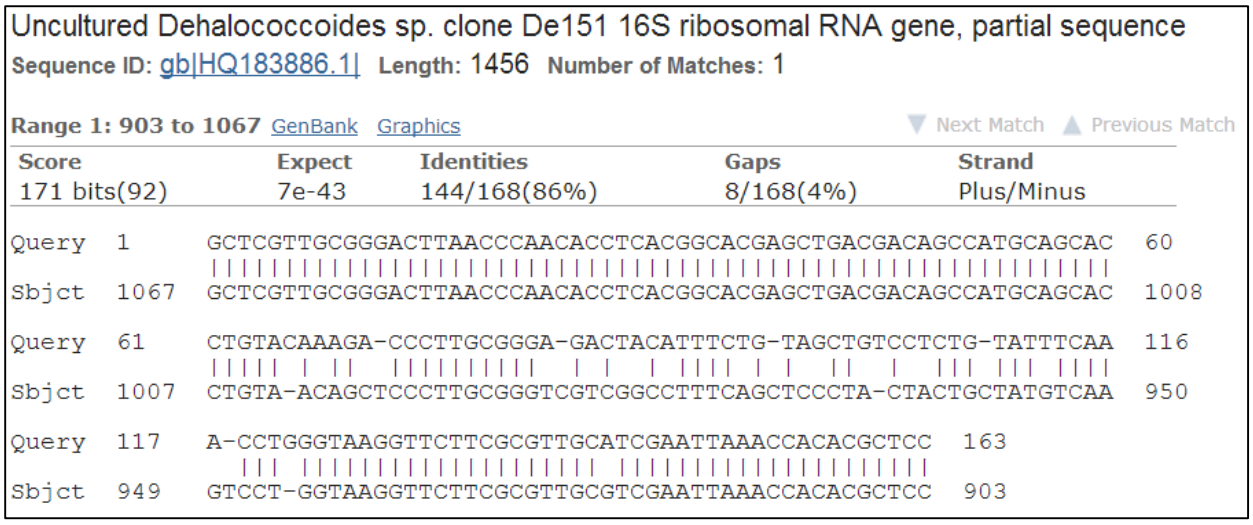


**Figure C.3.9: The alignment of the sequenced DMC 16S qPCR product (from column 3 port3 water DNA) and the best match among the *Dehalococcoidetes* (taxid: 301297).**

### *C.4. July 7th qPCR Test for DMC 16S rRNA Gene on Column Mulch and Water Samples*

For convenience, this qPCR event is named "*qPCR: DMC 16S No.2*." This qPCR run was modified from qPCR: *DMC 16S No.1*, with the only difference the annealing temperature (changed from 54 to 56$^{o}$C). From Figure C.3.10 and C.3.11 that show the amplification curves and melt curve for this qPCR run, it was found that all the samples, including standards, blanks as well as column samples passed the threshold, and the melting curve for column samples (not blanks) overlapped well with the standards. The sequencing of the qPCR product from column 3 port 3 again showed an uncultured *Chlamydia*-like 16S rRNA sequence (EU403857) (not a *Dehalococcoides* sequence), indicating that non-specific amplification was still happening.

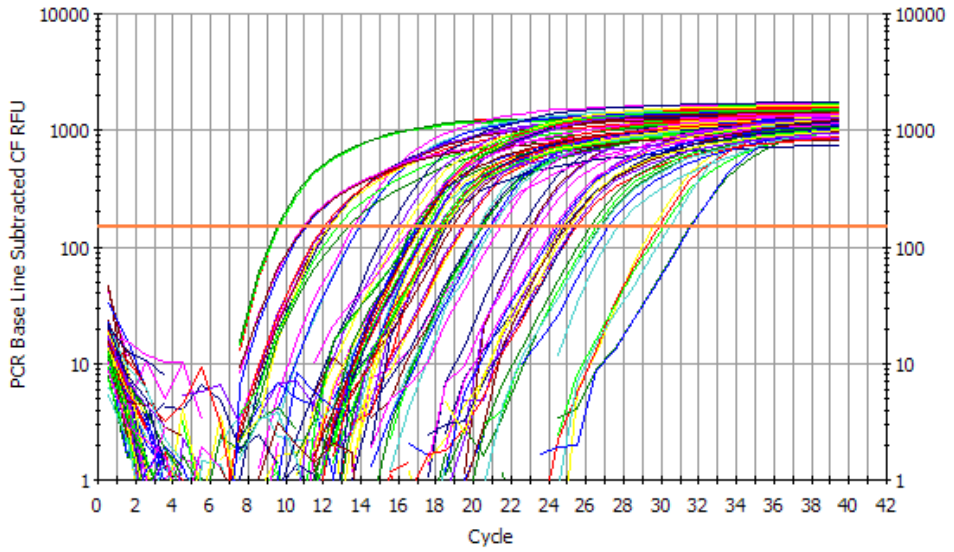


**Figure C.10: qPCR amplification curves for standards (long amplicons of the DMC 16S rRNA gene) and DNA samples from column 3 and 6 mulch and water samples. The fluorescence (RFU on y-axis) passed the threshold for all of the samples. The orange bold horizontal line is the threshold. This qPCR was done on July 7th, using DMC 16S rRNA primers, with an annealing temperature of 56°C.**

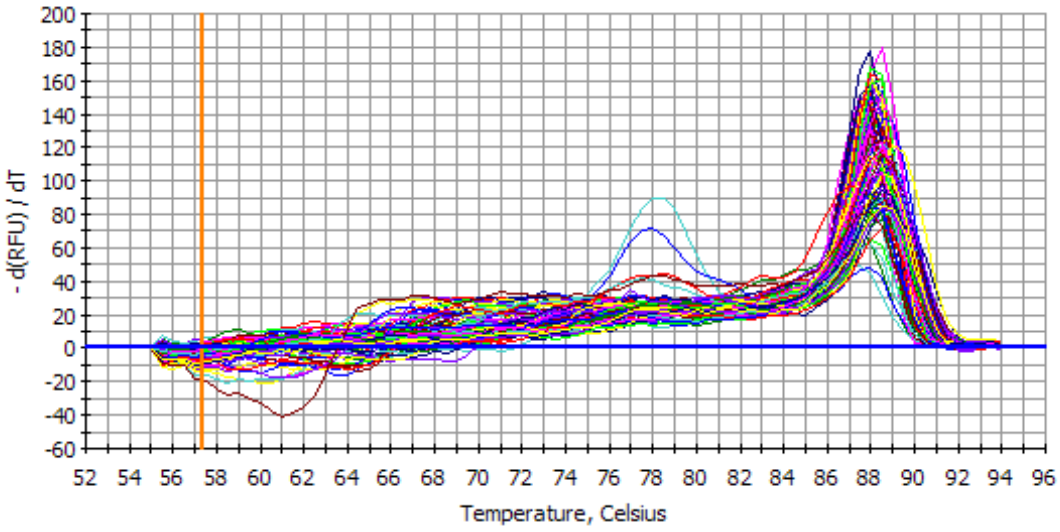


**Figure C.11: qPCR melting curves for July 7th qPCR test on DMC 16S rRNA gene (including standards, blanks and experimental samples). The good melt curves for all column samples (not blanks) suggest that the correct amplicon was achieved, but the sequencing result (below) suggested nonspecific amplification of other organisms' 16S rRNA genes. The annealing temperature used was 56°C.**

### *C.5 Quantification of the 16S rRNA Copies in Columns' Mulch and Aqueous Samples*

The four tables listed below are the gene copies concentration data obtained and modified from the two qPCR events for DMC 16S. Table C.1 and C.2 are for *DMC 16S No.1*, and Table C.3 and C.4 are for *DMC 16S No.2*.

**Table C.1: qPCR data of attached growth gene copies of column 3 and 6, from DMC 16S No.1. SQ stands for starting quantity (copies/µL reaction); SD stands for standard deviation; and co stands for copies.**

| Attached Growth | | | | | | | |
|---|---|---|---|---|---|---|---|
| ports | SQ mean | co/g wet | co/g dry | co/ml | rel SD | SD, co/ml | SD, co/g dry |
| *column 3* | | | | | | | |
| 1 | 3.69E+06 | 7E+08 | 2E+09 | 7E+08 | 0.25 | 1.79E+08 | 6.09E+08 |
| 2 | 2.10E+05 | 5E+07 | 2E+08 | 5E+07 | 0.77 | 3.54E+07 | 1.21E+08 |
| 3 | 4.53E+05 | 1E+08 | 4E+08 | 1E+08 | 0.13 | 1.36E+07 | 4.63E+07 |
| 5 | 3.36E+05 | 8E+07 | 3E+08 | 8E+07 | 0.51 | 3.87E+07 | 1.32E+08 |
| 6 | 1.51E+06 | 4E+08 | 1E+09 | 4E+08 | 0.83 | 3.01E+08 | 1.03E+09 |
| *column 6* | | | | | | | |
| 1 | | | | | | | |
| 2 | 1.40E+06 | 3E+08 | 9E+08 | 3E+08 | 0.09 | 2.37E+07 | 8.08E+07 |
| 3 | 1.99E+05 | 3E+07 | 1E+08 | 3E+07 | 0.27 | 8.99E+06 | 3.07E+07 |
| 5 | 1.20E+06 | 2E+08 | 8E+08 | 2E+08 | 0.30 | 6.81E+07 | 2.33E+08 |
| 6 | 1.93E+06 | 4E+08 | 1E+09 | 4E+08 | 0.36 | 1.29E+08 | 4.42E+08 |

**Table C.2: qPCR data of the planktonic phase gene copies of column 3 and 6, from DMC 16S No.1. SQ stands for starting quantity (copies/µL of reaction); SD stands for standard deviation; and co stands for copies.**

| Planktonic Growth | | | | |
|---|---|---|---|---|
| ports | SQ mean | co/ml | rel SD | StdDev co/ml |
| *column 3* | | | | |
| 1 | 1.13E+03 | 1E+04 | 0.32 | 3.57E+03 |
| 2 | 1.02E+04 | 1E+05 | 0.54 | 5.48E+04 |
| 3 | 1.76E+04 | 2E+05 | 0.07 | 1.17E+04 |
| 5 | 7.36E+04 | 7E+05 | 0.12 | 9.09E+04 |
| 6 | 3.08E+03 | 3E+04 | 0.43 | 1.33E+04 |
| 7 | 6.47E+03 | 6E+04 | 0.31 | 2.03E+04 |
| *column 6* | | | | |
| 1 | 4.22E+03 | 4E+04 | 0.38 | 1.60E+04 |
| 2 | 3.92E+02 | 4E+03 | 0.24 | 9.34E+02 |
| 3 | 5.29E+03 | 5E+04 | 0.44 | 2.34E+04 |
| 5 | 1.69E+03 | 2E+04 | 0.11 | 1.91E+03 |
| 6 | | | | |
| 7 | 3.59E+03 | 4E+04 | 0.17 | 6.11E+03 |

**Table C.3: qPCR data of attached growth gene copies of column 3 and 6, from DMC 16S No.2. SQ stands for starting quantity (copies/µL of reaction); SD stands for standard deviation; and co standrs for copies.**

| Attached Growth | | | | | | | |
|---|---|---|---|---|---|---|---|
| Column 3 Port: | SQ mean, co/uL | co/g wet | co/g dry | co/ml | rel SD | SD, co/ml | SD, co/g dry |
| 1 | 1.2E+06 | 2.3E+08 | 7.8E+08 | 2.3E+08 | 0.32 | 7.4E+07 | 2.5E+08 |
| 2 | 2.0E+05 | 4.4E+07 | 1.5E+08 | 4.4E+07 | 0.16 | 7.1E+06 | 2.4E+07 |
| 3 | 3.5E+05 | 7.9E+07 | 2.7E+08 | 7.9E+07 | 0.06 | 4.5E+06 | 1.5E+07 |
| 5 | 2.1E+05 | 4.8E+07 | 1.6E+08 | 4.8E+07 | 0.06 | 3.1E+06 | 1.0E+07 |
| 6 | 1.5E+06 | 3.6E+08 | 1.2E+09 | 3.6E+08 | 0.14 | 4.8E+07 | 1.7E+08 |
| Column 6 Port: | | | | | | | |
| 1 | 7.72E+05 | 1.4E+08 | 4.7E+08 | 1.4E+08 | 0.19 | 2.6E+07 | 8.7E+07 |
| 2 | 7.16E+05 | 1.3E+08 | 4.5E+08 | 1.3E+08 | 0.04 | 4.7E+06 | 1.6E+07 |
| 3 | 1.46E+05 | 2.4E+07 | 8.2E+07 | 2.4E+07 | 0.17 | 4.2E+06 | 1.4E+07 |
| 5 | 5.57E+05 | 1.1E+08 | 3.6E+08 | 1.1E+08 | 0.10 | 1.1E+07 | 3.7E+07 |
| 6 | 6.59E+05 | 1.2E+08 | 4.2E+08 | 1.2E+08 | 0.06 | 8.0E+06 | 2.7E+07 |

**Table C.4: qPCR data of the planktonic growth phase gene copies of column 3 and 6, from DMC 16S No.2. SQ stands for starting quantity (copies/µL reaction); SD stands for standard deviation; and co stands for copies.**

| Planktonic Growth | | | | |
|---|---|---|---|---|
| ports | SQ mean | co/ml | rel SD | StdDev co/ml |
| *column 3* | | | | |
| 1 | 4.67E+03 | 5E+04 | 0.27 | 1.24E+04 |
| 3 | 3.09E+04 | 3E+05 | 0.39 | 1.21E+05 |
| 7 | 1.63E+04 | 2E+05 | 0.23 | 3.74E+04 |
| *column 6* | | | | |
| 1 | 6.69E+03 | 7E+04 | 0.16 | 1.06E+04 |
| 3 | 2.00E+04 | 2E+05 | 0.18 | 3.55E+04 |
| 7 | 1.34E+04 | 1E+05 | 0.08 | 1.07E+04 |

## *Appendix D. DNA Sequencing Results*

### *D.1 Summary of the DNA Sequencing Results*

Table D.1 below is a summary of all the DNA sequencing conducted on the PCR and qPCR tests of column DNA samples. All obtained sequences are shown in Table D.2.

**Table D.1: Summary of DNA sequencing results for PCR and qPCR tests. Sanger sequencing was performed by the Cornell Genomics facility.**

| DNA sequencing Date | Sequence No. | qPCR plate/PCR run | qPCR platewell No. | DNA Sample amplified | Annealing Temperature $^{o}C$ | Melting curve? | DNA Sequencing | | |
|---|---|---|---|---|---|---|---|---|---|
| | | | | | | | primer used | Obtained sequence? | Top hit from BLAST* |
| 30-Apr | 10314763 | qPCR: GeopceA No.1 | A 1 | long amplicon standard | 52 | good | GeopceA | yes | *G.lovleyi* strain KB1*pceA gene (1) |
| | | | D 2 | column 4 port 2 | 52 | triple peaks | GeopceA | no | - |
| 8-May | 10315305 | qPCR: GeopceA No.2 | A 1 | long amplicon standard | 54 | good | GeopceA | no | - |
| | | | C 4 | bottom mulch from column 6 | 54 | late peak | GeopceA | no | - |
| | | qPCR: DMC 16S No.1 | B 5 | bottom mulch from column 3 | 54 | good | DMC 16S | no | - |
| 14-May | 10315732 | qPCR: DMC 16S No.1 | B 6 | bottom mulch from column 3 | 54 | good | DMC 16S | yes | *Acidobacteria* 16S rRNA gene (2) |
| | | | E 6 | column 3 port 3 | 54 | good | DMC 16S | yes | Uncultured *Chlamydia* 16S rRNA gene (see Figure 3.23) (3) |
| 2-Apr | 10314337 | PCR: 2-Apr vcrA & GeopceA column 3 to 6 | - | column 3 port 7 | 51 | - | VcrA | yes | *Dehalococcoides* sp. KB1 vcrA gene (4) |
| 7-July | 10318683 | PCR: 2-Apr vcrA & GeopceA column 3 to 6 | - | column 3 port 7 | 51 | - | GeopceA | yes | *G.lovleyi* strain KB1*pceA gene (5) |
| | | | | column 4 port 7 | 51 | - | GeopceA | yes | *G.lovleyi* strain KB1*pceA gene (6) |
| 8-July | 10318826 | qPCR: DMC 16S No.2 | F 5 | mulch from column 6 port 3 | 56 | good | DMC 16S | no | - |
| | | | G 5 | column 3 port 3 | 56 | good | DMC 16S | yes | Uncultured *Chlamydia* 16S rRNA gene (7) |
| 10-July | 10318996 | qPCR: GeopceA No.2 | C 2 | column 3 port 6 | 54 | late peak | GeopceA | yes | Only matched forward primer sequence (8) |
| | | | D 2 | column 6 port 5 | 54 | late peak | GeopceA | yes | Random result (9) |

*The numbering of the BLAST result (i.e. (1), (2),..) refers to the sequencing result in Table D.2, as well as there FASTA format information following Table D.2.

**Table D.2: A list of all the sequences obtained from Sanger sequencing (excluding those that failed), and their trimmed sequences used for BLASTing, which correspond to Table D.1.**

| | Trimmed sequence (FASTA format) | Top hit from BLAST* |
|---|---|---|
| (1) | GenBank Accession Number: JX081248.1<br>GCTGTTGATAAAGCATTAGAGTTAGCAGGATGGGCAACAAATGATGAATTTTCCCCATATGCACAATTCGGCAGGAGGAATTCTTTAATTGGAACACACATCGTAAATCCAGTGACTGGAAAGATTGCTAAGGATAAGCCTGTGTTTGTCCCAGGCTTTCATACATGGGA | *G.lovleyi* strain KB1 pceA gene (rdhA gene) |
| (2) | Genbank Accession Number: KJ081620.1<br>AGTCTCTTCAGAGTGCCCAGCTTGACCTGNTGGCAACTGANGACANGGGTTGCGCTCGTTGCGGGACTTAACCCAACATCTCACGNCACGAGCTGACGACAGCCATGCAGCACCT | *Acidobacteria* 16S rRNA |
| (3) | Genbank Accession Number: EU403857.1<br>AGTCTCATTAGAGTTCCCACCTCGCGGTGTTGGCAACTAATGATAAGGGTTGACGCTCGTTGCGGGACTTAACCCAACACCTCACGGCACGAGCTGACGACAGCCATGCAGCACCTGTACAAAGACCCTTGCGGGAGACTACATTTCTGTAGCTGTCCTCTGTATTTCAAACCTGGGTAAGGTTCTTCGCGTTGCATCGAATTAAACCACACGCTCCA | Uncultured *Chlamydia* 16S rRNA |
| (4) | GenBank Accession Number: DQ177519.1<br>TGATCGATGCAAAATTTTATCCCAAGGTTCCTGACCATGCCGTACCTATTAACTTTAAGGAAGCGGATTATAGCTACTACAATGATGCAGAGTGGGTTATTCCAACAAAGTGTGAATCCATTTTCACCTTCACCCTACCTCAACCAA | *Dehalococcoides* KB1 RdhAB14 gene (vcrA gene homolog) |
| (5) | GenBank Accession Number: JX081248.1<br>TTTACGNATGGTGGTGGTTCCAATTAAAGAATTCCTCCTGCCGAATTGTGCATATGGGGAAAATTCATCATTTGTTGCCCATCCTGCTAACTCTAATGCTTTATCAACAGCTGTAAAACCAGGCTCTCCATGCTGTTCAGGGTGAACAAATCCATCGAGTGATGACGCCAACATTAA | *G.lovleyi* strain KB1 pceA gene (rdhA gene) |
| (6) | GenBank Accession Number: JX081248.1<br>ATGTGTGTTCCAATTAAAGAATTCCTCCTGCCGAATTGTGCATATGGGGAAAATTCATCATTTGTTGCCCATCCTGCTAACTCTAATGCTTTATCAACAGCTGTAAAACCAGGCTCTCCATGCTGTTCAGGGTGAACAAATCCATCGAGTGATGACGCCAACATTAA | *G.lovleyi* strain KB1 pceA gene (rdhA gene) |
| (7) | GenBank Accession Number: EU403857.1<br>GCTACAGAAATGTAGTCTCCCGCAAGGGTCTTTGTACAGGTGCTGCATGGCTGTCGTCAGCTCGTGCCGTGAGGTGTTGGGTTAAGTCCCGCAACGAGCGCAACCCTTATCATTAGTTGCCAACACGCGAGGTGGGAACTCTAATGAGACTGCCCGGGTTAACCGGGAGGAAGGTGAGGATGACGTCAAGTCAGCATGGCCTTTATATCTTGGGCA | Uncultured *Chlamydia* 16S rRNA |
| (8) | GenBank Accession Number: JX081248.1<br>TACGGCCATTAAGCCCTTCGCGATCAAGAAGTTGTTCCAGGACAACGGCTACGAACGGGTAATCTATCTCGATCCGGACATCGTCGTCTATCGCCCGCTGGAAGAGTTGATCGACCTGCTGAAGAGTCACGATGTCATTTTGACGCCTCACCTGACCGATTTCTTGCCAGATGACGGCTGCTTGCCCAGCAACGTGCGGATCCTTCAGACAGGCACCAACAATTTGGGGTTTGTGGCCCTGCGTCGAAGTGAACAAGTGTTCCAGTTGGTCGAGTGATGACGCCAACATTAA | Only matched the forward primer of GeopceA |
| (9) | AAGCNTGGCCGGCGATGGGGCTGGTTATCGAACGCACCGAAGCGAGNTGATGACGCCAACATTAA | Incomplete matches to random microorganisms |

*For detailed BLAST results, please see the list provided in the next few pages.

*Appendix E. The Design of Piping System for the Column Experiment*

**McMaster Carr**

**[D]** 316 Stainless Steel—Coils 1/16" OD, 0.046" ID, .008" Wall, 5'L (search 51755K37 in McMaster Carr)

**[G]** Female x Male x Female tee 1/8" (search 48805K192 in McMaster Carr)

**[J]** 316 Stainless Steel Tubing 1/8" OD, .105" ID, .01" Wall, 28" L (search 1800T227 in McMaster Carr)

**Cole Parmer**

**[A]** Syringes with PTFE luer lock; syringe capacity; 10 mL; needle gauge; 22 (Cole Parmer: EW-07939-84)

**[B]** Female luer lock x 1/8" NPT, 316 SS, each (Cole Parmer: WU-31507-46)

**[F]** Parker® three-way ball valve, stainless steel, 1/8" NPT(F)

**[H]** Barbed Fittings; NPT Male Pipe Adapter, 316 SS, 1/8" NPT(M) x 1/16" Tubing ID

**Swagelok**

**[E]** SS Swagelok Tube Fitting, Male Connector, 1/16 in. Tube OD x 1/8 in. Male NPT (SS-100-1-2)

**[C]** SS Swagelok Tube Fitting, Female Connector, 1/16 in. Tube OD x 1/8 in. Female NPT (SS-100-7-2)

**[I]** SS Swagelok Tube Fitting, Male Connector, 1/8 in. Tube OD x 1/8 in. Male NPT (SS-100-1-2)

**[J]** SS Swagelok Tube Fitting, Bulkhead Union, 1/8 in. Tube OD (swagelok SS-200-61)

**[K]** SS 1-Piece 40 Series Ball Valve, 0.2 Cv, 1/8 in. Swagelok Tube Fitting (swagelok SS-41GS2)

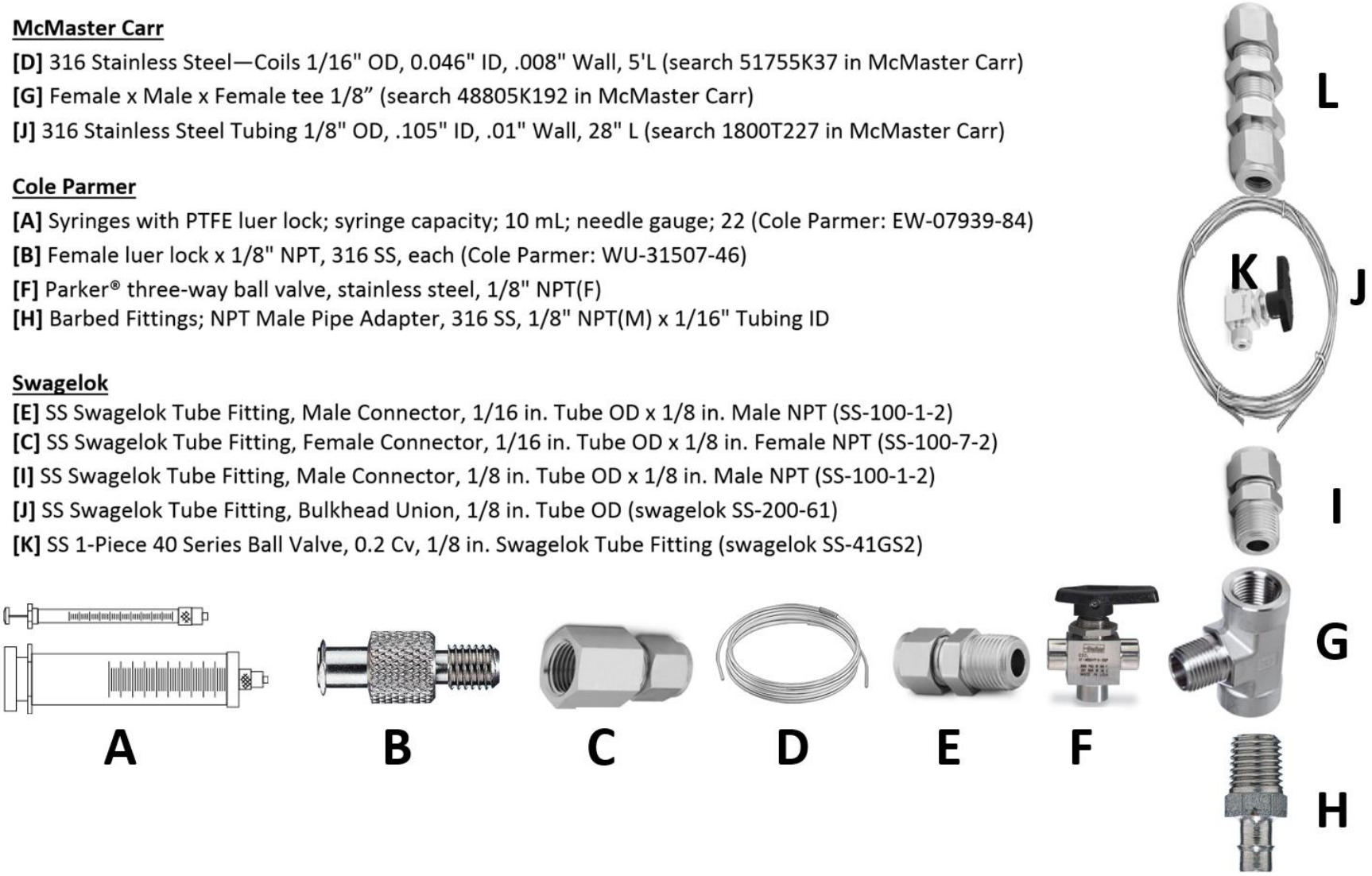

***Appendix F. Calculation of Mulch Consumption Rate from Oxidation by Dissolved Oxygen***

As reported from Runtian Yang (Yang R. , 2014), 1 gram of dry mulch (pine bark, same as used in the present column experiment) could ultimately consume 31.2 mg of DO in groundwater. Thus, knowing the DO level in column influent and the parameters of the column experiment, we can estimate the mass of mulch consumed just by the aerobic oxidation of mulch.

For 212 days of column operation, the total mass of DO that entered the column can be calculated by multiplying flow rate (287 mL/day), DO level (7.986 mg/L), and time of operation (212 days), and found to be 485.9 mg. Thus, the amount of dry mulch expected to be consumed is calculated by dividing 485.9 mg $O_2$ by 31.2 mg $O_2$/g mulch and found to be 15.6 grams mulch (dry weight).

Since the total dry mulch in each column was 185.6 gram, and the column height was 60 cm, the height of column consumed in 212 days is estimated to be 5.0 cm.

***Appendix G. Method of Measuring Column Porosity***

The porosity of the column is defined as the volume of water in the column (sorbed to mulch, as well as in column pores) divided by the total volume of the column. The total volume of the column was known to be 1226 mL, by multiplying cross sectional area of 20.43 $cm^2$ and column height of 60 cm. One of the six identical columns was filled with 320 grams of ambient-moisture mulch and limestone with weight equal to 40% of mulch dry weight; 720 mL water was poured in to completely fill the column with water. Due to the slow penetration of mulch by water, the column was capped and allowed to equilibrate for one day, and then a little more water was added to fill the entire column volume. Thus, a total volume of 823 mL of water was added to the column, to fully saturate it. The porosity of the column was then calculated, using the total added amount of water in the column (823 mL), plus the 134.4 mL water estimated as contributed by the 42% ambient moisture content of the added mulch, divided by the total column volume, to get 0.78.

# References


Amonette, J. E., Workman, D. J., Kennedy, D. W., Fruchter, J. S., & Gorby, Y. A. (2000). Dechlorination of carbon tetrachloride by Fe(II) associated with goethite. *Environmental Science and Technology, 34*, 4606-4613.

ATSDR. (1997). *Toxicological Profile for Trichloriethylene (TCE).* U.S. Centers for Disease Control Agency for Toxic Substances and Disease.

ATSDR. (2003, July). *ToxFAQs for Trichloroethylene (TCE).* Retrieved May 30, 2014, from Agency for Toxic Substances & Disease Registry: http://www.atsdr.cdc.gov/toxfaqs/TF.asp?id=172&tid=30

Azizian, M. F., Behrens, S., Sabalowsky, A., Dolan, M. E., Spormann, A. M., & Semprini, L. (2008). Continuous-flow column study of reductive dehalogenation of PCE upon bioaugmentation with the Evanite enrichment culture. *Journal of Contaminant Hydrology, 100*, 11-21.

Baker, M. A., Valett, H. M., & Dahm, C. N. (2000). Organic carbon supply and metabolism in a shallow groundwater ecosystem. *Ecology, 81*(11), 3133-3148.

Behrens, S., Azizian, M. F., McMurdie, P. J., Sabalowsky, A., Dolan, M. E., Semprini, L., & Spormann, A. M. (2008). Monitoring abundance and expression of "Dehalococcoides" species chloroethene-reductive dehalogenases in a tetrachloroethene-dechlorinating flow column. *Applied and Environmental Microbiology, 74*(18), 5695-5703.

Benner, S. G., Blowes, D. W., Gould, W. D., Herbert, D. H., & Ptacek, C. J. (1999). Geochemistry of a permeable reactive barrier for metals and acid mine drainage. *Environmental Science and Technology, 33*, 2793-2799.

Blowes, D. W., Gillham, R. W., Ptacek, C. J., Puls, R. W., Bennett, T. A., O'Hannesin, S. F., . . . Bain, J. (1999). *In situ permeable reactive barrier for the treatment of hexavalent chromium and trichloethylene in ground water: Volume 1. Design and Installation.* Washington, DC: U.S. Environmental Protection Agency.

Bouwer, E. J., & McCarty, P. L. (1983). Transformation of 1- and 2-carbon halogenated aliphatic organic compounds under methanogenic conditions. *Applied Environmental Microbiology, 45*, pp. 1286-1294.

Butler, E. C., & Hayes, K. F. (1999). Kinetics of the Transformation of Trichloriethylene and Tetrachloroethylene by Iron Sulfide. *Environmental Science and Technology, 33*, 2021-2027.

Champ, D. R., Gulens, R. L., & Jackson, R. E. (1979). Oxidation-reduction sequences in ground water flow systems. *Canadian Journal of Earth Sciences, 16*(1), pp. 12-23.

Chen, B. L., Johnson, E. J., Chefetz, B., Zhu, L. Z., & Xing, B. S. (2005). Sorption of polar and nonpolar aromatic organic contaminants by plant cuticular materials: role of polarity and accessibility. *Environmental Science and Technology, 39*(16), 6138-6146.

Chin, K. K. (1981). Anaerobic treatment kinetics of palm oil sludge. *Water Research, 15*, 199-202.

Cowan, D. (2000). Innovative abatement and remediation of perchlorate at McGregor, Texas Weapons Plant Site. *Soil Sediment & Groundwater, 5*, pp. 25-26.

Demirel, B., & Scherer, P. (2008). The roles of acetotrophic and hydrogenotrophic methanogens during anerobic conversion of biomass to methane: a review. *Reviews in Environmental Science and Biotechnology, 7*, 173-190.

Distefano, T. D., Gossett, J. M., & Zinder, S. H. (1991). Reductive dechlorination of high concentration of tetrachloroethene to ethene by an anaerobic enrichment culture in the absence of methanogenesis. *Applied Environmental Microbiology, 57*, pp. 2287-2292.

Duhamel, M., Wehr, S. D., Yu, L., Rizvi, H., Seepersad, D., Dworatzek, S., . . . Edwards, E. A. (2002). Comparison of anaerobic dechlorinating enrichment cultures maintained on tetrachloroethene, trichloroethene, cis-dichloroethene and vinyl chloride. *Water Research, 36*, 4193-4202.

Duryea, M. L., English, R. J., & Hermansen, L. A. (1999). A comparison of landscape mulches: chemical, allelopathic, and decomposition properties. *Journal of Arboriculture, 25*(2), 88-97.

Ebihara, T., & Bishop, P. L. (2002). Influence of supplemental acetate on bioremediation for dissolved polycyclic aromatic hydrocarbons. *Journal of Environmental Engineering, 128*(6), pp. 505-513.

Fennell, D. E., & Gossett, J. M. (1998). Modeling the production of and competition for hydrogen in a dechlorinating culture. *Environmental Science and Technology, 32*, 2450-2460.

Freedman, D. L., & Gossett, J. M. (1989). Biological reductive dechlorination of tetrachloroethylene and trichloroethylene to ethylene under methanogenic conditions. *Applied Environmental Microbiology, 55*, pp. 2144-2151.

Freundlich, H. M. (1906). Über die adsorption in lösungen. *Zeitschrift für Physikalische Chemie, 57*(A), 385-470.

Garbarini, D., & Lion, L. (1986). Influence of the nature of soil organics on the sorption of toluene and trichloriethylene. *Environmental Science and Technology, 20*(12), 1263-1269.

Gillham, R. W., & O'Hannesin, S. F. (1992). Metal-catalyzed abiotic degradation of halogenated organic compounds. *Waterloo Centre for Groudnwater Research, 29*(5), pp. 94-95.

Gomez, M. A., Hontoria, E., & Gonzalez-Lopez. (2002). Effect of dissolved oxygen concentration on nitrate removal from groundwater using a denitrifying submerged filter. *Journal of Hazardous Materials, 90*(3), 267-278.

Gossett, J. M. (1987). Measurement of Henry's law constants for C1 and C2 chlorinated hydrocarbons. *Environmental Science and Technology, 21*(2), pp. 202-208.

Gossett, J. M. (2010). Sustained aerobic oxidation of vinyl chloride at low oxygen concentrations. *Environmental Science and Technology, 44*, 1405-1411.

He, J., Sung, Y., Dollhopf, M. E., Fathepure, B. Z., Tiedje, J. M., & Löffler, F. E. (2002). Acetate versus hydrogen as direct electron donors to stimulate the microbial reductive dechlorination process at chloroethene-contaminated sites. *Environmental Science and Technology, 36*, 3945-3952.

He, Y. T., Wilson, J. T., & Wilkin, R. T. (2008). Transformation of reactive iron minerals in a permeable reactive barrier (Biowall) used to treat TCE in groundwater. *Environmental Science and Technology, 42*, 6690-6696.

Heavner, G. L. (2013). *Biokinetic modeling, laboratory examination and field analysis of DNA, RNA and protein as robust molecular biomarkers of chloroethene reductive dechlorination in* Dehalococcoides mccartyi*.* PhD Dissertation, Cornell University.

Henderson, A. D., & Demond, A. H. (2007). Long-term performance of zero-valent iron permeable reactive barriers: a critical review. *Environmental Engineering Science, 24*(4), pp. 401-423.

Huling, S. G., & Pivetz, B. E. (2006). In-situ chemical oxidation. *EPA Envineering Issue*(EPA/600/R-06/072).

IARC. (1974). Some Anti-Thyroid and Related Substances, Nitrofurans and Industrial Chemicals. In Lyon, *IARC Monographs on the Evaluation of Carcinogenic Risks to Humans.* World Health Organization.

ITRC. (2005). *Permeable reactive barriers: lessons learned/new directions.* Washington, DC: ITRC.

ITRC. (2008). *In situ bioremediation of chlorinated ethene: DNAPL source zones.*

Jarrell, K. F., Bayley, D. P., & Kostyukova, A. S. (1996). The archaeal flagellum: a unique motility structure. *Journal of Bacteriology, 178*, pp. 5057-5064.

Kovacich, M. S., Beck, D., Rabideau, T., Pettypiece, E., Smith, K., Noel, M., . . . Cannaert, M. T. (2007). *Full-scale bioaugmentation to create a passive biobarrier to remediate a TCE groundwater plume.* Tetra Tech GEO.

Krajmalnik-Brown, R., Holscher, T., Thomson, I. N., Saunders, F. M., Ritalahti, K. M., & Löffler, F. E. (2004). Genetic identification of a putative vinyl chloride reductase in *Dehalococcoides* sp. strain BAV1. *Applied Environmental and Microbiology, 70*, pp. 6347-6351.

Lee, W., & Batchelor, B. (2002). Abiotic reductive dechlorination of chlorinated ethylenes by iron-bearing soil minerals. *Environmental Science and Technology, 36*, 5348-5354.

Leeson, A., Beevar, E., Henry, B., Fortenberry, J., & Coyle, C. (2004). *Principles and practices of enhanced anaerobic bioremediation of chlorinated solvents.* DTIC.

Leisinger, T. (1983). Microorganisms and xenobiotic compounds. *Experientia, 39*(11), 1183-1191.

Liang, C., Bruell, C. J., Marley, M. C., & Sperry, K. L. (2004). Persulfate oxidation for in situ remediation of TCE. II. Activated by chelated ferrous ion. *Chemosphere, 55*(9), pp. 1225-1233.

Löffler, F. E., & Edwards, E. A. (2006). Harnessing microbial activities ofr environmental cleaup. *Current Opinion in Biotechmology, 17*, 274-284.

Löffler, F. E., Yan, J., Ritalahti, K. M., Adrian, L., Edwards, E. A., Konstantinidis, K. T., . . . Spormann, A. M. (2013). *Dehalococcoides mccartyi* gen. nov., sp. nov., obligate organohalide-respiring anaerobic bacteria, relevent to halogen cycling and bioremediation, belong to a novel bacterial class, *Dehalococcoidetes* classis nov., within the phylum Chloroflexi. *International Journal of Systematic Evolutionary Microbiology, 63*, 625-635.

Lovley, D. R. (1987). Organic matter mineralization with the reduction of ferric iron: A review. *Geomicrobiology Journal, 5*(3-4), 375-399. doi:10.1080/01490458709385975

Lu, X., Wilson, J. T., Shen, H., Henry, B. M., & Kampbell, D. H. (2008). Remediation of TCE-contaminated groundwater by a permeable reactive barrier filled with plant mulch (Biowall). *Journal of Environmental Science and Health Part A, 43*, pp. 24-35.

MacDougall, D., Lal, J., Amore, F. J., Langner, R. R., Cox, G. V., McClelland, N. I., . . . Crummett, W. B. (1980). Guidelines for data acquisition and data quality evaluation in environmental chemistry. *Analytical Chemistry, 52*, 2242-2249.

Magnuson, J. K., Romine, M. F., Burris, D. R., & Kingsley, M. T. (2000). Trichloroethene reductive dehalogenase from *Dehalococcoides ethenogenes*: Sequence of tceA and substrate range characterization. *Applied Environmental Microbiology, 66*, pp. 5141-5147.

Maymó-Gatell, X., Anguish, T., & Zinder, S. H. (1999). Reductive dechlorination of chlorinated ethenes and 1,2-dichloroethane by *Dehalococcoides ethenogenes* 195. *Applied Environmental Microbiology, 65*, pp. 3108-3113.

Maymó-Gatell, X., Chien, Y. T., Gossett, J. M., & Zinder, S. H. (1997). Isolation of a bacterium that reductively dechlorinates tetrachloroethene to ethene. *Science, 276*, pp. 1568-1571.

Maymo-Gatell, X., Tandoi, V., Gossett, J. M., & Zinder, S. H. (1995). Characterization of an H2-utilizing enrichment culture that reductively dechlorinates tetrachloroethene to vinyl chloride and ethene in the absence of methanogenesis and acetogenesis. *Applied and Environmental Microbiology, 61*(11), 3928-3933.

McCarty, P. L., Goltz, M. N., Hopkins, G. D., Dolan, M. E., Allan, J. P., Kawakami, B. T., & Carrothers, T. J. (1998). Full-scale evaluation of in-situ cometabolic degradation of trichloriethylene in groundwater through toluene injection. *Environmental Science and Technology, 32*, 88-100.

Moran, M. J., Zogorski, J. S., & Squillace, P. J. (2007). Chlorinated solvents in groundwater of the United States. *Environmental Science and Technology, 41*, pp. 74-81.

Moretti, C. J., & Neufield, R. D. (1989). PAH portioning mechanisms with activated sludge. *Water Research, 23*, pp. 93-102.

Müller, J. A., Rosner, B. M., Von Abendroth, G., Meshulam-Simon, G., McCarty, P. L., & Spormann, A. M. (2004). Molecular identification of the catabolic vinyl chloride reductase from *Dehalococcoides* sp. strain VS and its environmental distribution. *Applied and Environmental Microbiology, 70*, 4880-4888.

Oztürk, Z., Tansel, B., Katsenovich, Y., Sukop, M., & Laha, S. (2012). Highly organic natural media as permeable reactive barriers: TCE partitioning and anaerobic degradation profile in eucalyptus mulch and compost. *Chemosphere, 89*, 665-671.

Phillips, D. H., Gu, B. W., Roh, Y., Liang, L., & Lee, S. Y. (2000). Performance evaluation of a zerovalent iron reactive barrier: mineralogical characteristics. *Environmental Science and Technology, 34*, 4169-4176.

Powell, R. M., & Powell, P. D. (2002). *Economic analysis of the implementation of permeable reactive barriers for remediation of contaminated ground water.* Washington, DC: U.S. Environmental Protection Agency.

Rawls, W. J., Brakensiek, D. L., & Saxton, K. E. (1982). Estimation of soil water properties. *American Society of Aguicultural Engineering, 25*(5), pp. 1316-1320.

Reddy, K. R. (2008). Chapter 12: Physical and chemical groundwater remediation technologies. In C. J. Darnauly, *Overexploitation and contamination of shared groundwater resources* (pp. 257-274). Chicago, IL: Springer Science+Business Media B.V.

Richard, T. (2005). *The effect of lignin on biodegradability.* Ithaca: Cornell Waste Management Institute, Cornell University.

Richardson, R. E., Bhupathiraju, V. K., Song, D. L., Goulet, T. A., & Alvarez-Cohen, L. (2002). Phylogenetic characterization of microbial communities that reductively dechlorinate TCE based upon a combination of molecular techniques. *Environmental Science and Technology, 36*, 2652-2662.

Rose, S., & Long, A. (1988). Dissolved oxygen systematics in the Tucson basin aquifer. *Water Resources Research, 24*, pp. 127-136.

RTDF. (2001, August 1). *Permeable Reactive Barrier Installation Profiles.* Retrieved June 15, 2014, from RTDF: Permeable Reactive Barrier Action Team: http://www.rtdf.org/public/permbarr/prbsumms/default.cfm

Russell, H. H., Matthews, J. E., & Sewell, G. W. (1992). TCE removal from contaminated soil and ground water. *EPA Ground Water Issue*(EPA/540/S-92/002).

Scheutz, C., Durant, N. D., Dennis, P., Hansen, M. H., Jorgensen, T., Jakobsen, R., . . . Bjerg, P. L. (2008). Concurrent ethene generation and growth of *Dehalococcoides* containng vinyl chloride reductive

dehalogenase genes during an enhanced reductive dechlorination field demonstration. *Environmental Science and Technology, 42*, 9302-9309.

Seo, Y., & Bishop, P. L. (2008). The monitoring of biofilm formation in a mulch biowall barrier and its effect on performance. *Chemosphere, 70*, pp. 408-488.

Seshadri, R., Adrian, L., Fouts, D. E., Eisen, J. A., Phillippy, A. M., Methe, B. A., . . . Heidelberg, J. F. (2005). Genome sequence of the PCE-dechlorinating bacterium *Dehalococcoides ethenogenes*. *Science, 307*, pp. 105-108.

Shen, H., & Wilson, J. T. (2007). Trichloroethylene removal from groundwater in flow-through columns simulating a permeable reactive barrier constructed with plant mulch. *Environmental Science and Technology, 41*(11), 4077-4083.

Shen, H., Adair, C., & Wilson, J. T. (2010). Long-term capacity of plant mulch to remediate trichloroethylene in groundwater. *Journal of Environmental Engineering, 136*, pp. 1054-1062.

Singh, H. B., Salas, L. J., & Stiles, R. E. (1982). Distribution of selected gaseous organic mutagens and suspect carcinogens in ambient air. *Environmental Science and Technology, 16*(12), pp. 872-880.

Smatlak, C. R., Gossett, J. M., & Zinder, S. H. (1996). Comparative kinetics of hydrogen utilization for reductive dechlorination of tetrachloroethene and methanogenesis in an anaerobic enrichment culture. *Environmental Science and Technology, 30*, pp. 2850-2858.

Su, C., & Puls, R. W. (2007). Removal of added nitrate in cotton burr compost, mulch compost, and peat: mechanisms and potential use for groundwater nitrate remediation. *Chemosphere, 66*(1), 91-98.

Sung, Y., Fletcher, E. K., Ritalahti, K. M., Apkarian, R. P., Ramos-Hernandez, N., Sanford, R. A., . . . Löffler, F. E. (2006). *Geobacter lovleyi* sp. nov. Strain SZ, a novel metal-reducing and tetrachloroethene-dechlorinating bcterium. *Applied Environmental Microbiology, 72*(4), pp. 2775-2782.

Tang, S., Chan, W. M., Fletcher, K. E., Seifert, J., Liang, X., Loffler, F. E., & Edwards, E. A. (2013). Functional characterization of reductive dehalogenases by using blue native polyacrylamide gel electrophoresis. *Applied Environmental Microbiology, 79*(3), pp. 974-981.

TEACH, U. E. (2007). *Trichloroethylene (TCE): TEACH Chemical Summary.* U.S. Environmental Protection Agency, Toxcity and Exposure Assessment for Children's Health (TEACH).

USEPA. (1987e). *An Overview of Sediment Quality in the United States.* U.S. Environmental Protection Agency.

USEPA. (2001). *National air toxics program: the integrated urban strategy: report to congress.* U.S. Environmental Protection Agency.

USEPA. (2009). *National primary drinking water regulations.* U.S. Environmental Protection Agency.

USEPA. (n.d.). *Superfund: Basic Information.* Retrieved May 30, 2014, from United States Environmental Protection Agency: http://www.epa.gov/superfund/about.htm

Vainberg, S., Condee, C. W., & Steffan, R. J. (2009). Large-scale production of bacterial consortia for remediation of chlorinated solvent-contaminated groundwater. *Journal of Industrial Microbiology and Biotechnology, 36*, 1189-1197.

Wagner, D. D., Hug, L. A., Hatt, J. K., Spitzmiller, M. R., Padilla-Crespo, E., Ritalahti, K. M., . . . Löffler, F. E. (2012). Genomic determenants of organohalide-respiration in *Geobacter loveyi*, an unusual member of the Geobacteraceae. *BMC Genomics, 13*(200).

Warner, S. D., Longino, B. L., Zhang, M., Bennett, P., Szerdy, F. S., & Hamilton, L. A. (2005). The first commercial permeable reactive barrier composed of granular iron: Hydraulic and chemical performance at 10 years of operation. In G. Boshoff, & B. D. Bone, *First International Symposium on Permeable Reactive Barriers* (p. 32). Oxfordshire, UK: IAHS Press.

Wei, Z., & Seo, Y. (2010). Trichloroethylene (TCE) adsorption using sustainable organic mulch. *journal of Hazardous Materials, 181*(1-3), pp. 147-153.

Wilkin, R. T., & Puls, R. W. (2004). *Evaluation of permeable reactive barrier performance.* Washington, DC: U.S. Environmental Protection Agency.

Wilson, J. T., & Wilson, B. H. (1985). Biotransformation of Trichloroethylene in soil. *Applied and Environmental Microbiology, 49*(1), 242-243.

Wilson, J. T., Enfield, C. G., Dunlap, W. J., Cosby, R. L., Foster, D. A., & Baskin, L. B. (1981). Transport and fate of selected organic pollutants in a sandy soil. *Journal of Environmental Quality, 10*(4), pp. 501-506.

Yang, R. (2014). *Capacity of bark mulch to deoxygenate groundwaters remediated anaerobically in biobarrier walls.* Ithaca: M.S. Thesis: Cornell University. Retrieved July 4, 2014

Yang, Y., & McCarty, P. L. (1998). Competition for hydrogen within a chlorinated solvent dehalogenating anaerobic mixed culture. *Environmental Science and Technology, 32*, pp. 3591-3597.

Zytner, R. G. (1992). Adsorption desorption of trichloroethylene in granular media. *Water, Air, and Soil Pollution, 65*, 245-255.